



<https://theses.gla.ac.uk/>

Theses Digitisation:

<https://www.gla.ac.uk/myglasgow/research/enlighten/theses/digitisation/>

This is a digitised version of the original print thesis.

Copyright and moral rights for this work are retained by the author

A copy can be downloaded for personal non-commercial research or study,  
without prior permission or charge

This work cannot be reproduced or quoted extensively from without first  
obtaining permission in writing from the author

The content must not be changed in any way or sold commercially in any  
format or medium without the formal permission of the author

When referring to this work, full bibliographic details including the author,  
title, awarding institution and date of the thesis must be given

Enlighten: Theses

<https://theses.gla.ac.uk/>  
[research-enlighten@glasgow.ac.uk](mailto:research-enlighten@glasgow.ac.uk)

THE FLUID DYNAMICS OF THE LOWER URINARY TRACT

Thesis presented to the University of Glasgow

for the Degree of Ph.D.

W. T. Millar, Esq., B.Sc.,  
Department of Clinical Physics and Bio-engineering,  
11 West Graham Street,  
Glasgow.

ProQuest Number: 10647209

All rights reserved

INFORMATION TO ALL USERS

The quality of this reproduction is dependent upon the quality of the copy submitted.

In the unlikely event that the author did not send a complete manuscript and there are missing pages, these will be noted. Also, if material had to be removed, a note will indicate the deletion.



ProQuest 10647209

Published by ProQuest LLC (2017). Copyright of the Dissertation is held by the Author.

All rights reserved.

This work is protected against unauthorized copying under Title 17, United States Code  
Microform Edition © ProQuest LLC.

ProQuest LLC.  
789 East Eisenhower Parkway  
P.O. Box 1346  
Ann Arbor, MI 48106 – 1346

## A C K N O W L E D G E M E N T S

I should like to thank Mr. S. Alexander, Senior Lecturer in Surgery, University Department of Surgery, Glasgow Royal Infirmary and Mr. D. Rowan, Principal Physicist, Department of Clinical Physics and Bio-engineering, Western Regional Hospital Board for their invaluable help and co-operation during these studies. All clinical procedures were performed by Mr. S. Alexander. I should also like to than Professor W. Mackey, University Department of Surgery, Glasgow Royal Infirmary and Dr. J. M. L. Lenihan, Regional Physicist, Department of Clinical Physics and Bio-engineering, Western Regional Hospital Board for their continued support.

These studies were, in part, supported by grants from the M.R.C. and A.C.M.R.

## S U M M A R Y

Chapter 1 contains a general review of the physiology and fluid dynamics of the lower urinary tract.

A radioisotope technique for the measurement of urine flowrate simultaneously with bladder pressure has been developed and is discussed in Chapter 2. The method also permits the measurement of residual urine. The techniques used for the measurement of bladder pressure and abdominal pressure are also discussed. The rigid tube model of the urethra is presented in Chapter 3.

The measurements obtained from a group of female patients suffering from stress incontinence are presented in Chapter 4. No direct correlation between the peak urine flowrate, and the bladder pressure at peak flowrate, initial volume in bladder, volume voided and the micturition time was obtained. Multiple linear correlation, however, revealed an interdependence between all of the variables. Using data measured by Krøigaard (1970) in a group of young children, for which no direct correlation was found, it was found that there was again an interdependence. The analyses, however, suggested that the two groups of patients were different. This method of analysis may, therefore, help in the classification of incontinent patients.

The comparison of parameters determined using the rigid tube model and the clinically obtained values showed that the rigid tube model correlated well with the observations. However, the high degree of correlation between the resistance index (bladder pressure/flowrate<sup>2</sup>) directly obtained from clinical measurements and the

resistance defined by the rigid tube model show that the model is an unnecessary complication.

The theory of flow in elastic tubes is discussed in Chapter 5. It is shown that the tissue defines a critical flowrate which determines the general shape of the urethral profile during micturition. The occurrence of supercritical flow (that is, the urine flowrate is greater than the critical flowrate) may explain certain urethral profiles observed during micturition cystography, and the associated high resistances. The high transient flowrates with subsequently reduced flowrate may also be explained using the concept of supercritical flow. This is discussed in Chapter 6. It is also shown in Chapter 6 that the critical flowrate in excised dog urethras is of the order of 10 ml/sec upwards and that the occurrence of supercritical flow in the human subject is probable in certain cases.

## C O N T E N T S

|                   |  | <u>Page</u> |
|-------------------|--|-------------|
| <u>Chapter 1</u>  | GENERAL REVIEW                                       | 1.1         |
| 1.1               | The Micturition Process                              | 1.1         |
| 1.2               | Micturition Dynamics                                 | 1.5         |
| <u>Chapter 2</u>  | MEASUREMENT TECHNIQUE                                | 2.1         |
| 2.1               |  | 2.1         |
| 2.2               | Bladder Pressure                                     | 2.1         |
| 2.3               | Abdominal Pressure                                   | 2.3         |
| 2.4               | Urine Flowrate                                       | 2.6         |
| 2.5               | Theory   | 2.8         |
| 2.6               | Clinical Technique                                   | 2.16        |
| 2.7               | Data Processing                                      | 2.18        |
| <u>Chapter 3</u>  | RIGID TUBE THEORY                                    | 3.1         |
| <u>Chapter 4</u>  | DATA ANALYSIS  | 4.1         |
| 4.1               |  | 4.1         |
| 4.2               | Multiple Correlation Analyses                        | 4.13        |
| <u>Chapter 5</u>  | ELASTIC TUBE THEORY - I                              | 5.1         |
| 5.1               | Elastic Tube Theory                                  | 5.1         |
| 5.2               | The Flow Equation                                    | 5.1         |
| 5.3               | Method of Characteristics                            | 5.7         |
| 5.4               | Solution of the Flow Equations                       | 5.9         |
| 5.5               | Pressure-area Relationship                           | 5.10        |
| 5.6               | Numerical Solution of the<br>Pressure Flow Equations | 5.13        |
| <u>Chapter 6</u>  | ELASTIC TUBE THEORY - II                             | 6.1         |
| <u>Appendix I</u> | Elastic Tube Programme                               |             |

CHAPTER 1General Review1.1 The Micturition Process

The urinary bladder is a large muscular organ capable of accommodating a large volume of urine. The outlet from the bladder, the urethra, is a highly distensible and muscular tube whose length in the adult human is of the order of 3 cm in the female and 18 cm in the male (Gray's Textbook of Anatomy).

The musculature of the bladder is smooth and the motor supply to the bladder, which is both parasympathetic and sympathetic, stems from the sacral roots S2, S3 and S4, McCrea and Kimmell (1952), Learmonth (1931), Schlyvitsch and Kosintzev (1939). When the bladder muscle is stimulated, the volume of urine is expelled via the urethra by the forcible contraction of the detrusor.

The bladder wall also contains cells which are stimulated by the tension in the wall and therefore their activity relates to the volume in the bladder. The activity is not necessarily linearly related to the bladder volume. It has been observed by Sherrington (1915), Tang and Ruch (1955), Ruch (1960), Sabetian (1965) that in the normal bladder the bladder pressure slowly increases at physiological rates of filling. Normally some volume is eventually attained where there is a rapid change in the rate of change of the pressure with volume. At this point, it is probable that the elastic limit of the muscle fibres has been reached. Ruch (1960), Hinman and Miller (1963) used Lapides law relating the pressure  $p$ , radius  $R$  and the tension  $T$  in a balloon -

$$p = \frac{2T}{R}$$

The gentle rise normally observed in the pressure volume curve is due to the dependence of the pressure on the radius of the bladder, the mural tension however increasing more slowly than the pressure. Ruch (1960) also suggested that the thickness of the bladder wall decreased as the volume increased.

The tension exerted by the bladder wall in the resting state is a purely myogenic response. This has been shown by Langley and Whiteside (1951), Veneema et al (1952), Tang and Ruch (1955) and Sabetian (1965). The tension response was observed in bladders which had been denervated. These authors, therefore, concluded that the tonus was independent of the intact nerve supply. Sabetian (1965) quotes "The hypotonocity or hypertonicity of the bladder appears to be independent of neural influences ....." . Nesbit and Lapidus (1948) showed that the paralysed bladder in man elicited a tension response provided that the muscle fibres had not been overstretched. According to Barrington (1921) the proprioceptors in the bladder wall stimulate a spinal reflex in the spinal cord which results in detrusor contraction. This effect can be inhibited by higher centres. The basic voiding reflex, however, depends on an intact cord Langworthy et al (1940).

The urethra is composed of both smooth and striated muscle, with an abundance of elastic fibres in the region of the bladder neck, Woodburne (1968), Tanagho, Meyers and Smith (1968, 1969).

The striated musculature is concentrated in the region of the urogenital diaphragm. The smooth muscle is innervated by fibres from the pelvic nerves whilst the striated musculature is supplied by the pudendal nerves.

Micturition normally requires that the intravesical pressure increases. Initiation of micturition may also occur with a decrease in urethral resistance without a subsequent rise in the bladder pressure. Muellner and Fleischner (1949), Ritter and Sporer (1949) and Roberts (1953) suggested that on micturition abdominal pressure increase and pelvic floor relaxation occurred with a subsequent rise in the intravesical pressure due to detrusor contraction. These conclusions were mainly determined from micturition cystography studies. Denny Brown and Robertson (1933) found that a rise in abdominal pressure was not necessary for micturition to occur. Lapidus, Sweet and Lewis (1957) showed that normal persons could initiate micturition following pudendal block with curare. Peterson, Kellberg and Dhumer (1961) found that ninety per cent of their patients could not initiate micturition when the urethral sphincter was relaxed suggesting that in these instances pelvic floor relaxation was not the initiating factor in micturition. Lund, Benjamin et al (1957) observed that on initiation of micturition the posterior base of the bladder descended with a shortening of the proximal urethra. They also observed that on interruption of micturition the base of the bladder was elevated. Elevation of the bladder on interruption of micturition has also been observed by Ardran,

Simmons and Stewart (1956) and Vincent (1959).

The opening of the bladder neck is considered by Woodburne (1950) to open due to the action of the elastic fibres in that region. However, the urethra at the bladder neck often shows funnelling, Barnes (1940), Hodgkinson (1953), Ingelman-Sundbert (1949), Jeffcoate and Roberts (1952) and Mueller (1949), Enhorning (1963). Jeffcoate and Roberts (1952) also suggested that the angle between the posterior wall of the urethra and the bladder base was important in the diagnosis of stress incontinence. They considered that the closer this angle approached  $180^{\circ}$ , the more likely were the urethral closure forces to be insufficient to maintain continence. Enhorning (1963) suggested that, since the bladder is subjected to abdominal pressure, partial transmission of the abdominal pressure to the posterior urethra may result in the total pressure in the bladder overcoming the urethral resistance.

The urethral shape during micturition was investigated by Nordenstrom (1952) using urethrocytography. The female urethra was observed to narrow slightly at the bladder neck, subsequently widen in the posterior urethra and then gradually narrow down towards the external meatus. The slight narrowing in the bladder neck region may or may not be seen to occur during micturition. This general urethral shape has been observed by Nel (1955), Lund, Benjamin et al (1957), Gullmo (1962) and Gleason and Lattimer (1963). Essenhigh (1968) stated that a wide bladder neck was indicative of a normal detrusor contraction. The interpretation

of urethral shapes obtained during micturition are frequently a matter of controversy.

Lapides, Ajemian et al (1960), Backmann (1966), Tanagho, Meyers, Smith (1969) used a catheter in the urethra to determine the pressure exerted by the urethral tissue at rest. The maximum pressure was developed in the region of the membranous urethra with the pressure on each side of this segment decreasing towards the internal meatus and external meatus respectively. Paralysis of the striated musculature by spinal anaesthesia resulted in a reduction of the pressure in the membranous urethra in most of the patients investigated by Lapides, Ajemian et al (1960). During micturition however, the striated muscle is inactive Petersen, Stener et al (1962), Abramson, Housson and D'Onofrio (1966). Tanagho, Miller, Meyers and Corbett (1966) demonstrated that on initiation of micturition, the intraurethral pressure ceased but returned at the end of voiding.

### 1.2 Micturition Dynamics

Smith (1968) discussed the methods currently used to diagnose urethral obstruction.

- (a) The history of the patient may indicate the severity of the obstruction.
- (b) The physical examination may reveal a large bladder and/or an enlarged prostate.
- (c) Radiology may be used for the demonstration of residual urine or urethral stricture.
- (d) Endoscopy may reveal trabeculation of the bladder,

residual urine or urethral shape.

None of these techniques give satisfactory or unequivocal diagnoses. In the attempt to elucidate the fluid dynamics of the lower urinary tract and enhance diagnostic techniques, methods based on the measurement of fluid dynamical parameters have been employed.

The intravesical pressure was first measured by Dubois (1876) using an elastic catheter under static conditions. However, the variation of the intravesical pressure with time is much more informative and was investigated by Messa and Pellacini (1882) using a urethral catheter. They were the first investigators to demonstrate an intravesical pressure rise at the onset of micturition. They also showed that the bladder could accommodate varying amounts of urine without a significant change in pressure. Adler (1929) used a suprapubic catheter but found that the bladder pressure remained fairly constant. Denny Brown and Robertson (1933) performed investigations using a fine catheter in the bladder and another urethral catheter positioned within the urethra. They demonstrated that the intravesical pressure rise on micturition was independent of abdominal pressure. They also observed a secondary rise in the intravesical pressure during voiding which they termed an "after contraction". Baumann (1955) found the micturition pressure to have an average value of 52 cm  $H_2O$  in the female and 60 cm  $H_2O$  in the male.

Von Garrelts (1957) investigated a number of normal male patients. He obtained maximum pressures during voiding between

60 cm H<sub>2</sub>O and 102 cm H<sub>2</sub>O. Von Garrelts also subtracted the resting bladder pressure from the maximum bladder pressure and obtained an average value of 43 cm H<sub>2</sub>O. The values of the pressure difference ranged between 35 cm H<sub>2</sub>O and 54 cm H<sub>2</sub>O. In fifty per cent of the voidings, an "after contraction" was observed. The contraction was more frequently observed in some patients than in others. The "after contraction" was not related to any rise in abdominal pressure. No sensation was associated with the pressure rise even when marked. Von Garrelts suggested that there may have been a tendency for the "after contraction" to occur more frequently if the pelvic floor was contracted during the final phase of micturition. The study also implied that abdominal pressure was not involved in initiating or sustaining micturition. Von Garrelts performed these measurements with the patient in the erect position.

Murphy and Schoenberg (1960) investigated patients in the supine position and determined pressures in the range 20 cm H<sub>2</sub>O to 115 cm H<sub>2</sub>O in patients with obstruction. Most of the patients were children. Suprapubic catheterisation was used by Sandøe and Bryndorf (1960) and Gertz (1960). In patients with no indication of obstruction, the bladder pressures during micturition ranged between 34 cm H<sub>2</sub>O and 90 cm H<sub>2</sub>O. Bryndorf and Sandøe (1960) investigated nineteen male patients and obtained an average bladder pressure of 67 cm H<sub>2</sub>O with the pressure ranging between 50 cm H<sub>2</sub>O and 80 cm H<sub>2</sub>O for a group of normal patients. In five patients with urethral strictures the pressures

were much higher lying between 140 cm H<sub>2</sub>O and 175 cm H<sub>2</sub>O. Normal female patients were investigated by Sinner and Paquin (1963) and the bladder pressure found to lie between 18 cm H<sub>2</sub>O and 64 cm H<sub>2</sub>O. Backmann (1966) studying fifteen normal women found the voiding pressure to lie in the range 30 cm H<sub>2</sub>O to 112 cm H<sub>2</sub>O.

In the studies of Gleason and Lattimer (1962), the maximum voiding pressure ranged between 30 cm H<sub>2</sub>O and 139 cm H<sub>2</sub>O in ten children, whilst in seven adults the pressure lay between 55 and 101 cm H<sub>2</sub>O. Arbuckle and Paquin (1963) obtained a mean voiding pressure of between 43 and 60 cm H<sub>2</sub>O, depending on the bladder volume, in twenty-seven female subjects. The smaller the volumes voided, the larger the pressures. In one healthy male subject Cardus, Guesada and Scott (1963) obtained a pressure at peak flow-rate of 56.7 cm H<sub>2</sub>O. Rasmussen, Sandøe, Zachariae (1964) found the pressure to vary between 57 cm H<sub>2</sub>O and 106 cm H<sub>2</sub>O whilst in a group of patients with prostatic hyperplasia, the pressure was in the range 72 cm H<sub>2</sub>O to 120 cm H<sub>2</sub>O. A group of patients suffering from neurological bladder dysfunction developed pressures between 30 cm H<sub>2</sub>O and 82 cm H<sub>2</sub>O. Whittaker, Johnston and Lawson (1969) found an average bladder pressure of 68 cm H<sub>2</sub>O. The male group had an average value of 85 cm H<sub>2</sub>O whilst the female group had an average value of 59 cm H<sub>2</sub>O. These results refer to children.

The "after contraction" observed by Denny Brown and Robertson (1933) was also observed by Arbuckle and Paquin (1963). The aftercontraction occurred during the terminal part of voiding in

some patients whilst in others it occurred after the flow had ceased. This phenomenon was observed in twenty-four per cent of the female patients. The magnitude of the contraction was small. The pressure increase was thought to be due to the result of the urethral smooth muscle contraction prior to termination of voiding. Rasmussen, Sandøe and Zachariae (1964) observed an aftercontraction in thirty per cent of their patients when it occurred prior to the termination of voiding. Backman, Von Garrelts and Sundblad (1966) observed the secondary pressure rise in fifty per cent of their patients. Lewin, Culp and Flocks (1967) found that the magnitude of the aftercontraction sometimes exceeded the peak pressure during voiding. Hodgkinson and Morgan (1969) observed "waves of contraction" in the terminal region of voiding. This was frequently associated with abdominal pressure.

Since the bladder is subjected to abdominal pressure variation, the intravesical pressure is the result of the intrinsic pressure produced by the contraction of the detrusor muscle and the external pressures. It is important to differentiate between these two components.

The intravesical pressure changes due to abdominal pressure have been monitored using an intra-gastric balloon by Backman, Von Garrelts and Sundblad (1966). Their investigations implied that, in women, voiding was initiated by increasing the intra-abdominal pressure although young women did not rely so much on the use of intra-abdominal pressure. Hodgkinson and Morgan (1969) measured the abdominal pressure fluctuations using a balloon inserted into the

rectum. They confirmed the results of Backman, Von Garrelts and Sundblad. Hodgkinson and Morgan calculated that the abdominal pressure on initiation of micturition ranged from thirty per cent to one hundred per cent of the total intravesical pressure.

The magnitude of the intravesical pressure must determine to some extent the urine flowrate developed during micturition. In the last twenty years, methods for measuring urine flowrate have been developed.

In 1948, Drake described a method of measuring urine flowrate based on the weight of urine voided. The weight of the urine on a spring assembly was fed to a kymograph.. He considered a flowrate of 20 ml/sec as normal. In a study on one patient, the flowrate was found to remain relatively constant on different voidings. The flowrate was also found to be smaller when the volume voided was reduced. Kouffman (1961) using a flowmeter working on the same principle as Drakes, made a large number of determinations of urine flowrate. The average flowrate was found to be 31.4 ml/sec in females and 28 ml/sec in males.

A new method of measuring urine flowrate was developed by Von Garrelts (1956). In this method, the flow was directed into a cylinder of uniform diameter and the pressure at the base of the cylinder continuously measured by means of a pressure transducer. The voltage output from the pressure transducer was differentiated electronically and so the flowrate could be determined as a function of time. Von Garrelts (1957) also found that in individual patients the flowrate tended to increase as the volume voided

increased. Holm (1962) devised a flowmeter which operated by displacing air, the volume of which was measured using an anaesthetic gas flowmeter. Cardus, Quesada and Scott (1963) used an electromagnetic flowmeter to measure urine flowrate. Although sensitive to flow, this method is open to many artefacts. If the flowrate is impeded by the flowmeter then the true patient flowrate will not be recorded whilst if the flowmeter cavity is too large, air will be trapped thus giving spurious data. The output from the flowmeter is dependent on the flowrate profile so that if it is calibrated using laminar flow the same flow under turbulent conditions will give a different result. Arbuckle and Paquin (1963), using Von Garrelts' method, determined the average peak flowrate developed in a group of normal females to be 22 ml/sec when the bladder volume was in the range 300 to 500 ml. They also observed a tendency for there to be a slight decrease in the peak flowrate as the volume voided decreased. Rasmussen, Sandøe and Zachariae (1964) obtained a peak flowrate between 11 ml/sec and 25 ml/sec in normal male patients. The patients with prostatic hyperplasia were also investigated and found to develop peak flowrates less than 12 ml/sec. The majority of the latter group developed flowrates less than 5 ml/sec. Smith (1964) obtained peak flowrates between 19.3 ml/sec and 50.0 ml/sec in ten "normal" females.

Palm (1966) developed a flowmeter similar to the one used by Holm (1962) in which the displaced air flow was measured using a constant temperature hot wire anemometer. This flowmeter was also

used by Krøigard (1970) in his study of a group of children. The children in the age range 4 - 12 years developed peak flows between 10 ml/sec and 28 ml/sec. There was a tendency for the peak flow to increase with age.

Whittaker, Johnston and Lawson (1969) determined the peak flowrate in two groups of control patients. The male group developed an average peak flow of 18.5 ml/sec whilst the group of girls developed a peak flow of 28.3. There was no significant difference in the groups of control patients compared with groups of patients exhibiting vesical-ureteric reflux.

There has been very little pressure flow data on groups of patients reported in the literature and it is therefore difficult to define the flowrates which one would expect from normal patients.

Residual urine is a parameter of some importance and is frequently estimated in urological laboratories using catheterisation techniques. The residual urine has also been estimated using intravenous urography and measuring with a planimeter the area of the contrast area on an X-ray film taken immediately after micturition (Hershman (1960) Klosterhalfen and Boeminghaus (1960)). Cotran and Cass (1958), Smith (1960), Jarvinen and Vastiainen (1963) injected phenolsulfonftalein intravenously. Assuming that most of the dye had been excreted in the urine within three hours, then by determining the quantity of phenolsulfonftalein voided after micturition the residual urine could then be calculated. Barnes and O'Hara (1961) and Mulrow, Huvas and Buchanan (1961)

used an intravenous injection of  $I^{131}$  labelled Diodrast for the determination of residual urine. A shielded scintillation counter was positioned over the bladder prior to micturition and the countrate determined. After voiding, the countrate was again measured. On subtracting the background, they determined the residual activity in the bladder. These results were subject to errors due to blood activity. Lindbjerg and Brandt (1964) employed a similar technique using  $I^{131}$  labelled Hippuran in place of Diodrast. They estimated the blood background after micturition by counting over the precordium. They obtained an error of the order of 25 ml between the estimated residual and the volume withdrawn via a catheter for volumes less than 200 ml. Shand, MacKenzie et al (1968) also used  $I^{131}$  labelled Hippuran for residual volume estimation but used a count over the umbilicus as a correction for blood background after micturition. They concluded that the residual urine in five normal males was less than 1 ml. Vahala, Koskela and Kokkonen (1969) using  $I^{131}$  labelled Hippuran found that in patients with small residual volumes, the differences between the calculated residuals and the volumes aspirated via the catheter were considerable. These methods all depend on adequate renal function.

Winter (1964) and Strauss and Blaufox (1969) have also used the clearance of the  $I^{131}$  labelled Hippuran from the bladder during micturition to estimate the average urine flowrate. The results however were subject to large errors due to the very low countrates obtained prior to micturition (less than 400

counts/sec). The counters were also positioned very close to the bladder so that any bladder movement would cause large errors in the clearance profile.

The measurements of bladder pressure, urine flowrate and residual urine by themselves do not supply sufficient understanding of the lower urinary tract. With this aim in view various derived parameters have been used. Assuming laminar flow in the urethra, then the pressure loss is proportional to the urine flowrate (Schlichting (1955)). Gleason and Lattimer (1962), Pierce, Braun et al (1963) calculated the resistance of the urethra as being  $\frac{P_{BL}}{Q}$  where  $P_{BL}$  = the bladder pressure at peak urine flowrate, and  $Q$  = peak flowrate. Claridge and Shuttleworth (1964) assumed turbulent flow to occur and estimated the resistance using the ratio  $\frac{P}{Q^2}$ . The pressure  $P$  was obtained by subtracting the abdominal pressure from the bladder pressure. They obtained values for the resistance lying between 0.2 and 97.5 in patients with obstruction but thought that a value of 0.4 was the upper limit for the resistance in normal persons.

Considering the urethra as a rigid tube of circular cross-section and uniform diameter, Ritter, Zinner and Paquin (1964) calculated the equivalent diameter for normal females to have a mean value of 2.7 mm. Backmann (1966) calculated a mean value of 3.0 mm in a group of normal females. In a large group of normal female patients, Smith (1968) calculated resistance indices in the range 0.01 to 0.28 cm  $H_2O/ml^2/sec^2$ . He also calculated the equivalent diameters and found them to lie between

1.8 mm and 4.2 mm for a group of obstructed and non-obstructed patients.

Smith (1968) measured the exit energy of the stream using an open ended catheter inserted into the urethra just beyond the external urethral meatus. This measurement was performed simultaneously with the measurement of bladder pressure and urine flowrate. Knowledge of the exist energy  $P_E$  allowed Smith to calculate the urethral resistance using the formula -

$$R_f = \frac{P_{BL} - P_E}{Q^2}$$

This measurement was considered by Smith to be difficult and not always reliable. Whittaker and Johnston (1966) developed a  $P_E$  meter. The meter consisted of a fluid sensitive tambour which measured the force of the urinary stream as it left the urethra. This determination therefore also allowed Whittaker and Johnston to calculate the resistance factor  $R_f$ . In a large group of children, Whittaker and Johnston (1969) found no significant difference for the resistance factor  $R_f$  between male and female children, or children with and without reflux. Whittaker and Johnston (1968) attempted to correlate the resistance  $R_f$  with radiographic findings. Patients exhibiting conical and cylindrical urethral profiles were found to have resistances between 0.0135 mm Hg/ml<sup>2</sup>/sec<sup>2</sup> and 0.048 mm Hg/ml<sup>2</sup>/sec<sup>2</sup>. Those urethras showing narrowing, for example, string urethras and those with bladder neck narrowing were found to have resistances significantly higher than the first two groups, with values lying in the range 0.08 mm Hg/ml<sup>2</sup>/sec<sup>2</sup> to 0.135 mm Hg/ml<sup>2</sup>/sec<sup>2</sup>. They suggested that 0.07

mm Hg/ml<sup>2</sup>/sec<sup>2</sup> was the upper limit for normal patients.

Gleason and Bottaccini (1968) and Eyrick, Many and Wise (1969) have segmented the urethral profile obtained using radiography and calculated the energy loss due to the profile change along the urethral length. The frictional losses determined using this method were, as expected, much less than those obtained considering the urethra to be a uniform rigid tube of circular cross-section. On the basis of their results, and observing that the exit diameter of the urethra on radiography was of the order of 2 mm to 3 mm, Gleason and Bottaccini concluded that the distal urethral segment controlled the flowrate developed in the urethra.

In order to interrelate the hydrodynamic variables without model dependence, Von Garrelts (1957) investigated the numerical dependence of the peak flowrate on the volume voided. He found good correlation between these two variables in an individual patient with the peak flowrate increasing as the volume voided increased. The peak flowrate was proportional to the volume voided to the power 0.7. The data from a group of patients with no evidence of urological disorders also showed good correlation. Backmann (1965) did not obtain such a good correlation between the peak flowrate and the volume voided for groups of normal women. Gleason and Lattimer (1967) found no correlation between the peak flowrate and the corresponding intravesical pressure or between the intravesical pressure and the volume voided. They, however, corroborated Von Garrelts' finding (1967) that there was a

correlation between the volume voided and the peak urine flowrate.

The hydrodynamic investigations reported have not yet allowed consistent criteria to be determined which may prove useful in the diagnosis of disorders of the lower urinary tract. The range of values of derived parameters such as the resistance and the equivalent rigid tube diameter obtained for normal patients, do not exclude values obtained from patients who clinically are obstructive or incontinent.

CHAPTER 2Measurement Technique

2.1 In order to investigate the lower urinary tract from a fluid dynamical aspect and its relation to urinary disorders it is necessary to be able to measure several variables independently.

The variables measured in the present studies were -

1. intravesical pressure :  $P_{BL}$  cm  $H_2O$
2. abdominal pressure :  $P_{ABD}$  cm  $H_2O$
3. urine flowrate :  $Q$  ml/sec
4. residual Urine :  $V_{RES}$  ml

The primary data from which these variables were determined were recorded on an Ampex 7-channel instrumentation tape recorder using the FM recording mode.

## 2.2 Bladder Pressure

The intravesical pressure is measured using a semiconductor strain gauge pressure transducer connected to the bladder via a suprapubic catheter. In these studies, it was felt that it was important not to interfere with the urethra directly if possible, since the resulting irritation could cause non-typical flow dynamics in the subject being investigated. It is also believed by the author that the use of a transurethral catheter for the measurement of intravesical pressure would cause a distortion of the fluid flow in the urethra during micturition. Since the frictional loss is inversely proportional to the diameter to the power 4.75 in a uniform rigid tube of circular cross-section (Chapter 3), it would seem that the use of a transurethral catheter,

which would be of outer diameter approximately that of the narrowest part of the normal female urethra, would significantly increase the resistance of the urethra to flow if the urethra were rigid. Since the urethra is not rigid it will tend to distend. The frictional loss will also increase since there is now more than one surface in contact with the fluid in the urethra. Von Garrelts (1957) used three catheters of different external diameters but the same internal diameters to measure the intravesical pressure prior to and during micturition in order to assess the effects of the outer diameter of the catheter. The same patient was investigated three times but with a different catheter in position on each occasion. Von Garrelts found no significant difference in the pressure profiles obtained. The catheters used were of internal diameter 0.38 mm and the outer diameters were 1.09 mm, 1.57 mm and 4.9 mm. The bladder pressures at maximum flowrate as obtained by Von Garrelts seem to be constant. This investigation does not imply that a transurethral catheter does not influence the flow in the urethra. Since in obstructed flow the flowrate is not only a function of the bladder pressure which can be developed, different degrees of obstruction will modify the flowrate even though the bladder pressure may remain approximately constant. Gleason and Lattimer (1962) reported, without much supporting evidence, that in their studies the flowrate was not impaired by transurethral catheterisation (catheter of outer diameter 1 mm), but that the bladder pressure may have been.

## 2.3

Ritter and his associates (1964) developed a flowrate of 18 ml/sec in a rigid tube with an internal diameter of 3.2 mm at a pressure of 40 mm Hg with a catheter of outer diameter 1.27 mm in position. The catheter was then removed and at the same pressure the flowrate increased to 24 ml/sec. This experiment shows effectively the significant differences which may result in the use of transurethral catheters. In the present studies a Number 11 suprapubic catheter was inserted into the bladder using the method developed by Sandøe, Bryndorf, Gertz (1959). Local anaesthetic was used. The catheter was connected to a semiconductor strain gauge pressure transducer which was used in conjunction with a pressure preamplifier. The voltage output was recorded on the instrumentation tape recorder. Prior to the clinical study, a 50 cm H<sub>2</sub>O pressure calibration was recorded on the tape recorder for subsequent analysis of the bladder pressure data.

### 2.3 Abdominal Pressure

The most common method of measuring abdominal pressure is to measure the pressure fluctuations in the rectum using a fluid filled balloon connected to a pressure transducer. This method has several disadvantages:-

1. It will measure non-abdominal pressure variation.
2. The recording position of the balloon may change.
3. The rectum has to be emptied.

It was desirable to measure abdominal pressure in the patients investigated in order to ascertain whether abdominal straining

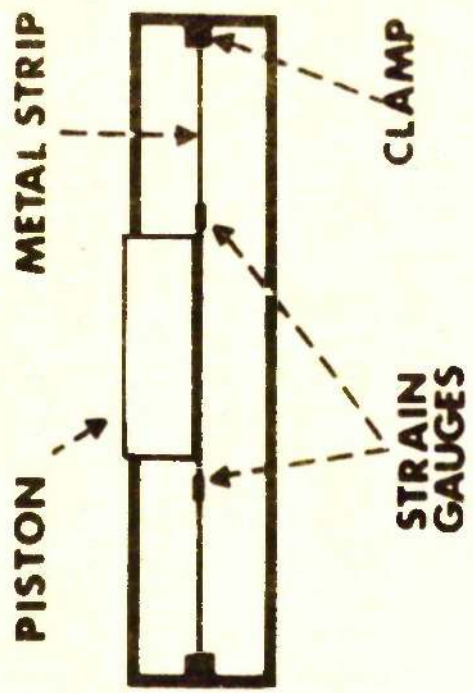


**FIG 2.1**

occurred prior to or during micturition.

The technique used in these studies is based on a device developed by Smythe (1957) called a Tochodynamometer.

If we consider a bubble, then -

$$\Delta p = \frac{2T}{R}$$

where  $\Delta p$  = pressure difference across the bubble surface,  $T$  = tension and  $R$  = radius of the bubble.

Thus as  $\frac{T}{R} \rightarrow 0$ ,  $\Delta p \rightarrow 0$ , i.e., pressure fluctuations are transmitted normally through a flat elastic surface.

The tochodynamometer, Figure 2.1, consists of a piston which is attached normally to a metal strip to which are attached strain sensors. Any pressure acting on the piston strains the metal strip. The magnitude of the strain is measured via the strain sensors.

A tochodynamometer was constructed using semiconductor strain gauges. These give a much higher electrical output than the sensors used in the original article so that it is possible to use a less "elastic" metal. The main reason for this is so that any deformation will be well within the elastic limit of the material resulting in a more linear output. Several gauges were used for temperature compensation. It is possible to obtain hysteresis if the piston is unable to return to its equilibrium position due to friction with the side of tochodynamometer. This will also limit its frequency response. Hysteresis was insignificant in the device used.

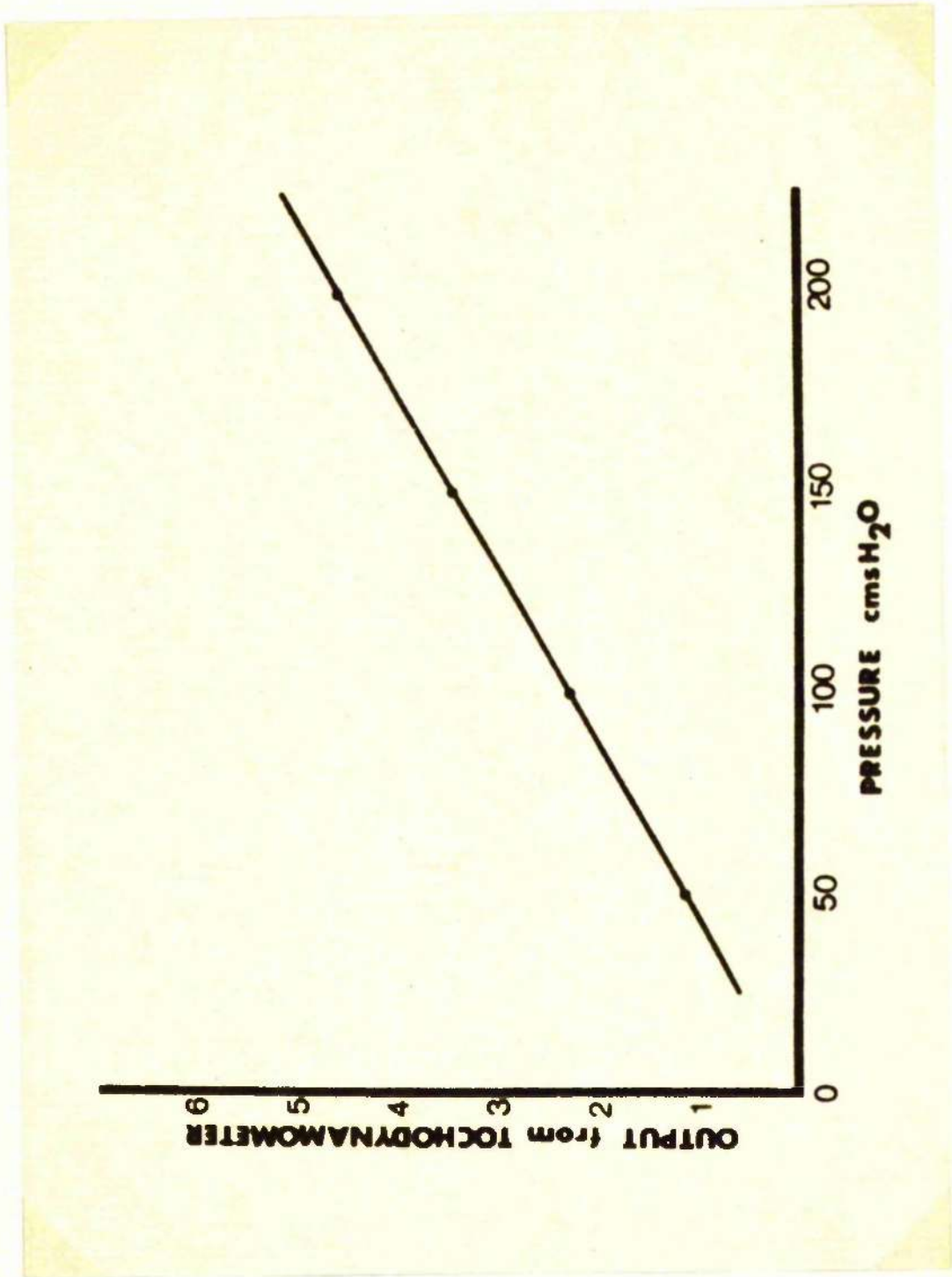


Fig. 2.2

The linearity of the device was investigated by applying different weights to the piston and measuring the output from the strain gauges. The results are shown in Figure 2.2.

The device was linear within the range 0 - 200 cm H<sub>2</sub>O. The pressure was calculated using the equation -

$$P = \frac{W}{A}$$

where  $W$  = weight on the piston and  $A$  = area of the piston.

It is imperative that the surface on which the piston sits is flat and so a plate was constructed which fits over the device and two straps, fitted with Velcro adhesive tape, were attached. When used clinically, the tochodynamometer was strapped tightly to the patient in the region of the umbilicus, and the patient asked to cough in order to ensure that the abdominal pressure was being transmitted. It should be pointed out that this device is capable only of measuring changes in abdominal pressure. The tochodynamometer is calibrated with a known weight, the calibration being recorded on the tape recorder.

It was sometimes found that the calibration of the tochodynamometer appeared to be incorrect, since the variations in intravesical pressure which were certainly abdominal were not completely accounted for by the abdominal pressure variations obtained. This is probably due to the fact that the abdominal pressure variations were not transmitted completely through the tissue. In these cases, the calibration of the abdominal pressure transducer was altered until the variations in abdominal pressure cancelled out the

obvious abdominal pressure variations in the resting intravesical pressure prior to micturition. This is justifiable since we are looking for changes during micturition. It is also possible to position the transducer incorrectly so that it is not completely sited on the abdominal cavity. If this were the case, it would be impossible to obtain the calibration factor since the observed variations from the tochodynamometer would be dependent on the magnitude of the abdominal pressure (the piston would no longer be effectively 'flat' as the abdominal pressure changed). The absolute accuracy, therefore, of the measurements of abdominal pressure is limited although it is useful clinically.

#### 2.4 Urine Flowrate

A technique for the measurement of urine flowrate simultaneously with intravesical pressure has been developed. This method is based on the clearance of a radioactive isotope instilled into the bladder prior to micturition. This technique also permits the measurement of residual urine. It is not possible with the apparatus used to ascertain the nature of the residual volume, i.e., whether it is true residual in the bladder or whether it is refluxed volume. The radioactive isotope used in these studies was Technetium 99 m. This particular isotope was chosen for several reasons -

1. Minimal radiation hazard to the patient.
2. The gamma radiation (130 Kev) easily detectable.
3. Short half-life - 6 hours.
4. It is possible to administer highly active

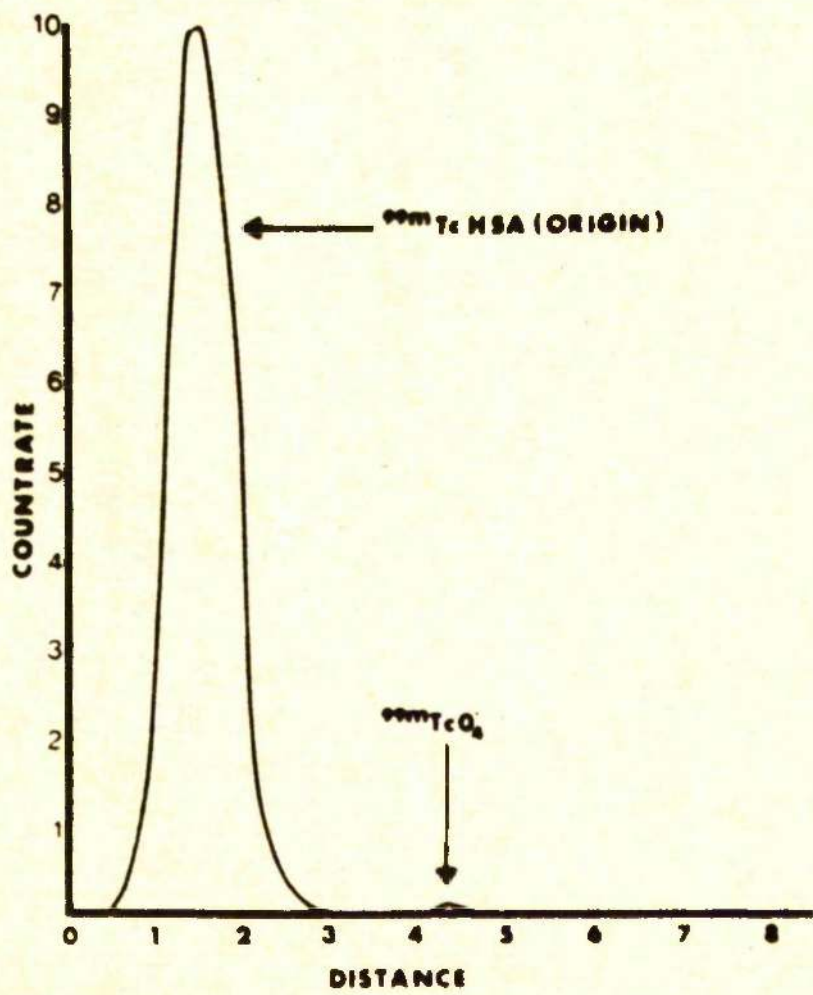


FIG 23

solutions thus obtaining high concentrations.

The technetium is normally dispensed in the form of pertechnetate ion  $TcO_4^-$ . In initial trials with dogs it was found that the pertechnetate ion readily diffused into the bladder tissue. This would lead to errors in the calculation of urine flowrate and residual urine if the rate of diffusion were sufficiently high. In order to reduce this effect, it was decided to label the protein molecule, human serum albumin with the pertechnetate ion. The method originally used to label the protein was that developed by Stern (1965). This method was found to be unpredictable with yields of labelled protein lying between nil and 30 per cent. The technique was modified by Gwyther and Field (1966) and the results obtained by the author using this technique were far superior with yields consistently lying in the range 70 - 90 per cent. Any free pertechnetate was removed by passing the solution through a column of Amberlite IRA400 ( $Cl^-$ ). The resulting solution of the pertechnetate labelled human serum albumin obtained using the latter technique was analysed for any free pertechnetate ion using thin layer chromatography. Figure 23 shows the distribution of the isotope on the chromatogram obtained using a chromatogram gamma scanner. The free technetium was less than 1 per cent of total labelled activity.

In order to check the stability of the labelled protein ascending thin layer chromatography was performed using an acetic acid/butanol solvent. Acetate buffers were prepared at pEs of 3, 4, 5, 6 and added to samples of the labelled protein. The

| <b>PH</b> | <b>% DISSOCIATION</b> |
|-----------|-----------------------|
| 3.0       | ↙ 1.0                 |
| 4.0       | ↙ 1.0                 |
| 5.0       | ↙ 1.0                 |
| 6.0       | ↙ 1.0                 |
| 7.4       | ↙ 1.0                 |

**FIG 2.4**

buffered labelled protein was allowed to stand for 1 hour to 4 hours at room temperature before performing the thin layer chromatography. The resultant chromatograms were then scanned with the chromatogram scanner, a run being performed with the pertechnetate ion only in order to determine its position on the chromatogram. The procedure was also performed using buffered solutions which had been left to stand for one hour at body temperature. It was then possible to calculate the degree of dissociation by comparing the count rate of the labelled protein band with the count rate due to the free pertechnetate. Negligible dissociation was found to occur under the conditions investigated. Figure 2.4 shows the percentage dissociations obtained.

Prior to the clinical investigations, the labelled protein is kept at a pH of 3.0 at which negligible dissociation occurs. A few minutes prior to use, the labelled protein is added to saline at body temperature bringing the pH up to about 6, at which point it is instilled into the patient's bladder. Thus the labelled complex is at a pH of 6 for a maximum period of 20 minutes during which time the dissociation is insignificant.

## 2.5 Theory

The isotope is instilled into the bladder prior to micturition. During voiding, this bladder volume decreases and so the bladder behaves effectively as a deflating sphere. It is therefore necessary to investigate the effects of changing self-absorption of the radiation in the sphere during deflation.

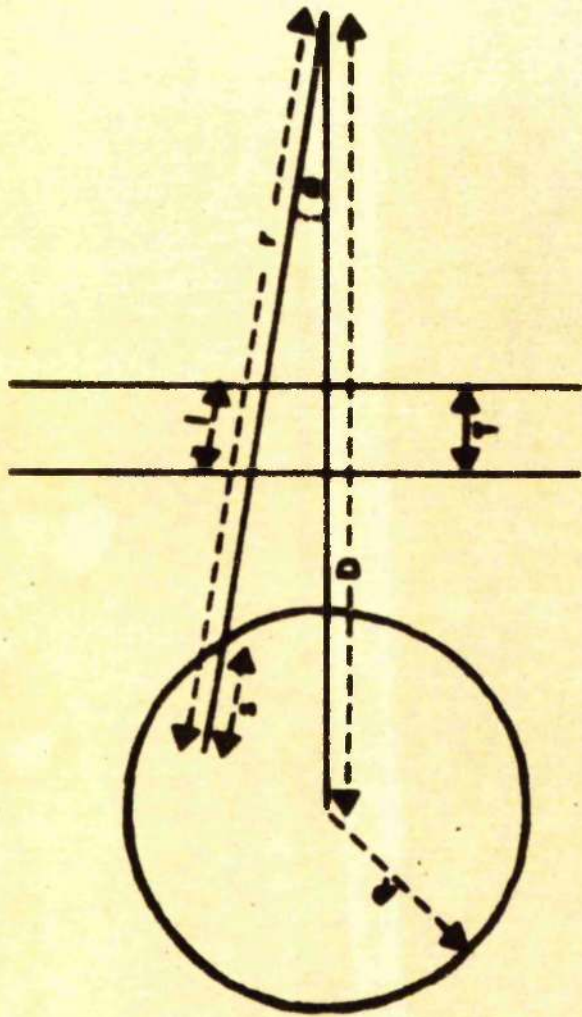


FIG 2.5

The subsequent theory permits the calculation of the dose rate at some point outside the sphere and separated from the sphere by an air gap and a wedge of tissue. Also, only monoenergetic gamma radiation is considered and so any dose due to scattered radiation is not taken into account. Referring to Figure 2.5, the dose rate at some point external to the sphere due to an infinitesimal volume  $\delta V$  of isotope is given by

$$d\dot{\mathcal{D}} = \frac{kc}{r^2} e^{-[\mu_1(s+1) + \frac{\mu_1}{\mu_2}(r-s)]} \delta V \quad 2.1$$

where  $k$  = specific gamma-ray emission of the source,  $c$  = specific activity,  $\mu_1$  = linear absorption coefficient of the fluid inside the sphere,  $l$  = length of tissue through which the radiation is passing, modified to equivalent length of fluid,  $r$  = distance of  $\delta V$  from the point,  $s$  = the length of  $r$  inside the sphere,  $\mu_2$  = linear absorption coefficient of air,  $D$  = distance of point from centre of sphere.

Since  $\mu_1 \gg \mu_2$  when the fluid inside the sphere is water, equation 2.1 tends to

$$\dot{\mathcal{D}}_d = \frac{kc}{r^2} e^{-[\mu_1(s+1)]} \delta V$$

If  $\dot{\mathcal{D}}$  = dose rate at the point distant  $D$  from centre of the sphere, then -

$$\dot{\mathcal{D}} = kc \int_V \frac{1}{r^2} e^{-[\mu_1(s+1)]} \delta V$$

where

$$\delta V = 2\pi r^2 \sin \theta \delta \theta \delta r$$

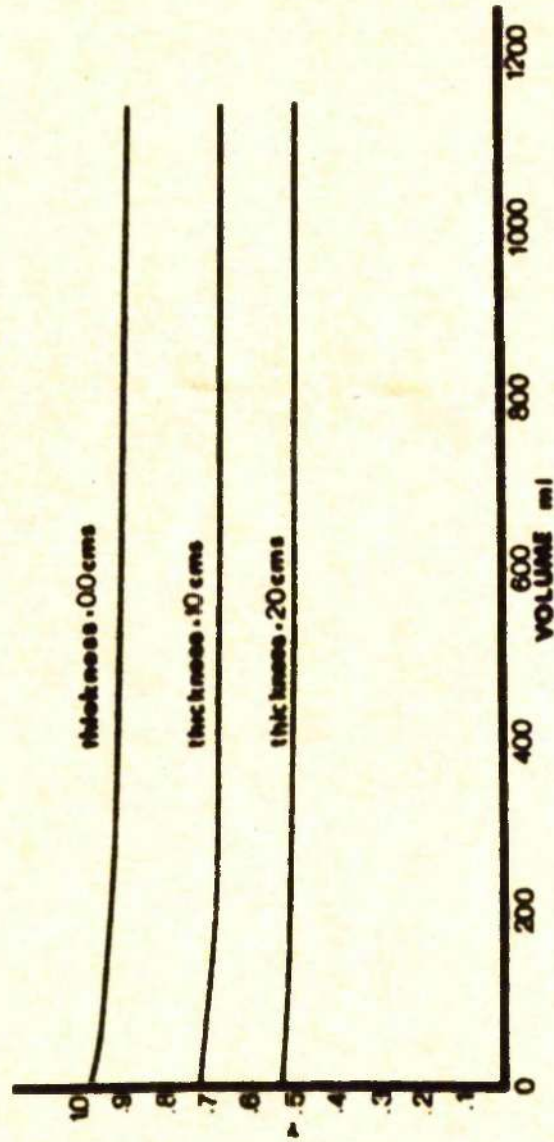


FIG 2.6

The integral is normalised by dividing by the dose rate which would be obtained at the point if there were zero absorption and the source were concentrated at the centre of the sphere. If this is denoted by  $\gamma_N$ , then -

$$\gamma_N = \frac{2\pi k c \int_V e^{-\mu(1+s)} \sin \theta \, d\theta \, dr}{\frac{(4\pi R^3 k c)}{3D^2}}$$

Therefore -

$$\gamma_N = \frac{3D^2}{2R^3} \int_V e^{-\mu(1+s)} \sin \theta \, d\theta \, dr$$

Using the substitution

$$u = \frac{(R^2 - D^2 \sin^2 \theta)^{1/2}}{2}$$

and observing that -

$$r = s + D \cos \theta = (R^2 - D^2 \sin^2 \theta)^{1/2}$$

and

$$1 = \frac{T}{X}$$

where  $T$  = thickness of tissue converted to "equivalent thickness of the fluid" for the  $\gamma$  radiation and  $X = \cos \theta$

$$\gamma_N = \frac{3D^2}{R^2} \int_0^1 \sqrt{1 - \frac{T}{X}} e^{-\mu(2Xu + \frac{T}{X})} du$$

A digital computer programme was written to perform the integration. The variation of  $\gamma_N$  with  $R$  volume is shown in Figure 2.6. The effects of the thickness  $T$  are also shown.

Now, suppose -

$I'$  = intensity measured at a distance  $d$  from the centre

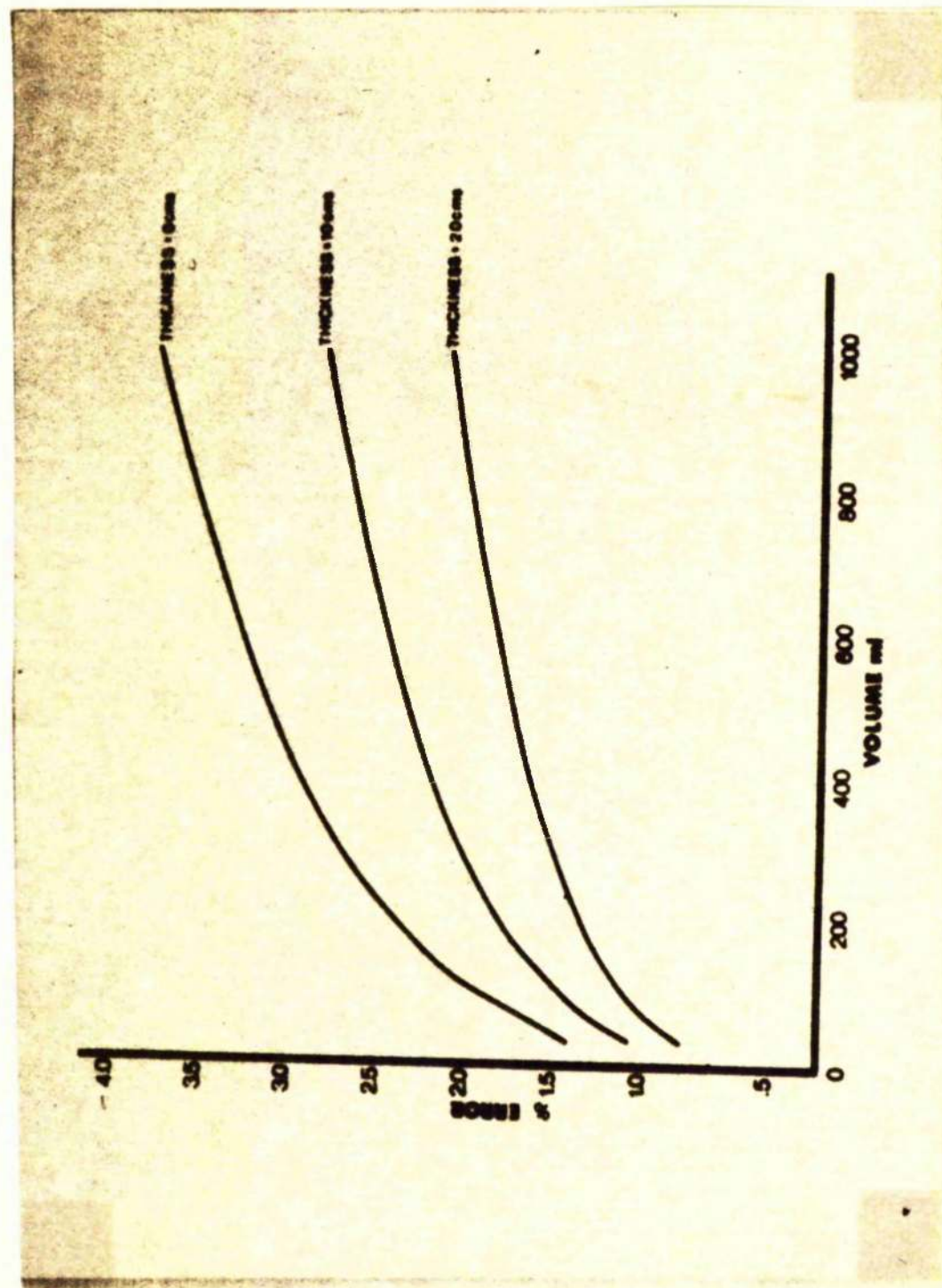


Fig. 2.7

of the sphere (bladder)

$I'_0$  = specific intensity

$I$  = intensity which would be observed if all the activity were concentrated at the centre of the sphere i.e. a point source with zero absorption,

then,

$$\begin{aligned}\gamma_N &= \frac{I'}{I} \\ I' &= \gamma_N I \\ &= I_0 \gamma_N V \quad 2.2\end{aligned}$$

where  $V$  = volume in the bladder.

Then -

$$\frac{dI'}{dt} = I_0 \gamma_N \left[ -Q + \frac{V}{dR} \frac{d\gamma_N}{dt} \right]$$

where  $Q$  = the flowrate.

Since

$$V = \frac{4}{3} \pi R^3$$

that is -

$$\frac{dV}{dt} = -Q = + 4 \pi R^2 \frac{dR}{dt}$$

Hence,

$$\begin{aligned}\frac{1}{I_0} \frac{dI'}{dt} &= -Q - \frac{V}{\gamma_N 4 \pi R^2} \frac{d\gamma_N}{dR} \\ &= -Q \left[ 1 + \frac{R}{3\gamma_N} \frac{d\gamma_N}{dR} \right]\end{aligned}$$

The variation of this error  $\frac{R}{3\gamma_N} \frac{d\gamma_N}{dR}$  with volume is shown in Figure 2.7 for various thicknesses of tissue.

From equation 2.2

$$\frac{I'_i}{I'_f} = \frac{\gamma_i V_i}{\gamma_f V_f} \quad 2.3$$

where  $\gamma_i$  = dose rate at distance d initially, i.e. prior to deflation,  $I'_i$  = initial observed intensity from the bladder,  $V_i$  = initial volume in the bladder,  $I'_f$  = observed intensity from bladder at some time t during or after micturition,  $V_f$  = volume in bladder at time t,  $\gamma_f$  = dose rate at distance d at time t.

If VO = volume voided at time t

$$\begin{aligned} V_i &= VO + V_f \\ &= VO + \frac{\gamma_i}{\gamma_f} \frac{I'_f}{I'_i} V_i \end{aligned}$$

Therefore,

$$V_i = VO \sqrt{\frac{1 - \gamma_i I'_f}{\gamma_f I'_i}}$$

and  $V_{RES} = V_i - VO$

Therefore,

$$V_i = \frac{\gamma_i I'_f}{\gamma_f I'_i} \sqrt{\frac{1 - \gamma_i I'_f}{\gamma_f I'_i}} VO$$

If  $\frac{\gamma_i}{\gamma_f} \approx 1.0$ , then

$$V_{RES} = \frac{I'_f}{I'_i} \sqrt{\frac{1 - I'_f}{I'_i}} VO \quad 2.4$$

This is the formula used in practice to calculate the residual urine.

If  $V_{i\text{calc}}$  = calculated initial volume in the bladder, then

since the change in absorption is ignored in practice

$$V_{\text{icalc}} = V_0 \left[ 1 - \frac{I'_f}{I'_i} \right]$$

that is,

$$V_{\text{icalc}} = \frac{\left[ 1 - \frac{I'_f}{I'_i} \right]}{\left[ 1 - \frac{\delta_i I'_f}{\delta_f I'_i} \right]} V_i \quad 2.5$$

Since

$$Q = - \frac{V_i}{I'_i} \frac{dI'_i}{dt} \frac{1}{\left[ 1 + \frac{R}{3\delta_f} \frac{d\delta_f}{dR} \right]}$$

then

$$Q = - \frac{dI'_i}{dt} \frac{V_i}{\left[ 1 + \frac{R}{3\delta_f} \frac{d\delta_f}{dR} \right]} \frac{1}{I'_i}$$

that is,

$$\begin{aligned} Q &= - \frac{V_{\text{icalc}}}{I'_i} \frac{dI'_i}{dt} \frac{\left[ 1 - \frac{\delta_i I'_f}{\delta_f I'_i} \right]}{\left[ 1 + \frac{R}{3\delta_f} \frac{d\delta_f}{dR} \right] \left[ 1 - \frac{I'_f}{I'_i} \right]} \\ &= - \frac{V_{\text{icalc}}}{I'_i} \frac{dI'_i}{dt} \end{aligned}$$

In the practical routine calculation the assumption that  $\epsilon = 1$  is made. Hence, the error involved is

$$\text{Error} = (1 - \epsilon) \times 100\%$$

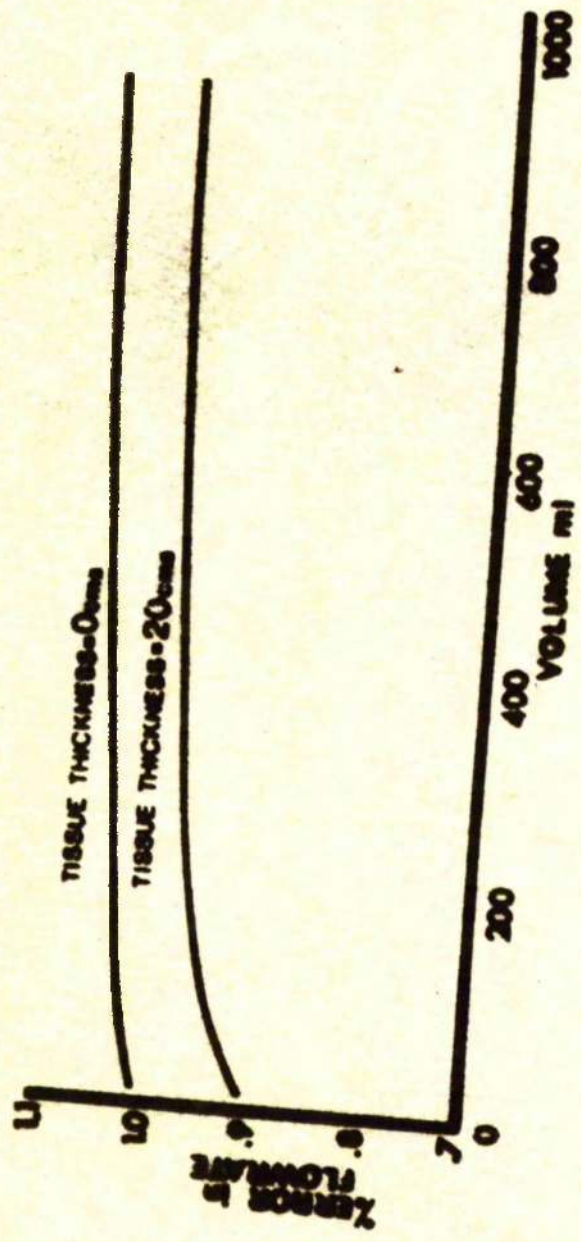


FIG 2.8

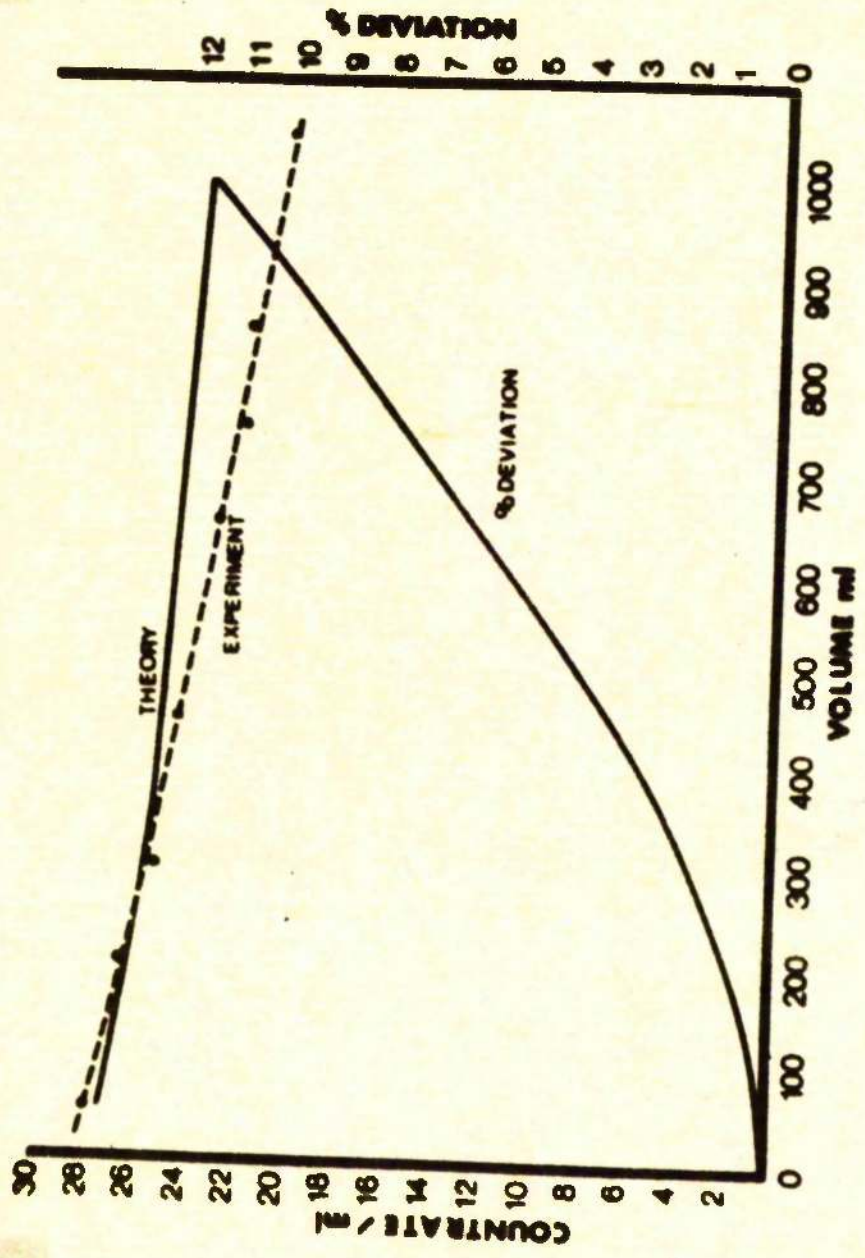


FIG 2.9

Using the data resulting from the analysis of the integral for  $\chi_N$ , this error can be computed. These errors are shown in Figure 2.8 for different thicknesses of tissue.

The analysis is dependent on the shape of the volume, the values used for  $\chi_N$  and  $\frac{d\chi_N}{dR}$  being for spherical volumes only. However, the fact that the errors involved are small and that the bladder is not greatly non-spherical, the conclusions to be drawn from the results can be regarded as reasonably accurate. Thus, according to the theory for spherical sources, the error in flow-rate is of the order of 1 per cent and the error in residual  $<10$  per cent for normal physiological volumes, the accuracy of the latter increasing as the residual increases.

In order to check the effects of self absorption, a balloon was filled with a solution of pertechnetate in increments of 50 ml. The centre of the balloon was positioned 75 cm from a sodium iodide scintillation counter connected to a pulse height analyser timer-scaler which was calibrated on the  $Tc^{99m}$  photopeak. The counts over a period of 60 seconds were measured for each increment of 50 ml of the pertechnetate solution instilled into the balloon. The countrate/ml was then calculated at each increment and corrected for decay. The results obtained are shown in Figure 2.9. These results were then compared with the theoretical predictions using equation 2.1. The comparison is shown also in Figure 2.9. It can be seen that the theoretical and experimental results agree to within 10 per cent for volumes up to 300 ml.

The dose-rate on the surface of the sphere can be approximated

by the equation --

$$D = 2\pi k\alpha R$$

where  $R$  = the radius of the bladder.

Thus, for 5 mCi  $Tc^{99m}$  labelled human serum albumin in 300 ml saline, the dose rate to the surface of the bladder is approximately 100 mrad/30 mins. This is the activity used in the clinical study. If it was found necessary to increase the volume in the patient's bladder, extra saline was added so that the specific activity decreases. This results in a lower dose rate. If the patient is unable to accept the full 300 ml then, although the specific activity is the same, the total activity is less than 5 mCi resulting in a lower dose rate. Thus, in all cases, the maximum dose rate to the surface of the bladder is less than or equal to 100 mrad/30 mins. The dose rate to the gonads is lower than this but no real estimate can be given since the distance of the gonads from the surface of the bladder is variable from patient to patient.

It is also possible to have errors in the technique due to bladder movement. It has been observed by the author and Hinman et al (1955) using micturition cystography that the bladder falls from its premicturition position by about 2 cm at the onset of micturition. Thus, it is possible that:-

- (a) The reference used to calculate the residual urine, that is, the count rate prior to micturition, may

be in error. If  $D_m$  = the distance of the scintillation detector from the centroid of the bladder prior to micturition,  $D$  = the distance at the onset of micturition, then -

$$D_m^2 = D^2 + h^2$$

where  $h$  = the distance moved by the bladder. Thus for  $D \approx 60$  cm and  $h \approx 3$  cm, then the error in the reference is of the order of 0.5 per cent. This error is therefore negligible.

- (b) There are errors in the flowrate during the period of movement. It is impossible to quantitate this error since it depends on the rate of movement. When this occurred in practice, comparison of the flowrates determined by the isotope technique and Von Garrelts' technique show that this apparent flowrate (which was not detected by the Von Garrelts' apparatus) was less than 3 ml/sec.

## 2.6 Clinical Technique

The intravesical pressure is measured using a semiconductor strain gauge pressure transducer connected to the bladder via a suprapubic catheter. After the catheter has been inserted, the patient is seated on a specially constructed wooden chair. The chair was designed so that:-

- (a) it would be possible to incorporate a Von Garrelts' apparatus for the measurement of urine flowrate;
- (b) it would be possible to X-ray the patient with

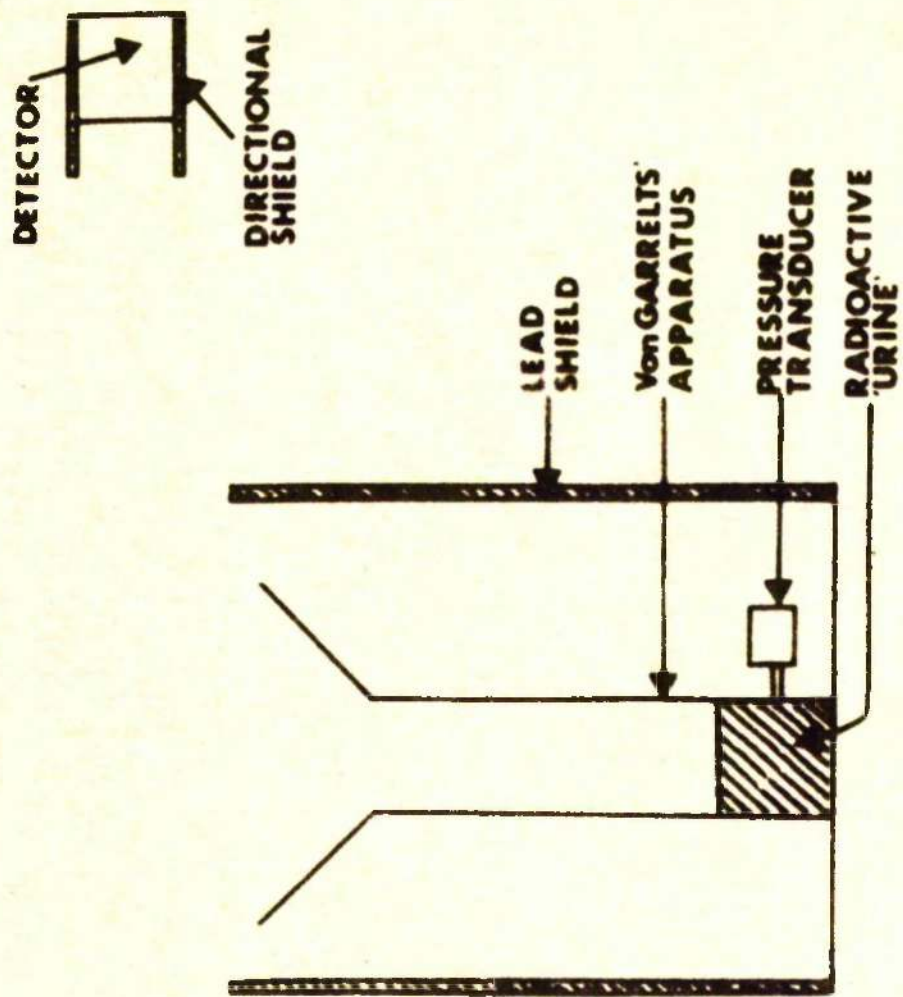


Fig. 2.10

minimal interference from the chair.

In these studies the urine flowrate was measured using both the isotope and Von Garrelts' techniques. The Von Garrelts' apparatus was shielded with lead so that only radiation from the fluid in the bladder would be detected, Figure 2.10.

At this point, the calibrations for the bladder pressure and the abdominal pressure were recorded on separate FM channels of the taperecorder. After catheterisation the patient was seated on the micturition chair. The tochodynamometer was strapped round the patient and positioned near the umbilicus for the measurement of abdominal pressure. 5 mCi of  $Tc^{99m}$  labelled human serum albumin were then dissolved in 300 ml sterile saline and instilled slowly into the patient's bladder via the suprapubic catheter. The solution was instilled in volumes of 50 ml at a rate of 50 ml/2 - 3 mins and the bladder pressure measured after each increment of volume. If the bladder pressure was found to increase rapidly, the rate of filling the bladder was reduced in order to allow the bladder to accommodate more readily to the instilled volume.

If the bladder capacity was greater than 300 ml and the patient could not initiate micturition, saline was instilled into the bladder until the patient could initiate micturition or the bladder capacity was reached. After the bladder was filled, 10 ml saline were flushed through the catheter used for filling in order to remove any residual activity. A sodium iodide scintillation counter fitted with a directional shield was positioned

approximately 3 ft from the patient's bladder which was viewed laterally. The field of view of the detector was of the order of 35 cm. The output from the detector was fed into an amplifier, pulse-height analyser and the pulses due to the  $Tc^{99m}$  photopeak were fed into a ratemeter. The analogue voltage from the ratemeter was fed into an FM channel of the taperecorder.

The bladder pressure, abdominal pressure and the countrate from the bladder were recorded simultaneously on separate FM channels of the taperecorder for two minutes prior to micturition.

The patient was then asked to micturate and the bladder pressure, abdominal pressure, the pressure from the Von Garrelts' flowmeter and the countrate from the bladder were recorded simultaneously on the taperecorder throughout micturition. The variables were also recorded for two minutes after micturition in order to record the residual activity. The residual was then aspirated from the bladder via the suprapubic catheter and the volume measured. The patient was then removed from the field of view of the counter and the background recorded on tape. The volume voided by the patient was measured. It should be noted that it is not necessary to know the initial volume in the bladder since it can be determined from the calculation of the residual urine. Hence, it does not matter if the kidneys secrete a significant amount of urine after bladder filling but prior to micturition.

## 2.7 Data Processing

The calculations on the analogue data recorded on the

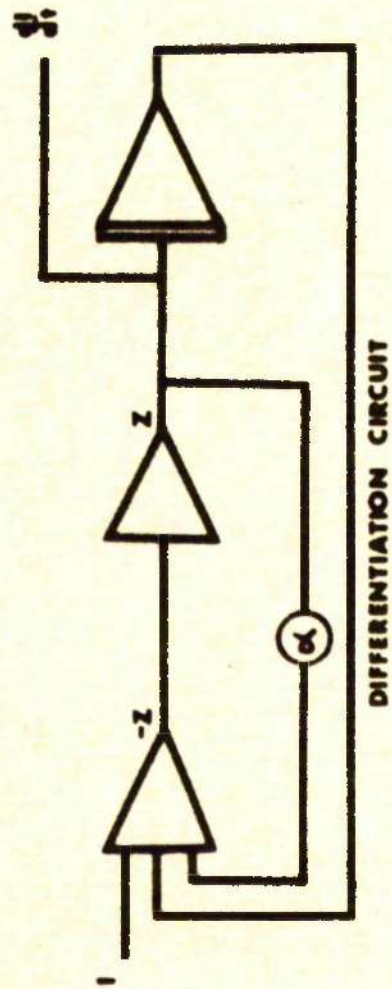


FIG 2.11

DIFFERENTIATION CIRCUIT

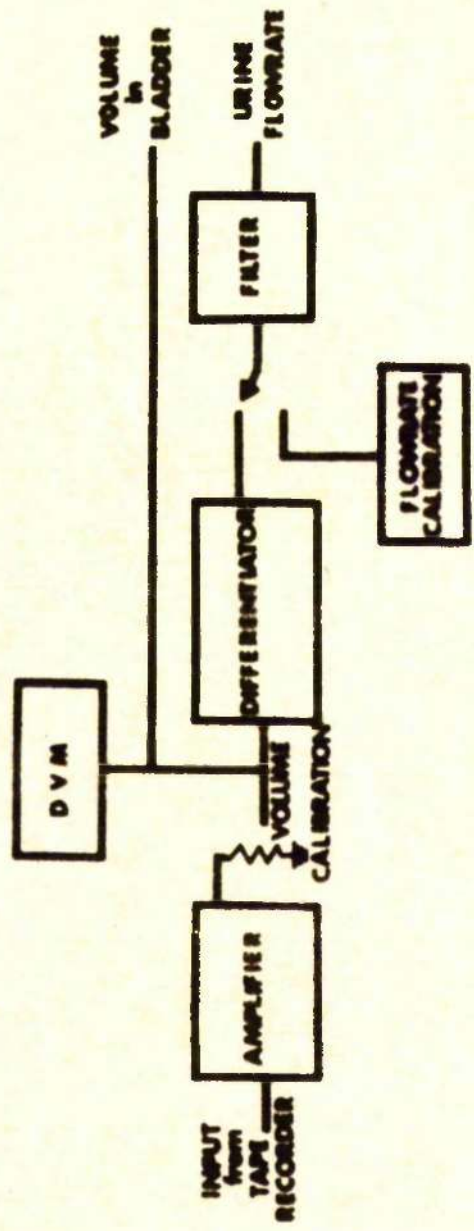


FIG 2.12

taperecorder were performed using an analogue computer for convenience.

In order to calculate the urine flowrate, it is necessary to differentiate the countrate from the bladder with respect to time. The circuit used to differentiate is shown in Figure 2.11 Jackson.

If in the equation -

$$I(t) + (1 - \alpha) Z(t) = \int_0^t Z(\tau) d\tau$$

Then as  $\alpha \rightarrow 1$ ,  $Z \rightarrow \frac{dI(t)}{dt}$ .

The value of  $\alpha$  controls the noise level inherent in the differentiation process. A value of 0.9 for  $\alpha$  was generally found to be acceptable.

A block diagram of the circuit used to calculate the residual urine and urine flowrate is shown in Figure 2.12. In order to calibrate the system for the urine flowrate it is necessary to first calculate the residual volume. This is done by measuring the voltages on the digital voltmeter (DVM) Figure 2.12 during playback and using the formula -

$$V_{RES} = \frac{\text{Volume Voided}}{\left[ 1 - \frac{I_1 - I_3}{I_2 - I_4} \right]}$$

where  $I_1$  = voltage representing the countrate from the bladder just prior to micturition,  $I_3$  = voltage representing the background from the bladder prior to voiding,  $I_2$  = voltage representing the countrate from the bladder after micturition and  $I_4$  = voltage representing the background from the bladder after micturition.

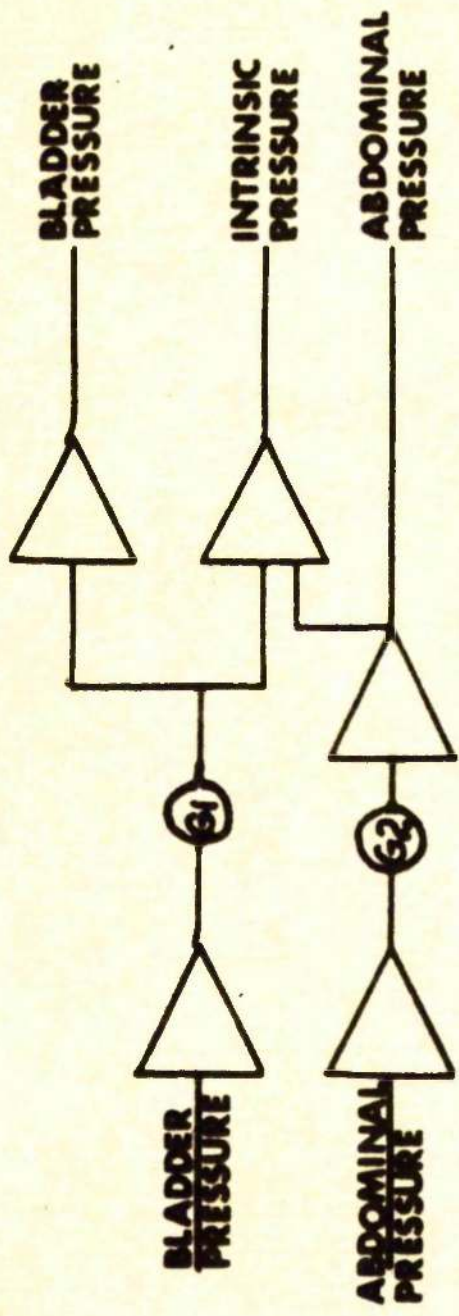


FIG 2.13

In order to obtain an accurate reading of these voltages, the time constant of the input filter was increased to 15 secs. Once the residual is calculated, the initial volume in the bladder can be determined.

In the isotope technique, the urine flowrate is calculated from the equation --

$$Q(t) = - \frac{V_i}{I_i} \frac{dI(t)}{dt}$$

where  $V_i$  = initial volume in the bladder,  $I_i$  = countrate from the bladder prior to micturition and  $I(t)$  = countrate from the bladder during micturition.

Thus, the pen recorder is easily calibrated by injecting a voltage = X mV from the calibration unit in Figure 2.12 and setting full scale deflection on the pen recorder to X ml/sec. It is then only necessary to set the voltage due to the countrate prior to micturition equal numerically to the initial volume in the bladder in millivolts. It was necessary to use filters with a time constant of 1 second in order to reduce the noise since it was undesirable to reduce beyond 0.9. The same method was used to determine the urine flowrate using the Von Garrelts' technique only in this instance  $I_i$  was set to the volume voided and the polarity of the output to the pen recorder was reversed.

The circuit for the analysis of the bladder pressure and abdominal pressure data is shown in Figure 2.13. The pressure due to detrusor contraction (intrinsic pressure) was determined by subtracting the abdominal pressure from the intravesical pressure.

The intravesical pressure, abdominal pressure and the intrinsic pressure were fed to separate channels of the pen recorder.

The pressure channels were calibrated independently by injecting the calibration voltages recorded on the taperecorder prior to micturition. The gains  $G_1$  and  $G_2$  were adjusted to give the same pressure calibration before the subtraction unit.

CHAPTER 3Rigid Tube Theory

In order to try to understand the fluid dynamics of the lower urinary tract many investigators have used the theory of flow in rigid tubes as a first order approximation. The flow was considered to be steady. If the flowrate was not constant then the it was considered as a sequence of steady flowrates. The theory has been used to correlate the bladder pressure and flowrate and the clinical condition of the patient by Gleason and Lattimer (1962) and Pierce et al (1963) who considered the flow to be laminar. Using turbulent flow conditions, Litter, Zinner and Faquin (1964) and Bachman (1966) calculated the energy losses in a rigid tube approximating the urethra.

If we consider the steady flow in a rigid tube of uniform circular cross-section  $A$ , then we have (Figure 3.1) -

$$P_{BL} = p(x) + \frac{1}{2} \frac{Q^2}{A^2} + \int_0^x E_{\text{loss}}(Q, A) dz \quad 3.1$$

where  $E_{\text{loss}}(Q, A)$  = energy loss/cm,  $p(x)$  = pressure at point  $x$  within the tube and  $Q$  = flowrate.

Since, in general, the bladder neck on entry from the bladder is not a sharp physical boundary, the energy loss on entry will be small. When the basic flow equation (the Navier Stoke's equations) are solved for non-turbulent flow in rigid tubes, it can be shown (Schlichting (1955)) that the velocity profile, being flat on entry, becomes progressively more parabolic downstream only attaining the laminar flow profile at a distance of the area of  $0.3 \times d \times R$

where  $R$  = Reynolds' No. =  $v \frac{d}{\nu}$ ,  $d$  = diameter of the tube,  $v$  = velocity of the fluid within the tube and  $\nu$  = kinematic viscosity of the fluid.

These variables are all in c.g.s. units.

Thus, for a Reynolds' No.  $\approx 1,000$ , and a diameter  $\approx 3$  mm, the inlet length  $L_I \approx 100$  cm. This is much greater than the length of the urethra. It would, therefore, appear that laminar flow does not occur in the urethra during the main part of micturition.

If swirling occurs on entry to the tube, but of an order less than the axial velocity, then this will decay downstream dying out after a distance of the order of forty diameters at a Reynolds' No. of 1,000. Assuming a diameter of 3 mm, this distance is of the order of 12 cm. Thus one would possibly expect swirling to occur occasionally in the female on exit at the external meatus but not in the male.

Energy losses may also occur at bends but in general these losses will be small in the female although they are probably not insignificant in the male. Most of the energy dissipated is due to frictional loss between the fluid and the urethral surface. In order to quantitate the loss it is necessary to determine the type of flow in the urethra. Measurements of the urine flowrate and the diameter of the urethra from X-ray photographs of the urethra during micturition show that the Reynolds' No. is generally in excess of 2,000 at flowrates greater than 10 ml/sec. This implies (Schlichting (1955)) that the flow will not be laminar and will be approximately turbulent. This has also been reported

by Morales (1952).

In 1911, Blasius surveyed the literature on turbulent flow in pipes and established an empirical equation relating the frictional resistance  $\lambda$  to the velocity  $v$  of the fluid and the diameter  $d$  of the tube.

$$\lambda = 0.3164 \left( \frac{vd}{\nu} \right)^{-0.25}$$

The frictional pressure loss is related to  $\lambda$  by the following equation -

$$\begin{aligned} \Delta P_{\text{loss}} &= l \frac{\lambda}{d} \left( \frac{1}{2} \rho v^2 \right) \\ &= l \frac{\lambda}{d} \left( \frac{1}{2} \rho \frac{Q^2}{A^2} \right) \end{aligned}$$

where  $l$  = length of the tube.

In terms of equation 3.1 -

$$\int_0^l \Delta P_{\text{loss}}(Q, \lambda) ds = l \frac{\lambda}{d} \left( \frac{1}{2} \rho \frac{Q^2}{A^2} \right)$$

Hence -

$$P_{\text{BL}} = \frac{Q^2}{A^2} + \frac{8l}{\pi^2} \rho \frac{Q^2}{d^5} \quad 3.2$$

if it is assumed that the pressure at the exist of the tube is atmospheric.

It can be seen that -

$$\Delta P_{\text{loss}} = \frac{C^{1.75}}{d^{4.25}}$$

Therefore, if the flowrate  $Q$  and the bladder pressure  $P_{\text{BL}}$  are known, then it is possible to calculate a diameter  $d_1$  which

satisfies equation 3.2. This diameter is called the equivalent rigid tube diameter.

This concept has been used by Backman (1966) and Smith (1968). However, in these instances the coefficient  $\lambda$  in equation 3.2 was taken to be a constant with a value of 0.005 in c.g.s. units. The use of a constant value will tend to cause an error in the estimation of  $d_1$  as the Reynolds' No. increases. This error will be of the order of 0.2 mm.

Since  $\Delta P_{\text{loss}}$  is proportional to  $Q^{1.75}$ , Backman (1966) and Smith (1968) have used the ratio  $R_f = \frac{\Delta P_{\text{loss}}}{Q^2}$  as an indication of the resistance of the urethra. Using this definition of  $R_f$  -

$$P_{\text{BL}} = \left( \frac{1}{2} \lambda_c^2 + R_f \right) Q^2$$

The term  $R = \frac{P_{\text{BL}}}{Q^2}$  may also reflect the resistance of the urethra. The factor  $R$  has been used frequently since it does not require any knowledge of the equivalent rigid tube diameter. Both  $R_f$  and  $R$  are approximately independent of the flowrate and, therefore, reflect the calibre and length of the urethra.

Values of bladder pressure, equivalent rigid tube diameter, flowrate and the corresponding resistance factors  $R$  and  $R_f$  have been tabulated using a digital computer. Hence, knowing the flowrate and the corresponding bladder pressure one can determine the other parameters characterising the urethra from the tables.

The bladder pressure and urine flowrates have an error of the order of 5 per cent associated with them. Hence, it is important to determine the effect of these errors on the estimation of the equivalent rigid tube diameter and the other parameters.

In the rigid tube model, the basic equation is -

$$P_{BL} - \frac{1}{2} \frac{C^2}{A_e^2} = \alpha \frac{C^{1.75}}{d_e^{4.25}}$$

Therefore -

$$\frac{\delta \left[ P_{BL} - \frac{1}{2} \frac{C^2}{A_e^2} \right]}{\left[ P_{BL} - \frac{1}{2} \frac{C^2}{A_e^2} \right]} = 1.75 \frac{\delta C}{C} - 4.75 \frac{\delta d_e}{d_e}$$

Since -

$$\Delta P_{loss} = P_{BL} - \frac{1}{2} \frac{C^2}{A_e^2}$$

Then -

$$\frac{1}{\Delta P_{loss}} \delta P_{BL} - \frac{1}{2 \Delta P_{loss}} \left( \frac{C^2}{A_e^2} \right) = 1.75 \frac{\delta C}{C} - 4.75 \frac{\delta d_e}{d_e}$$

Therefore -

$$\frac{P_{BL}}{\Delta P_{loss}} \frac{\delta P_{BL}}{P_{BL}} - \frac{1}{2 \Delta P_{loss}} \frac{C^2}{A_e^2} \left[ 2 \frac{\delta C}{C} + 2 \frac{\delta A_e^2}{A_e^2} \right] = 1.75 \frac{\delta C}{C} - 4.75 \frac{\delta d_e}{d_e}$$

$$\text{Let } \beta = \frac{P_{BL}}{\Delta P_{loss}}$$

Then -

$$\beta \frac{\delta P_{BL}}{P_{BL}} - \left[ \frac{P_{BL} - \Delta P_{loss}}{\Delta P_{loss}} \right] \left[ 2 \frac{\delta C}{C} + 4 \frac{\delta d_e}{d_e} \right] = 1.75 \frac{\delta C}{C} - 4.75 \frac{\delta d_e}{d_e}$$

$$\beta \frac{\delta P_{BL}}{P_{BL}} - 2(\beta - 1) \frac{\delta C}{C} - 4(\beta - 1) \frac{\delta d_e}{d_e} = 1.75 \frac{\delta C}{C} - 4.75 \frac{\delta d_e}{d_e}$$

Hence -

$$\beta \frac{\delta P_{BL}}{P_{BL}} - (2\beta - 0.25) \frac{\delta \zeta}{\zeta} = (4\beta - 3.75) \frac{\delta d_e}{d_e}$$

Therefore -

$$\frac{\delta d_e}{d_e} \approx \frac{[(2\beta - 0.25) \frac{\delta \zeta}{\zeta} + \beta \frac{\delta P_{BL}}{P_{BL}}]}{(4 - 3.75)}$$

Thus if  $P_f \approx 10$  per cent  $P_{BL}$ ,  $\frac{\delta \zeta}{\zeta} \approx 5$  per cent and  $\frac{\delta P_{BL}}{P_{BL}}$  5 per cent we have  $\frac{\delta d_e}{d_e} \approx 5$  per cent.

The error increases as  $\beta$  decreases, i.e., as the frictional loss increases.

The equivalent rigid tube diameter is related to the diameter which would be obtained if there were negligible loss.

For a lossless tube, then -

$$P_{BL} = \frac{1}{2} \frac{\zeta^2}{A_{LL}^2}$$

therefore -

$$A_L^2 = \frac{1}{2} \frac{\zeta^2}{P_{BL}}$$

In the case of frictional loss -

$$\begin{aligned} P_{BL} &= \frac{1}{2} \frac{\zeta^2}{A} + 2 \frac{P_f}{\zeta} A_e^2 \cdot \frac{\zeta^2}{2A_e^2} \\ &= \frac{1}{2} \frac{\zeta^2}{A_e^2} \sqrt{1} + 2 \frac{P_f}{\zeta^2} L_e^2 \end{aligned}$$

Therefore -

$$A_e^2 = \frac{1}{2} \frac{Q^2}{P_{BL}} \left[ 1 + 2 \left( \frac{P_f}{Q^2} \right) A_e^2 \right]$$

Hence --

$$A_c^2 = A_L^2 \left[ 1 + 2 R_f A_e^2 \right] \quad 3.3$$

$$RN2 = \frac{A_e^2 - A_L^2}{A_e^2} = \frac{2 \Delta P_{loss}}{Q^2} A_e^2$$

Hence the percentage deviation of  $A_e^2$  from the lossless value  $A_L^2$  is proportional to the resistance  $\frac{P_f}{Q^2}$ .

Therefore, the resistance  $\frac{P_f}{Q^2}$  is an index of the deviation of the equivalent rigid tube model from the idealised lossless model

The percentage deviation of the equivalent rigid tube diameter from the lossless diameter is easily shown from equation 3.3 to be --

$$RN1 = \frac{d_e - d_L}{d_L} = 100 \left( \frac{1 - \alpha}{\alpha} \right)$$

where  $\alpha = \sqrt{1 - 2 R_f A_e^2}$ .

Since  $A_c$  depends on the flowrate, the parameters RN1 and RN2 may be more informative parameters relating the bladder pressure, urine flowrate and the resistance to flow than the resistances  $R_f$  and  $R_c$ .

Abdominal pressure is not considered separately from the bladder pressure since the model cannot incorporate the distinction. Thus any effects of abdominal pressure acting on the bladder/urethral systems may only be reflected by the magnitude of the equivalent rigid tube diameter.

CHAPTER 4Data Analysis

4.1 This chapter details the results obtained in a group of female patients suffering from incontinence. The majority of these patients fell into the category of stress incontinence coupled with urgency and or frequency.

In Chapter 2, the radioisotope method used to measure urine flowrate was discussed. Von Garrelts' method (1957) was also used simultaneously for comparative purposes.

The flow from a rigid tube of internal diameter equal to 3 mm was directed down the side of the Von Garrelts' apparatus. In this instance a flowrate of 10 ml/sec was recorded. When the same stream was directed down the centre of the apparatus, the flowmeter indicated an increase in the flowrate of 30 per cent. This increase was due to the kinetic energy of the impinging stream. This effect may, therefore, artificially elevate the peak flowrates observed during patient investigations. The correlation between the peak flowrates obtained from the group of patients using both techniques is shown in Figure 4.1. There is, therefore, a very close correlation between the two techniques. The standard deviation was 1.6 ml/sec. The results suggest that in the majority of patients the stream was directed down the side of the Von Garrelts' apparatus. The apparatus was positioned to minimise artefacts due to flow down the centre of the apparatus. However, there was a compromise between this requirement and positioning of the apparatus such that there was no

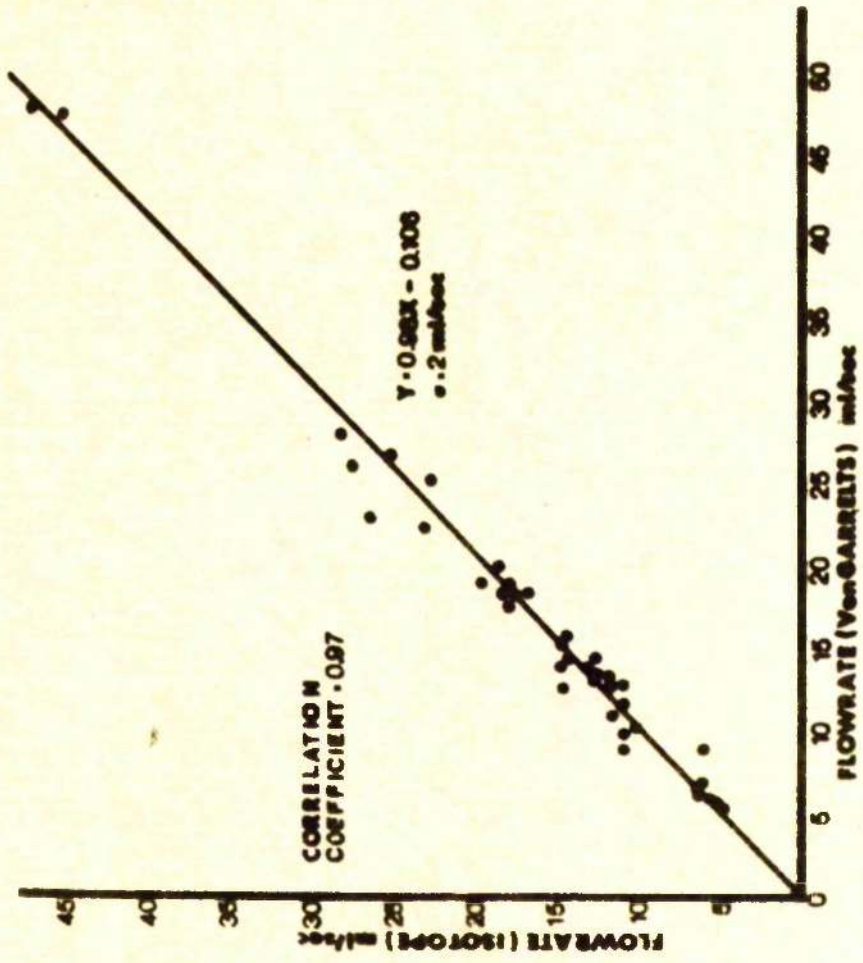
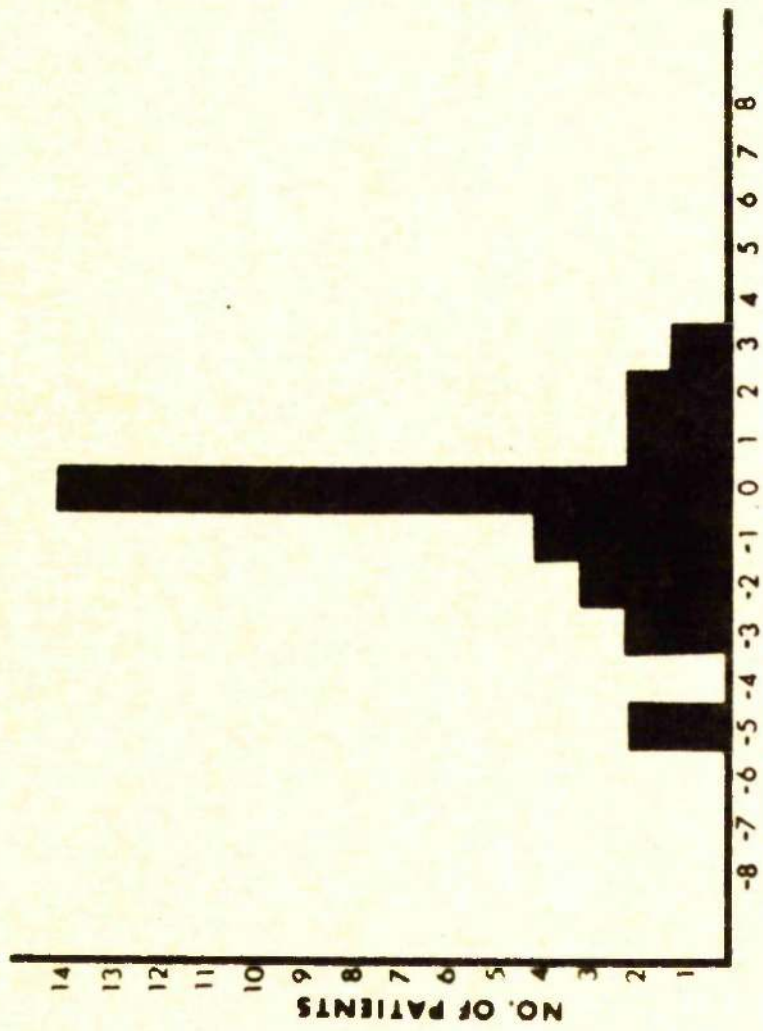


FIG 4.1



OPENING TIME DIFFERENCE: von GARRELTS - ISOTOPE  
 FIG 4.2

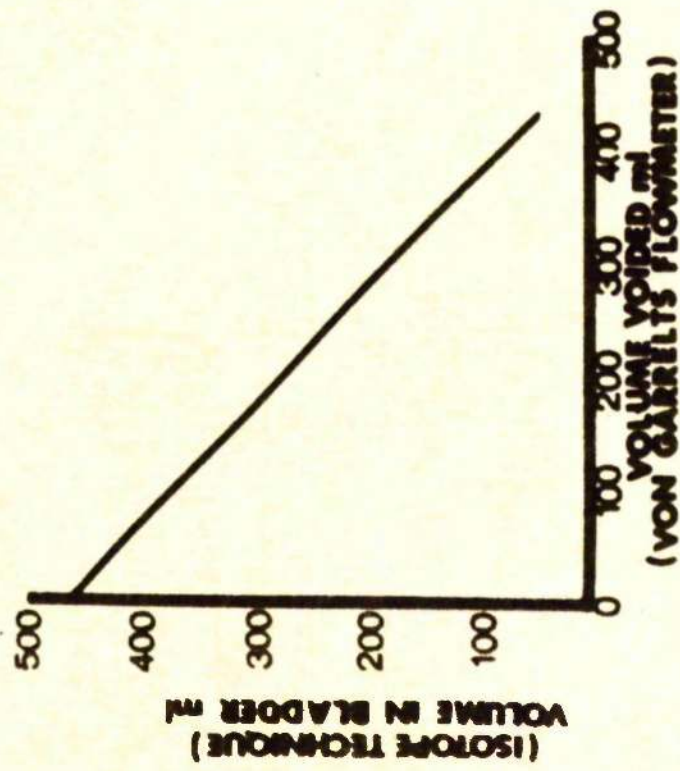


FIG 4-3

possibility of the stream missing the funnel. Increasing the diameter of the funnel was not desirable since this could lead to excessive delays in the detection of the flow.

In the Von Garrelts' apparatus, the delay in flow detection may be increased due to swirling occurring in the funnel. Using a standard reference, the times at which flow commenced, according to the two techniques, was determined. The deviations in these times were calculated and plotted (Figure 4.2). The majority of the flowrate recordings commenced within 0.5 sec of each other. There were larger discrepancies which were attributable to a combination of two main causes.

- (a) Swirling in the Von Garrelts' apparatus.
- (b) The inability to accurately ascertain the point at which the flow commenced in the radioisotope technique due to an apparent negative flowrate. This was probably due to the relaxation of the pelvic floor resulting in the descent of the bladder.

In order to determine the effects of self-absorption of the radiation, the countrate observed from the bladder was plotted continuously against the volume voided as determined from the Von Garrelts' apparatus in several patients using an x - y recorder. The graphs obtained were linear showing that there were no significant absorption variation effects (Figure 4.3).

These results imply that the two techniques give comparable results under clinical conditions. At low flowrates the

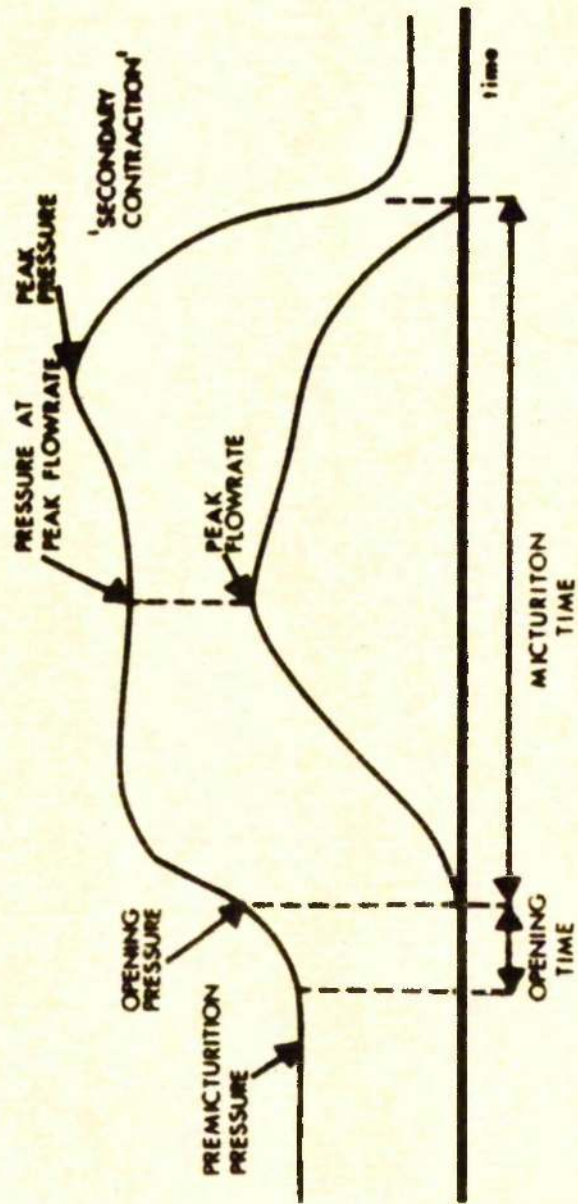


FIG 4.A

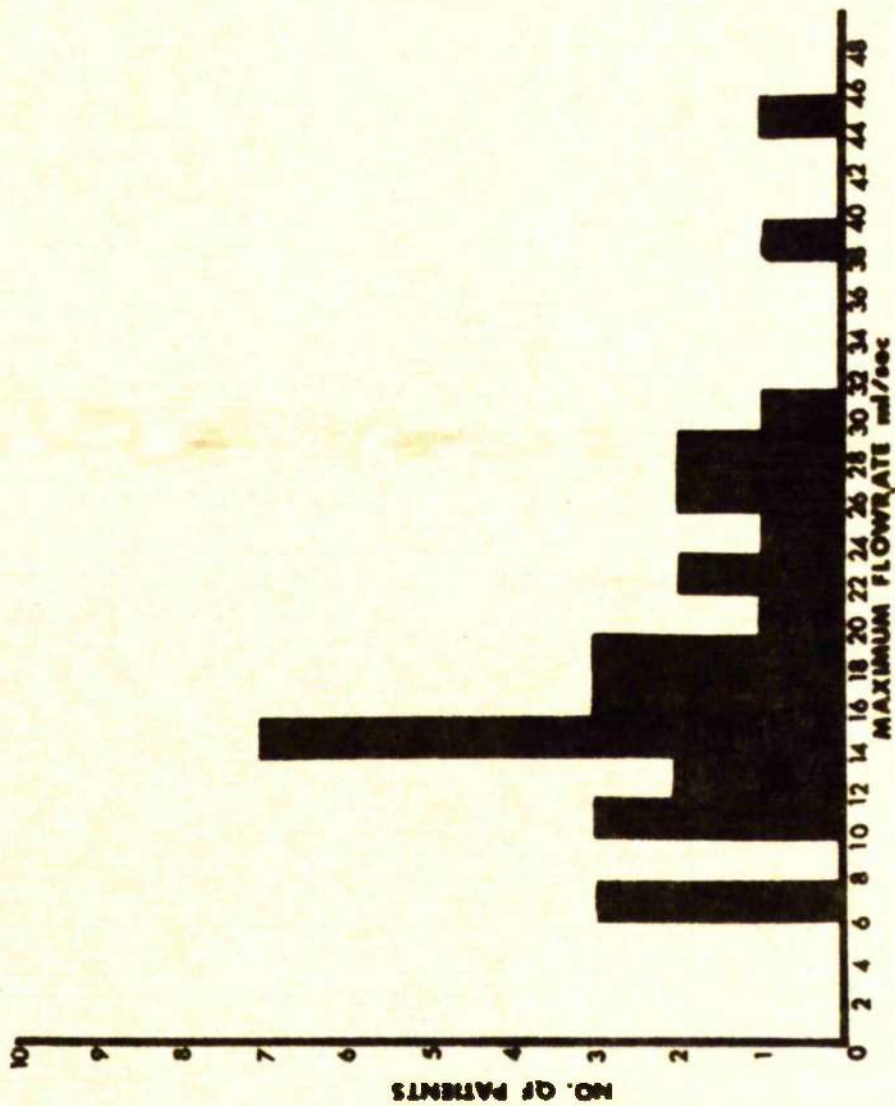


FIG 4.5

Von Garrelts' method is preferred due to its lower noise level. At high flowrates, the isotope technique is not susceptible to the artefacts resulting from kinetic energy effects. The radioisotope technique permits also the residual urine to be determined.

Following Cardus, Quesada and Scott (1963) Figure 4.4 shows the definition of several variables, which will be used subsequently, based on the general micturition pattern.

The distribution of the peak flowrates measured are shown in Figure 4.5. The average peak flowrate was 18 ml/sec with a standard deviation of 6.5 ml/sec. The average peak flowrate is significantly less than the value of 24 ml/sec obtained by Smith (1968) and even more significantly less than the value of 31.5 ml/sec obtained by Drake (1948). Several patients developed a peak flowrate of the order of 10 ml/sec but this was not necessarily related to a large residual urine and/or a small capacity bladder although the residual volume was generally higher than the normal value for the group. Overflow incontinence could, therefore, be eliminated. It is possible that the psychological state of the patients affected the micturition pattern. Neither the peak flowrate nor the pressure at peak flowrate indicate the nature of the flowrate or pressure profiles and, therefore, cannot give a complete picture of the state of the bladder or urethra.

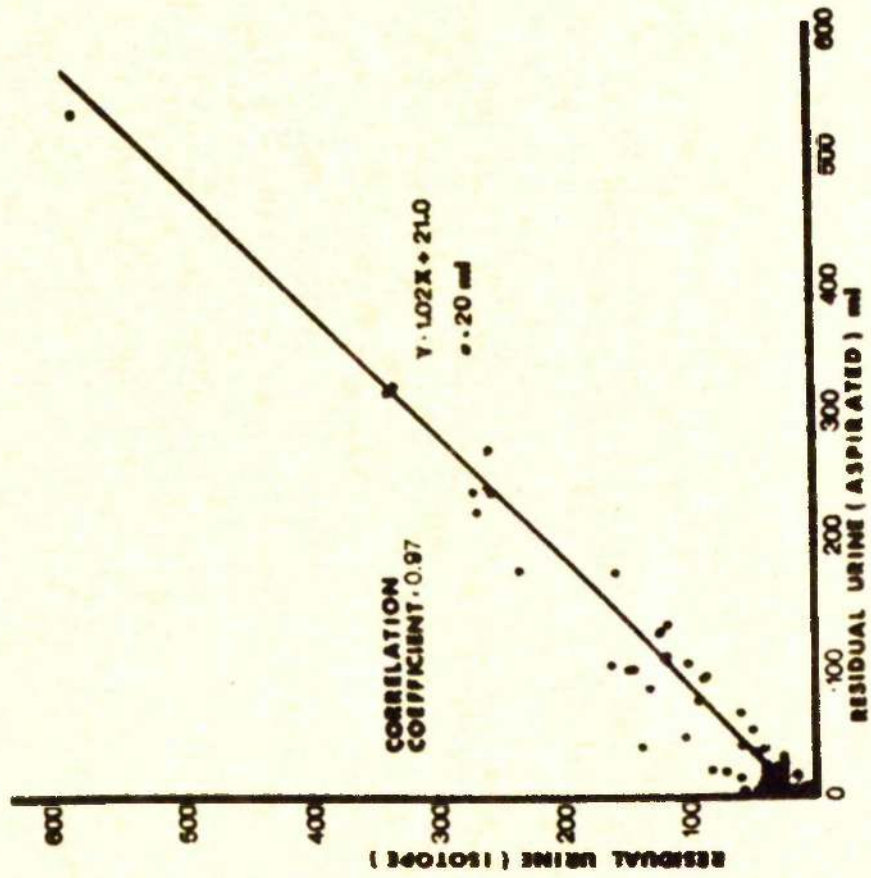


FIG 4.6

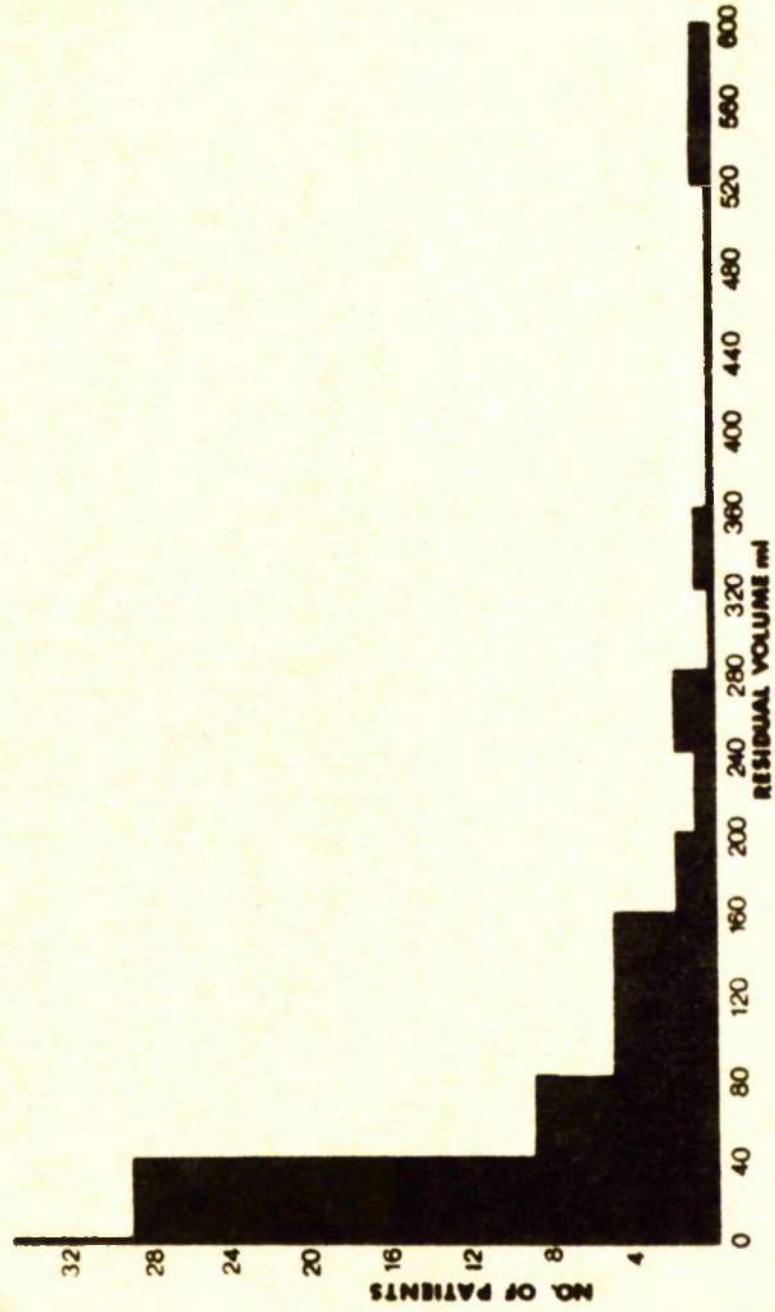


FIG 4.7

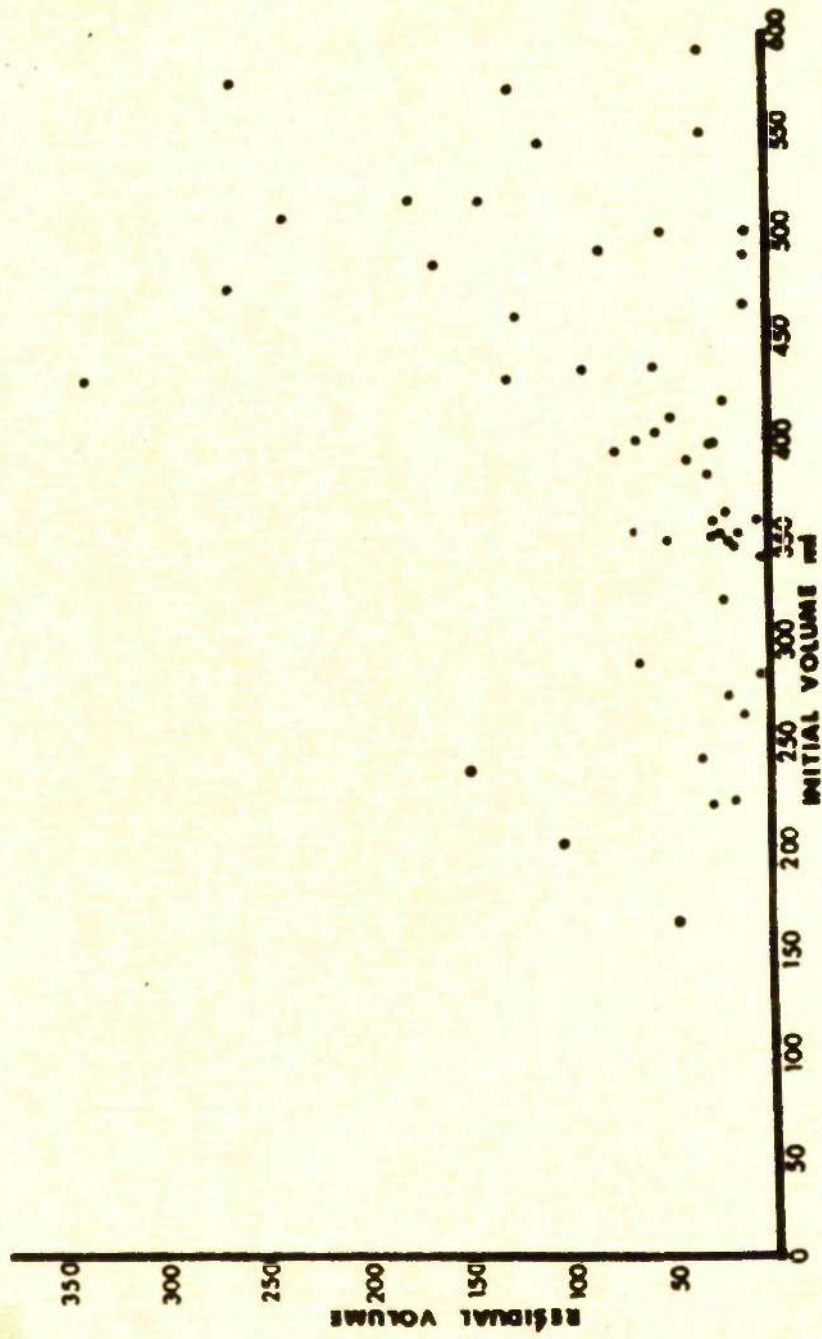


FIG 4.8

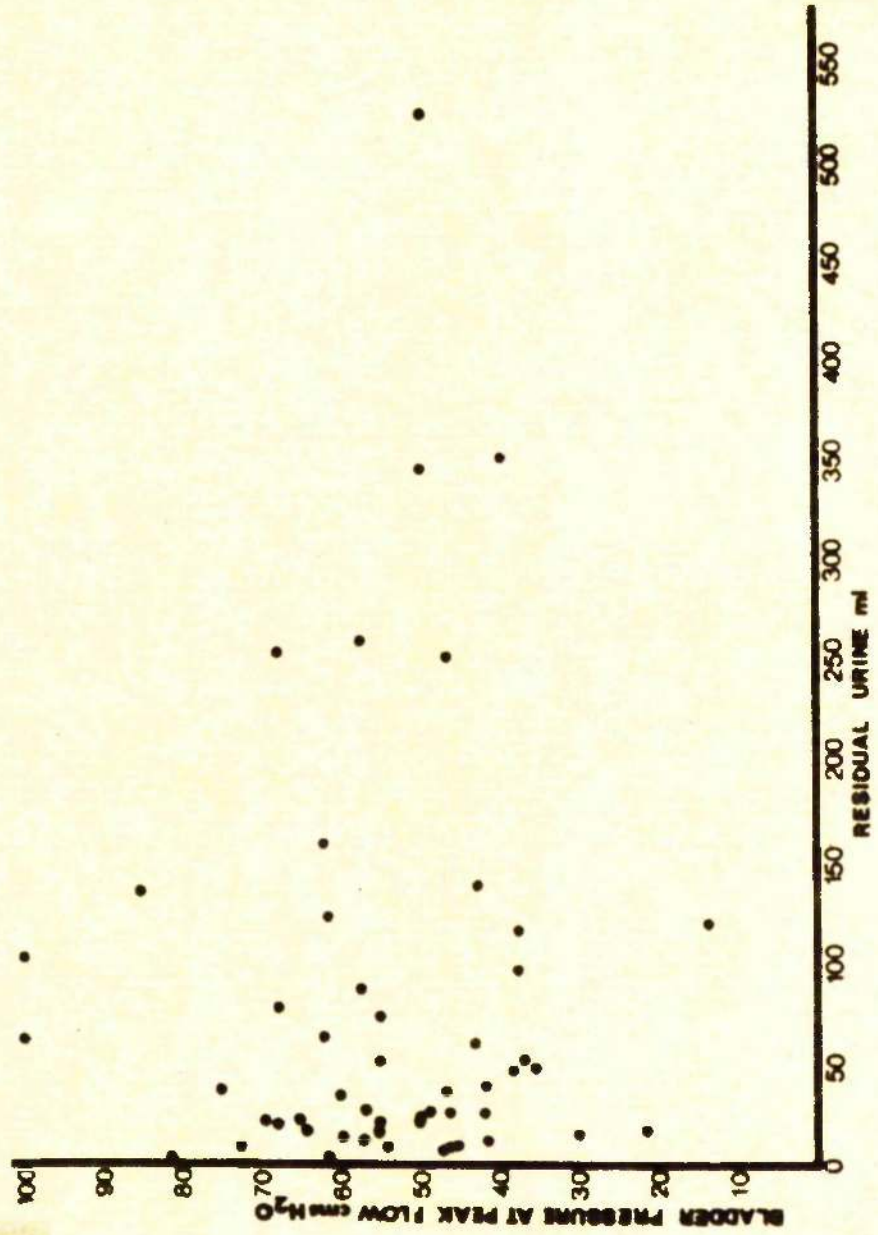


FIG 4.9

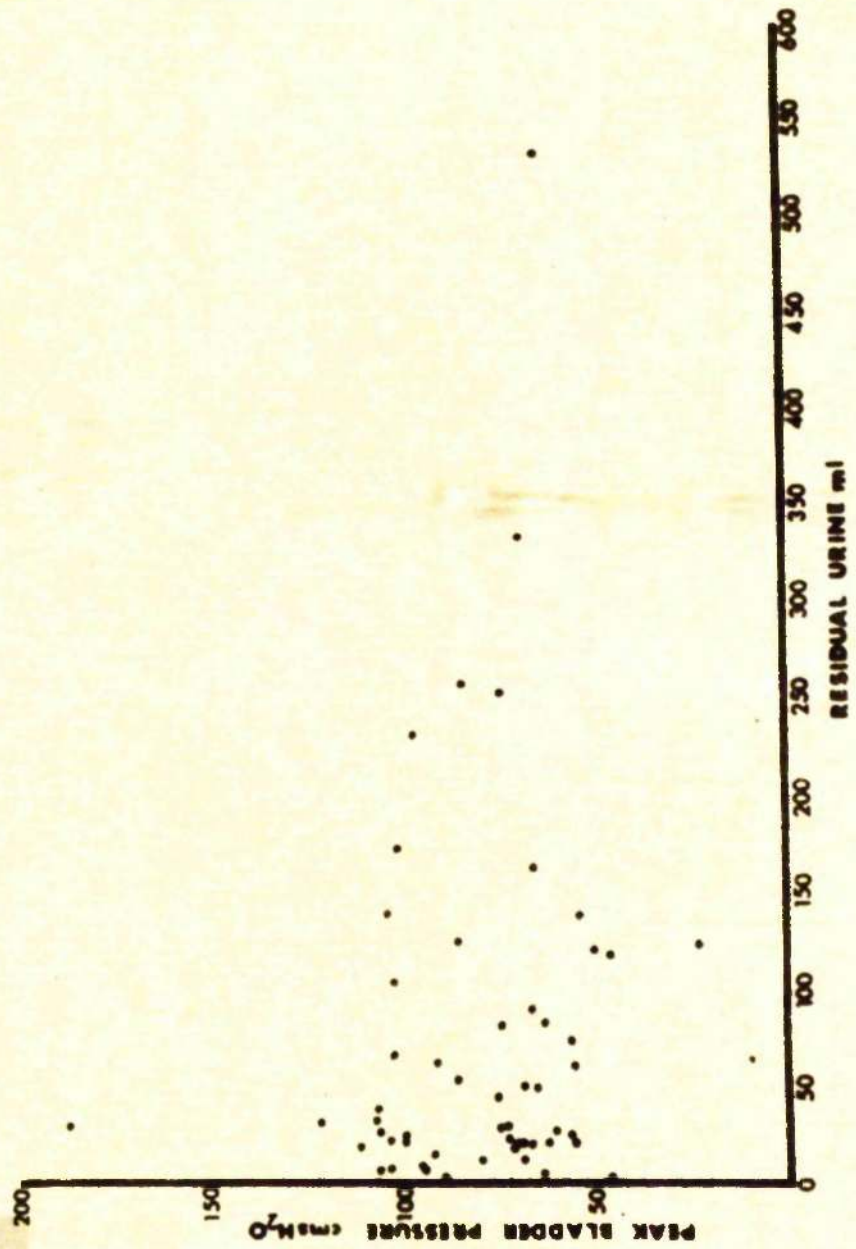


FIG 4.10

The residual urine determined by the isotope technique was correlated with the residual volume withdrawn from the bladder via the transurethral catheter. These results are shown in Figure 4.6. It can be seen that there is a tendency for the isotope technique to suggest residual volumes in excess of the volumes withdrawn. In each case where no residual could be withdrawn, there was isotope activity in the bladder significantly different from background. In only one patient was the residual volume less than 5 ml. In order to verify that the apparent residual volume was not due to diffused labelled human serum albumin, the bladder of a patient who had 20 ml residual was filled with 300 ml of saline and the patient asked to void. About 90 per cent of the activity was voided giving a similar residual. This justifies the assumption that there is negligible diffusion of the labelled serum albumin into the bladder wall.

The residual urine measured in this group of patients is significantly higher than the values obtained by Shand et al (1969) who reported residual volumes in normal subjects as being less than 2 ml. A histogram of the residual urines obtained is shown in Figure 4.7. The mean residual was 67 ml. This, however, is in excess of the most probable residual urine due to a small number of patients with exceedingly large residual volumes. The majority of residual volumes lay in the range 10 - 30 ml. The residual volumes were not significantly related to the initial volume in the bladder, the bladder pressure at the peak flowrate or the peak bladder pressure Figures 4.8, 4.9 and 4.10.

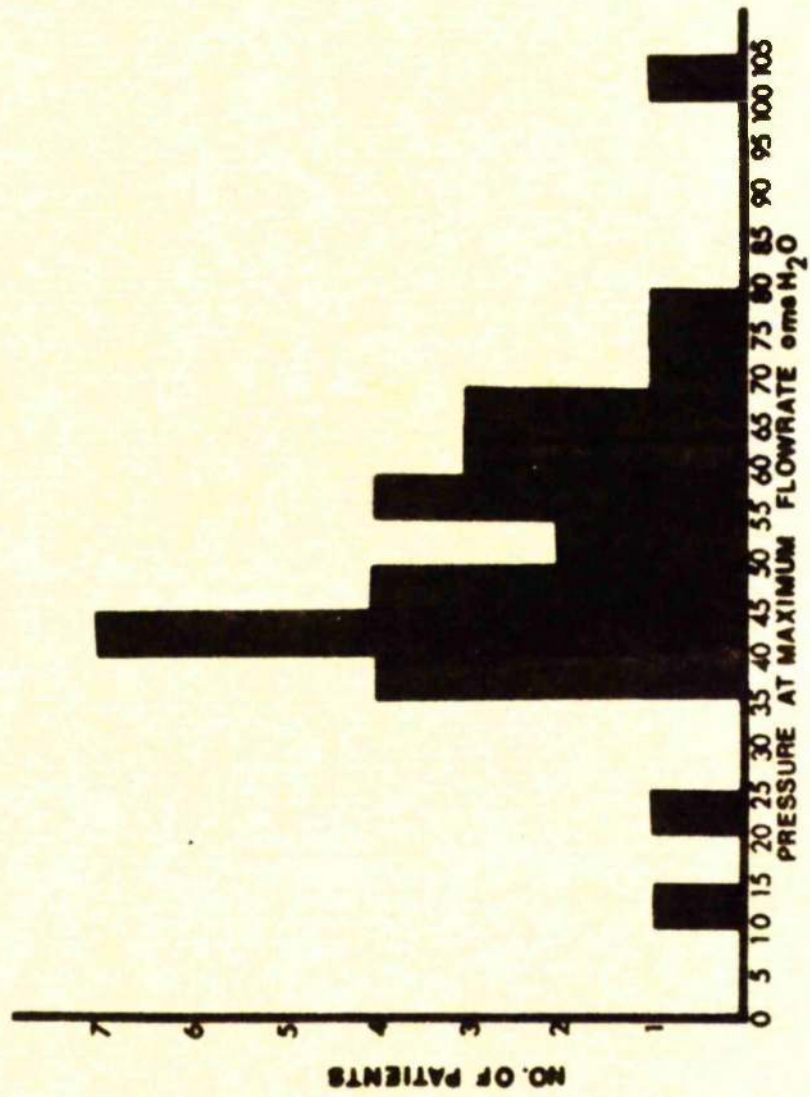
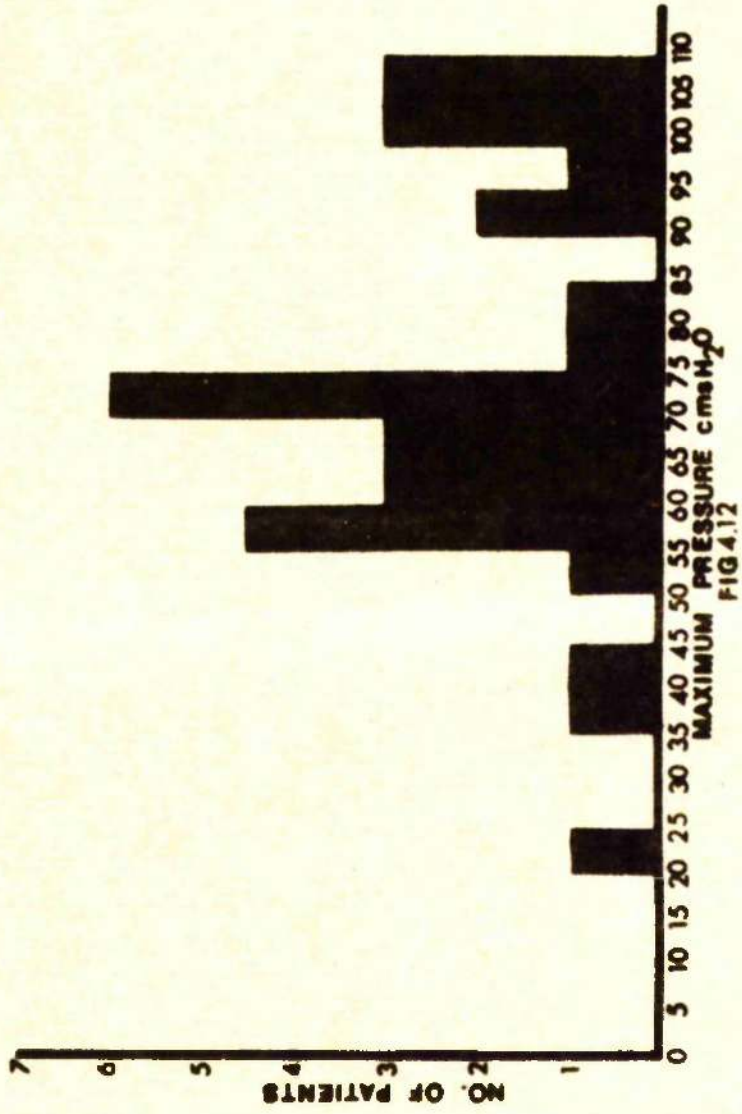


FIG 4.11



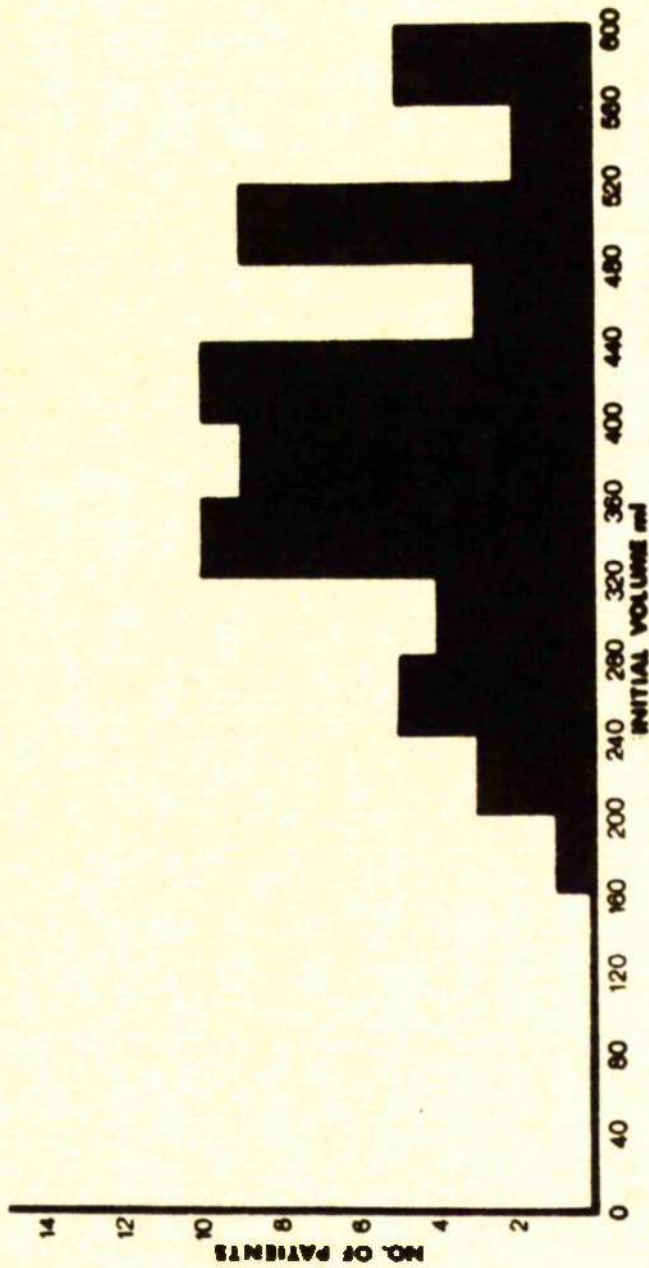


FIG 4.13

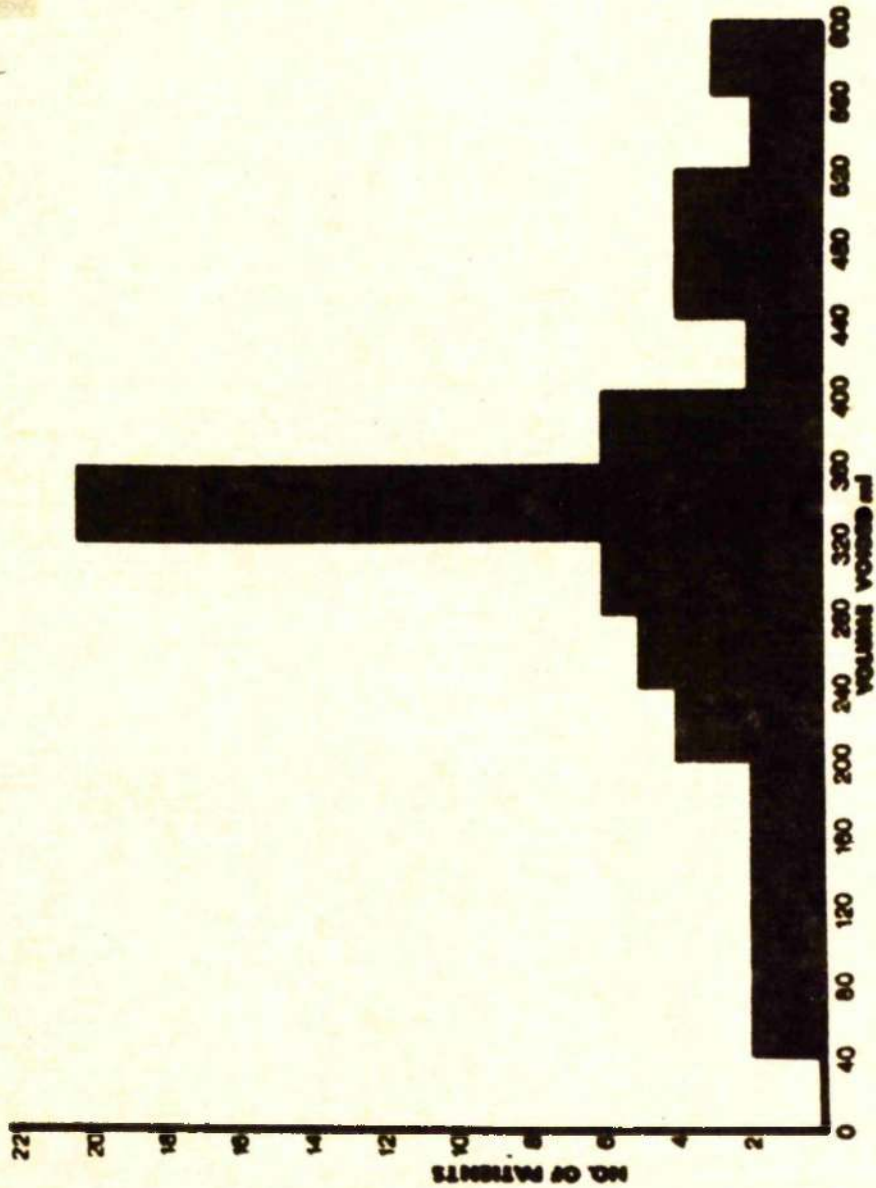


FIG 4.14

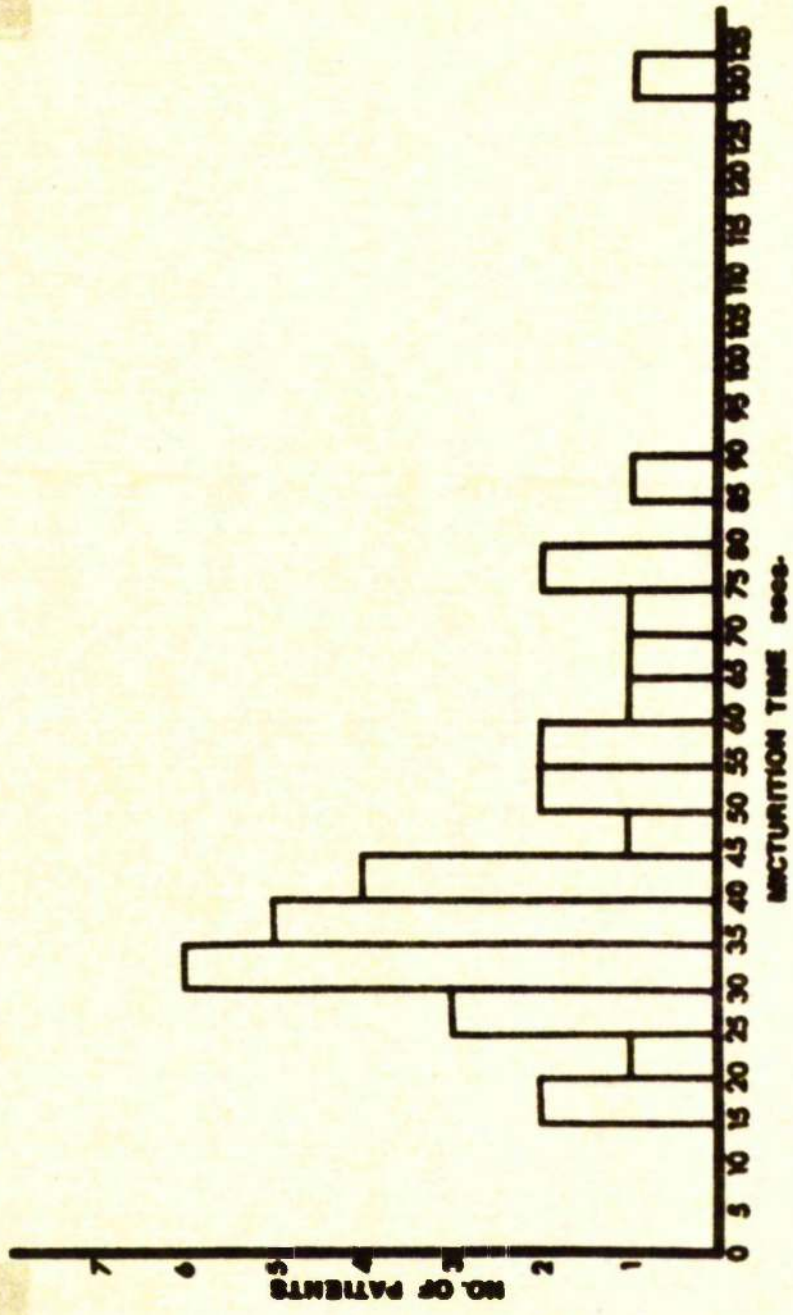


FIG 4.15

The mean bladder pressure at the peak urine flowrate was 52 cm H<sub>2</sub>O with a standard deviation of 19 cm H<sub>2</sub>O. The symphysis pubis was used as the zero pressure reference. The mean peak pressure, however, was 80 cm H<sub>2</sub>O. The peak pressure invariably occurred prior to the peak flowrate. The mean pressure at the peak flowrate agrees with the value obtained by Bauman (1955), Zinner and Paquin (1963) and Backman (1966). The distributions of the bladder pressure at peak flowrate and the peak bladder pressure are shown in Figures 4.11 and 4.12.

Figures 4.13 and 4.14 show the distributions of the initial volumes in the bladder prior to micturition and the volumes voided. The initial volume in the bladder does not in general relate to the bladder capacity since once the bladder was filled with 300 ml of the solution of the radioisotope, the patient was asked to initiate micturition if possible. Only in those patients who could not initiate micturition was more fluid instilled into the bladder until a desire to void was established. The bladder was, therefore, filled to capacity in those patients whose bladder capacity was less than 300 ml.

Two other parameters directly measured were the micturition time and the opening time. The mean micturition time was found to be 46 seconds with a standard deviation of 17 seconds. Several patients voided in more than one episode. The distribution of the micturition times is shown in Figure 4.15. The opening time was not always measurable since the pressure flow profiles were radically different from the defining profile in

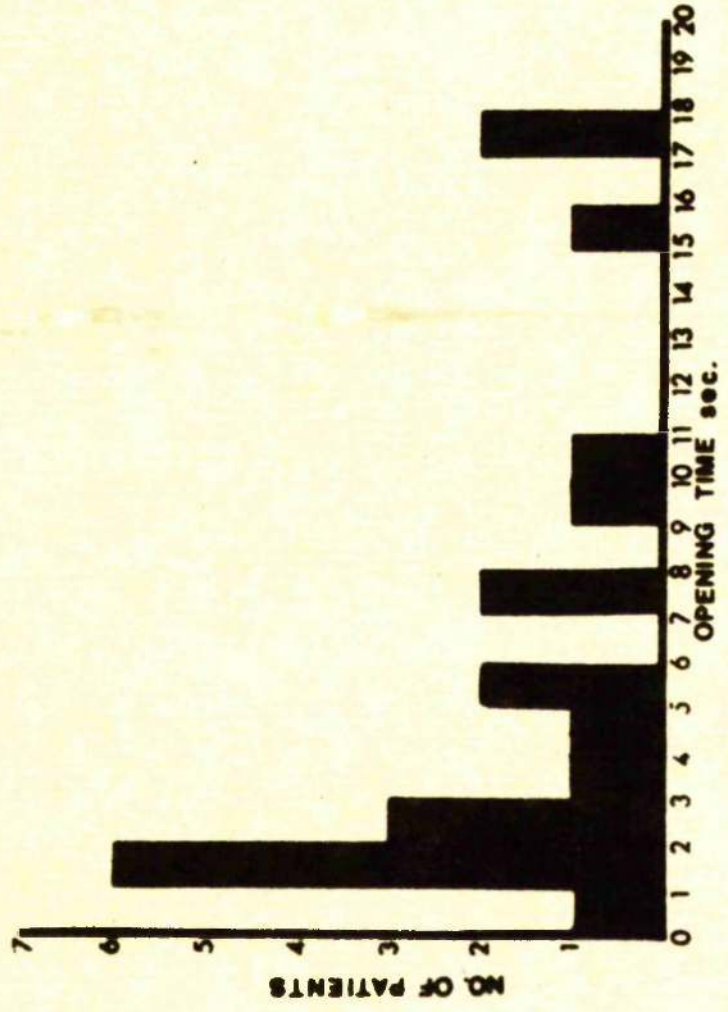


FIG 4.16

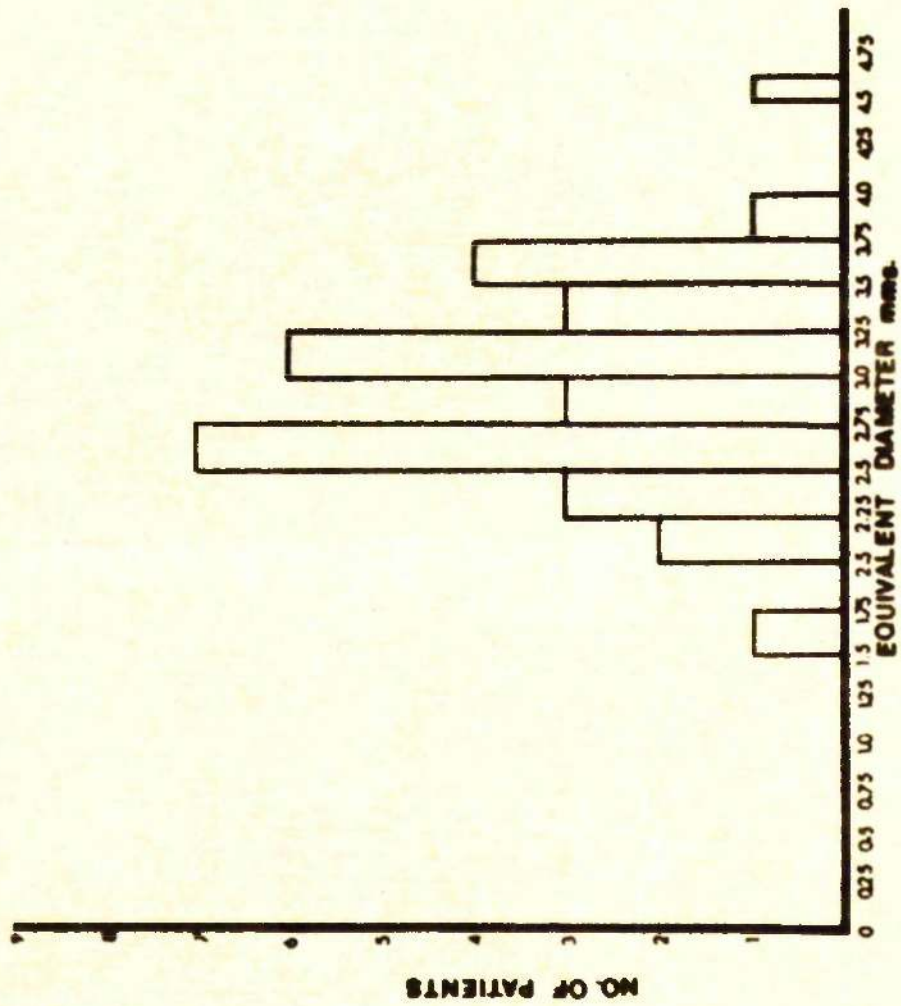


FIG 4.17

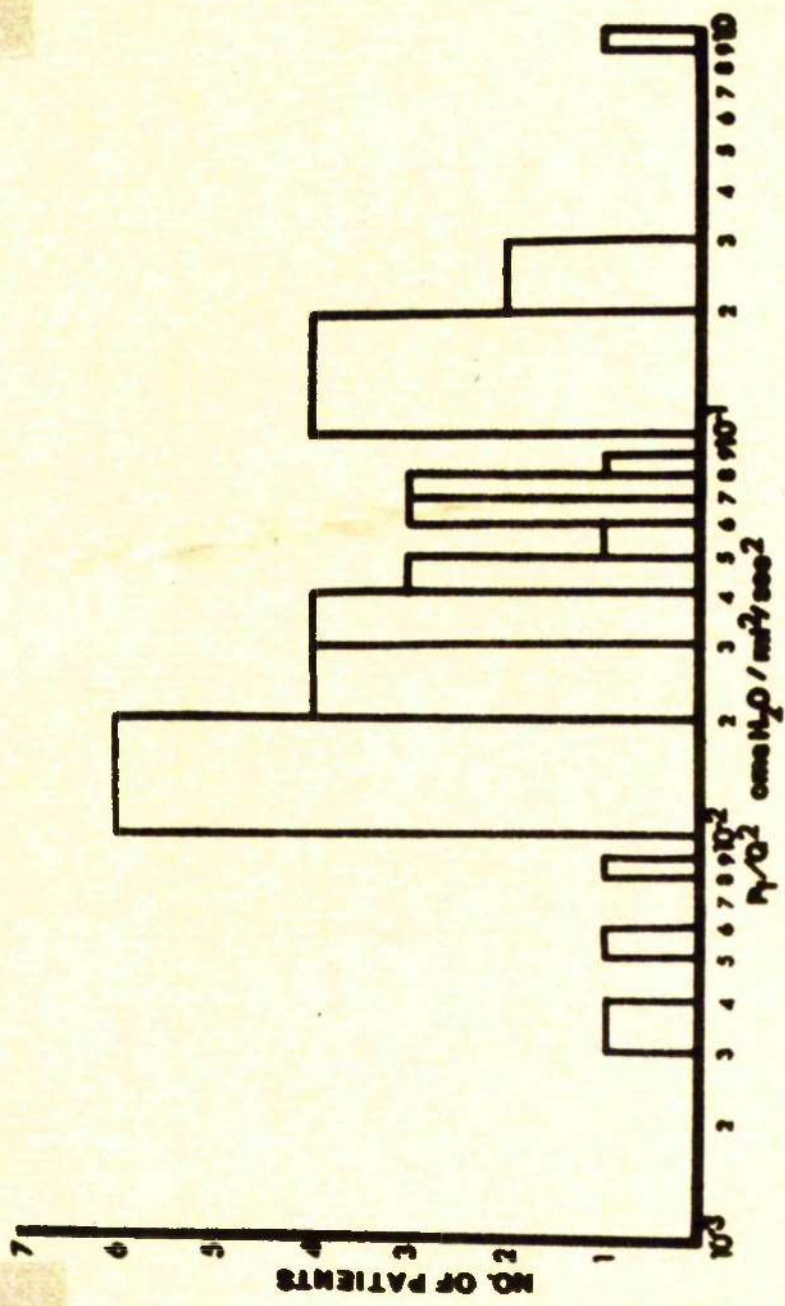


FIG 4.18

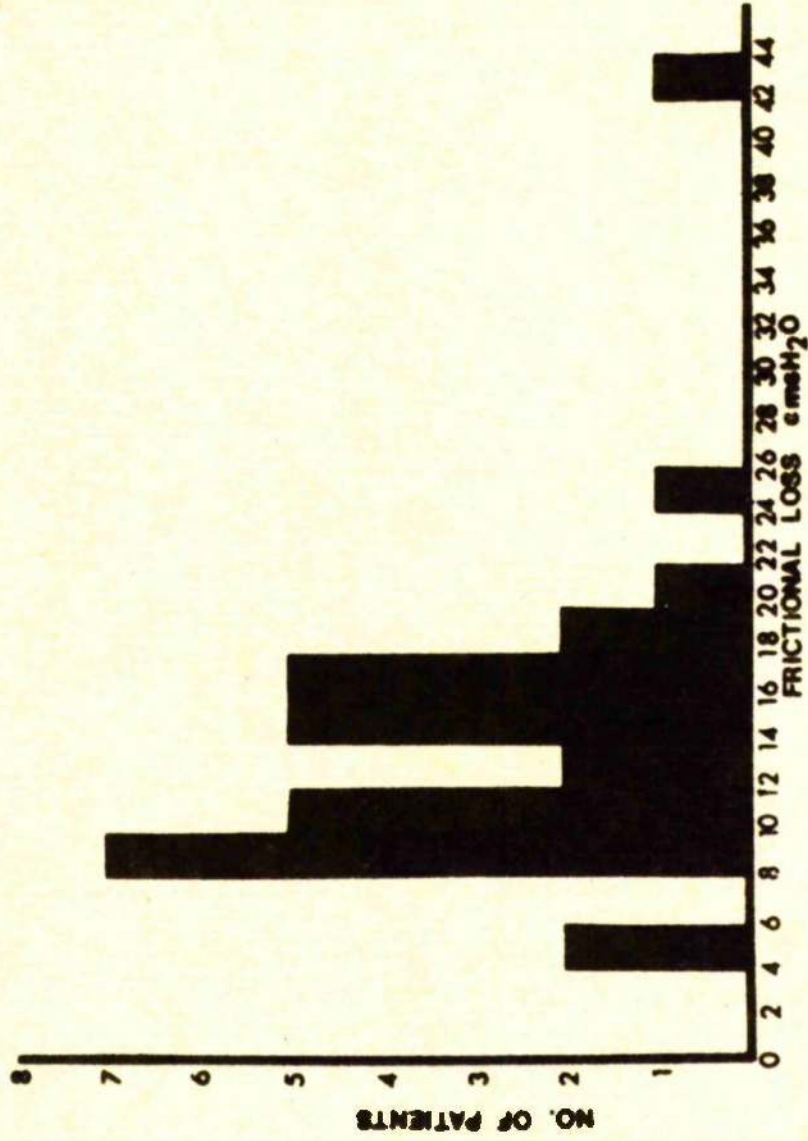


FIG 4.19

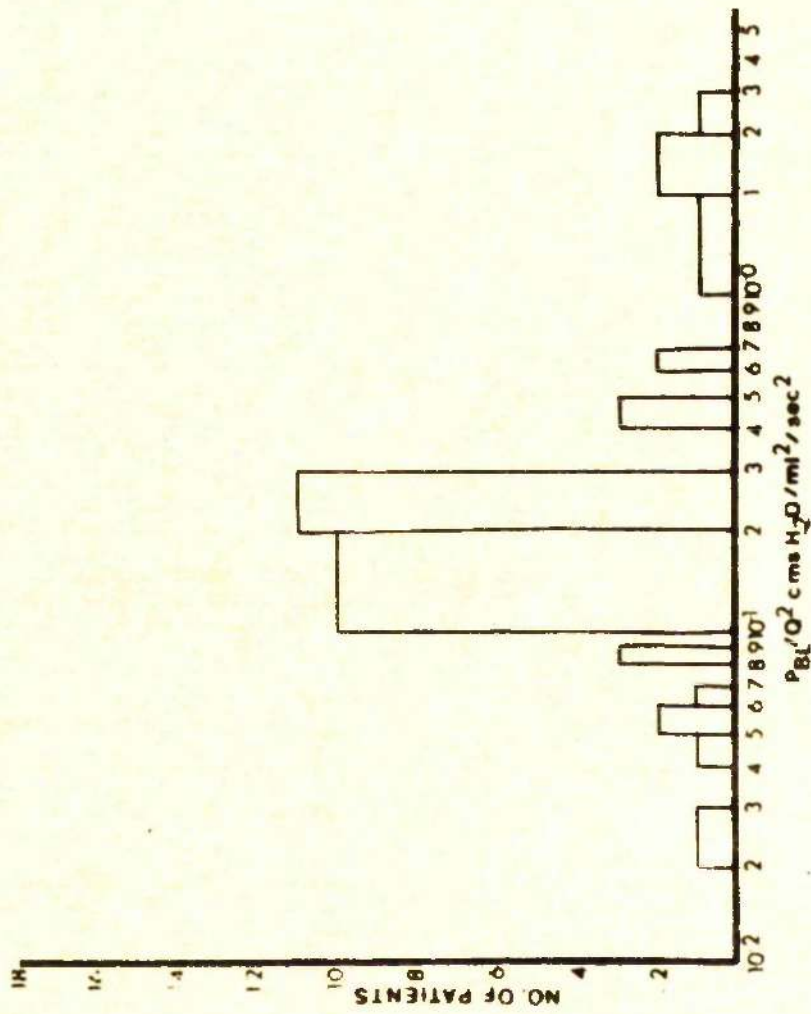


FIG 4.20

Figure 4.3. The distribution of the opening times is shown in Figure 4.16.

The equations in Chapter 3 were used to determine the equivalent rigid tube diameter, the frictional resistance and the frictional loss. The distributions of these parameters are shown in Figures 4.17, 4.18 and 4.19. The resistance index  $R = \frac{P_{BL}}{Q^2}$  was also determined Figure 4.20. It can be seen that 70 per cent of the frictional resistance estimations lie in the range 0.01 to 0.1 cm H<sub>2</sub>O/ml<sup>2</sup>/sec<sup>2</sup> and that 60 per cent of the equivalent diameter values lie between 2.5 and 3.5 mm. Ritter et al (1964) calculated a mean value of 2.7 mm for the equivalent rigid tube diameter for a group of normal women assuming the urethral length to be 4 cm, while Backman (1966) determined a mean diameter of 3 mm. These results agree well with the results obtained in the present study.

It was found that 75 per cent of the determinations of the resistance index lay in the range 0.08 to 0.5 cm H<sub>2</sub>O/ml<sup>2</sup>/sec<sup>2</sup>. Most of the frictional loss estimations lay in the range 8 to 20 cm H<sub>2</sub>O.

From the conservation of energy

$$P_{BL} = P_f + \frac{1}{2} \frac{Q^2}{gAc^2}$$

therefore,

$$\frac{P_{BL}}{Q^2} = \frac{P_f}{Q^2} + \frac{1}{2gAc^2} \quad 4.1$$

The last factor in the above equation ranges from 0.03 to 0.5

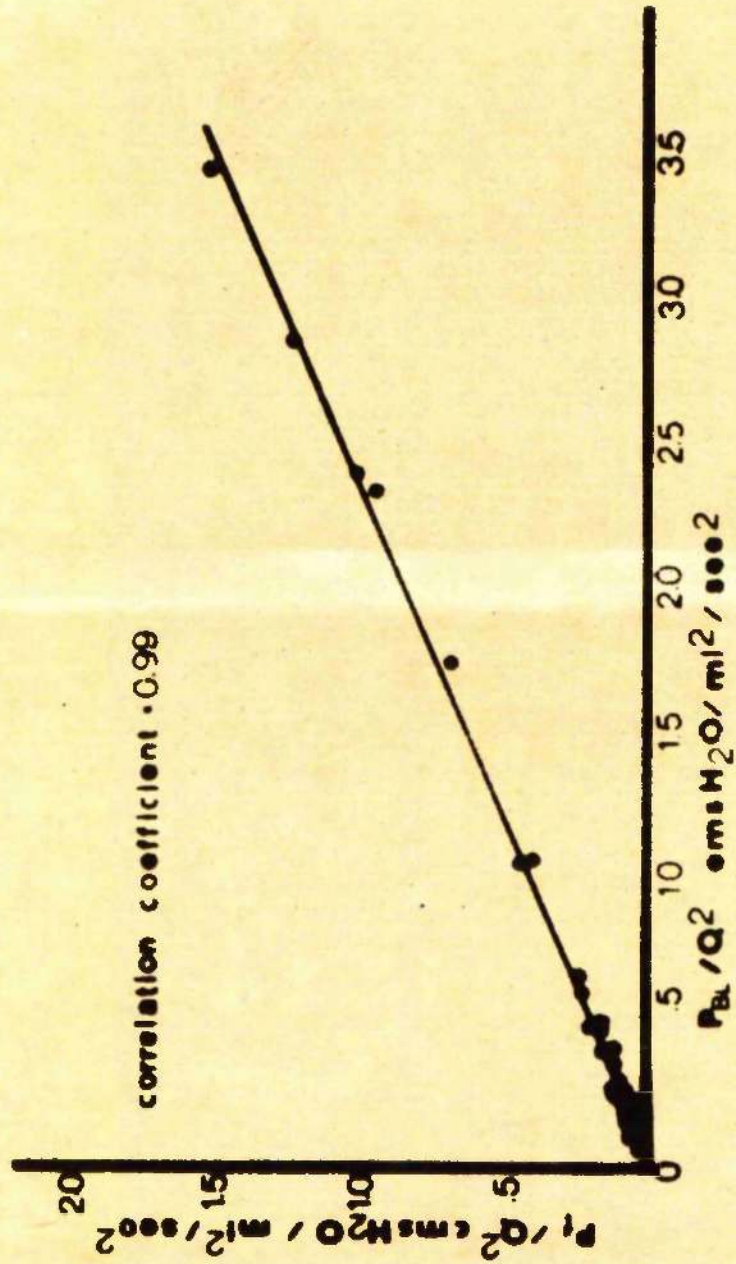


FIG 4 21

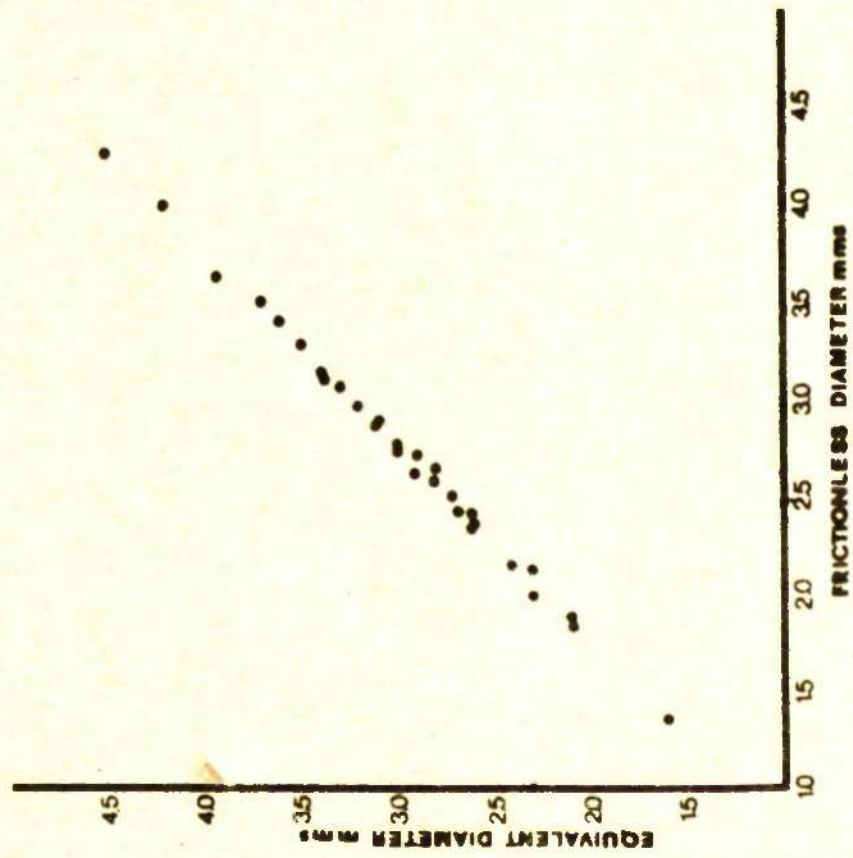


FIG 4.22

in the physiological ranges of diameters. This implies that the larger the equivalent diameter, the smaller the deviation of the resistance index from the frictional resistance. The correlation between these two variables was investigated Figure 4.21. The correlation coefficient was 0.99 and the standard deviation was 0.016. This result, therefore, implies that the resistance index is as useful as the frictional resistance in the interpretation of patient data since they appear to be approximately linearly related within the physiological range of values.

If it is assumed that there is no frictional loss, then the equivalent rigid tube lossless diameter can be determined from equation 4.1. The lossless diameter was plotted against the calculated equivalent rigid tube diameter assuming frictional loss Figure 4.22. A correlation coefficient of 0.99 was obtained. From equation 4.1 it can be seen that the lossless diameter is a function only of the resistance index.

These two results imply that the rigid tube model is an unnecessary complication and that the determination of the resistance index alone suffices to describe the urethra. This is only justifiable if it is assumed that the urethral length is constant in the patients being analysed.

The parameter RN2, defined in Chapter 3, was used to clarify the implication of the variation of the frictional resistance. The parameter R (resistance index) is an indication of the ease of micturition since it groups the properties of the bladder and the urethra. The parameter RN2 is an

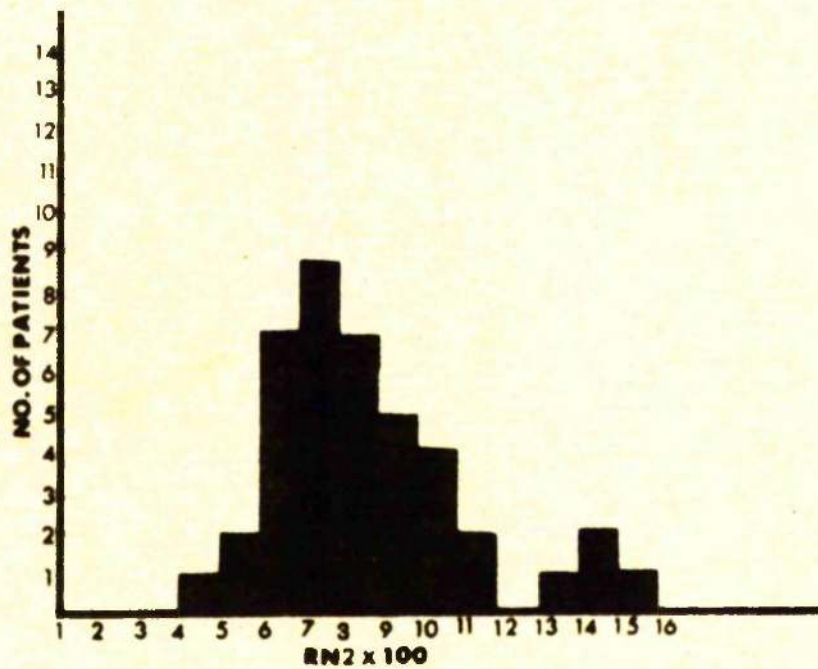


FIG 4.23

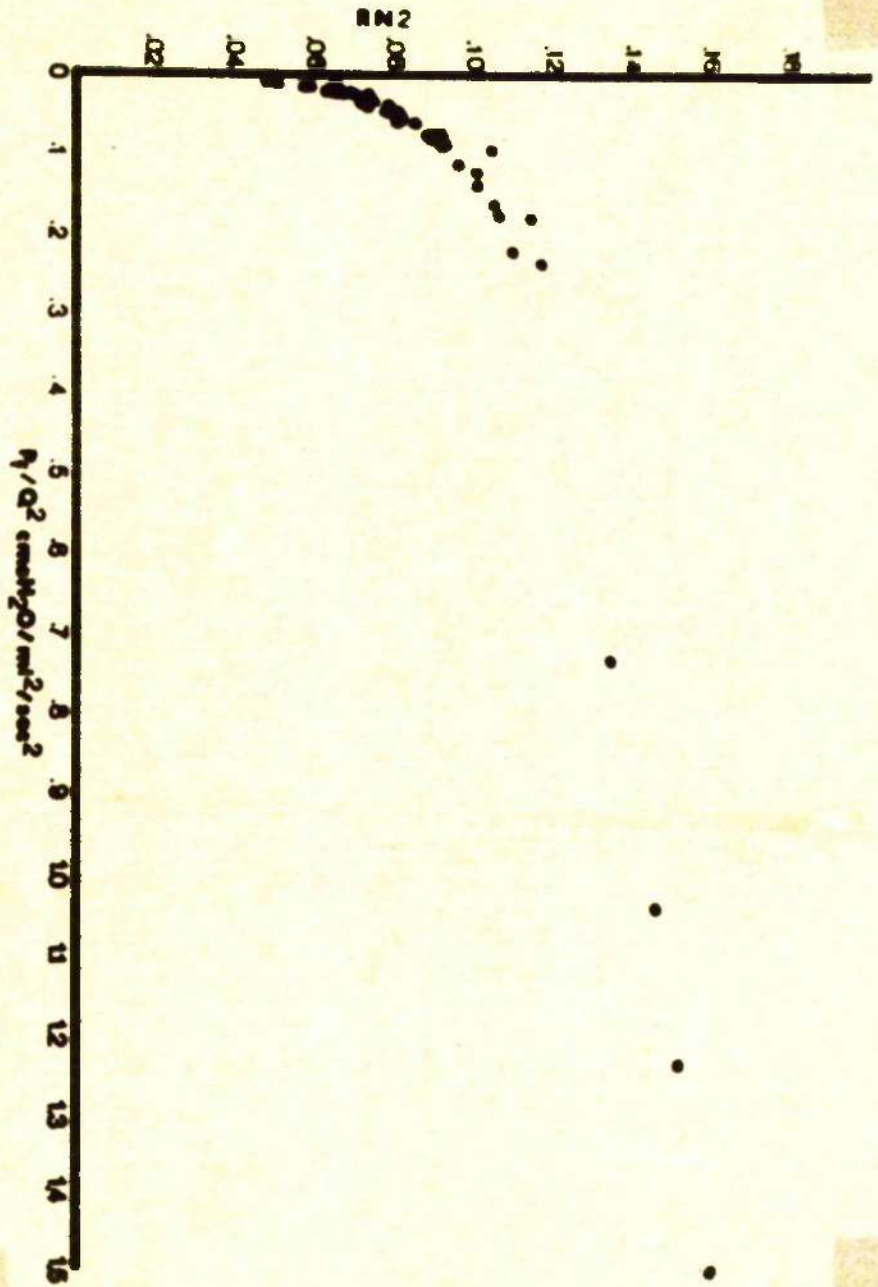
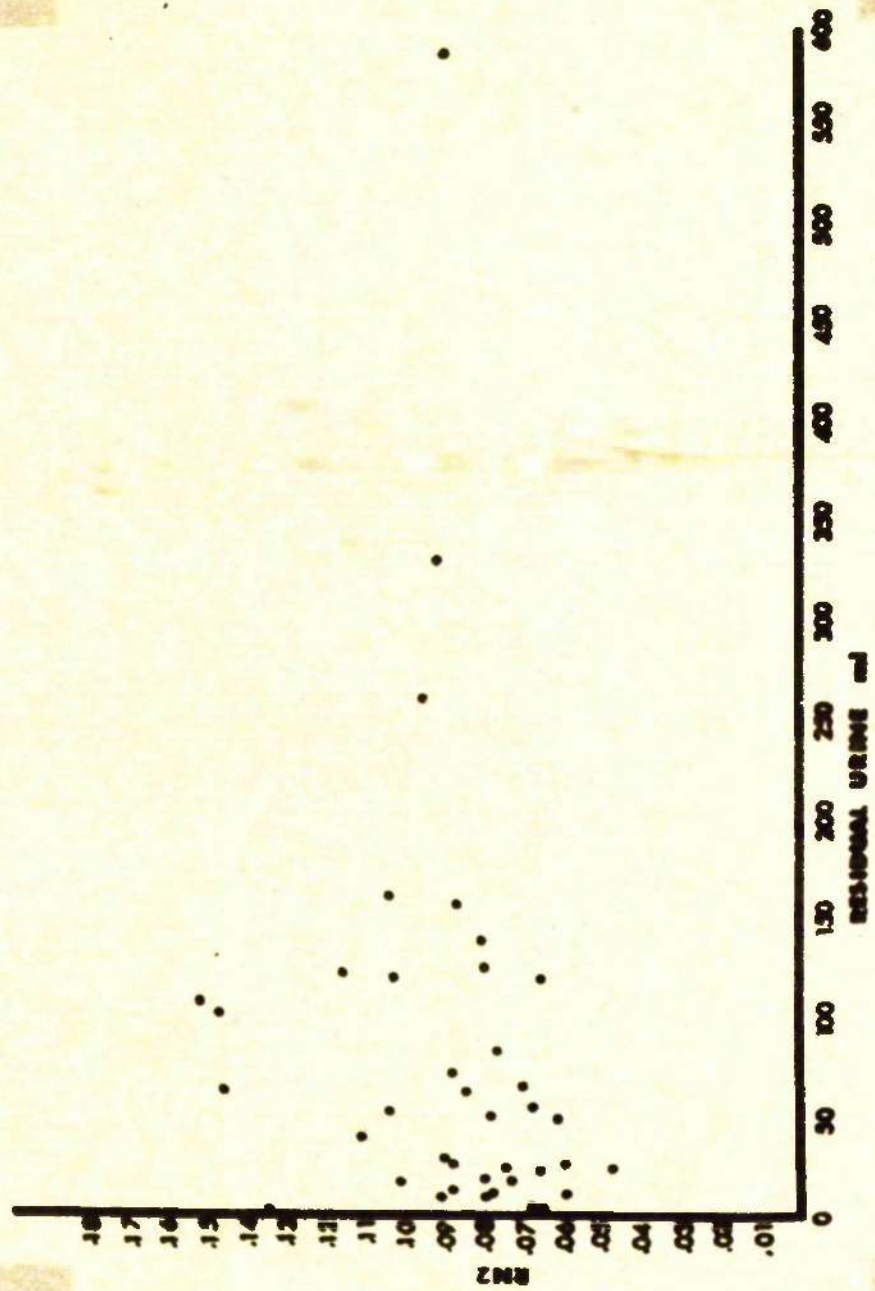


FIG 4.24

indication of the calibre of the urethra and relates the equivalent rigid tube diameter to the idealised lossless diameter. A histogram of RN2 is shown in Figure 4.23. The relationship between RN2 and the frictional resistance is shown in Figure 4.24. The parameter RN2, therefore, increases with the frictional resistance, so that the frictional resistance therefore in general does give an indication of the urethral calibre. At large values of frictional resistance, the rate of change of RN2 with the frictional resistance is small so that RN2 will tend to smooth out any individual variations at high resistances. The rate of change of RN2 with the frictional resistance is greater than 1.0 at low resistances and may, therefore, amplify patient differences in this region. The histogram for RN2 appears to be approximately symmetrical with the exception of four patients with high values of RN2. Three of these patients had peak flowrates between 6.0 and 6.5 ml/sec and one had a peak flowrate of 8 ml/sec. All of the patients developed bladder pressures greater than 100 cm H<sub>2</sub>O. The patient with the higher flowrate had the smallest value of RN2.

RN2 was found to decrease with the peak flowrate. This implies that the flowrate by itself is an indication of the calibre of the urethra although the bladder pressure and abdominal pressure would be necessary for a reliable diagnosis as found by Scott and McIlhaney (1961) and Stewart (1960). No significant correlation was found between the parameter RN2 and the residual



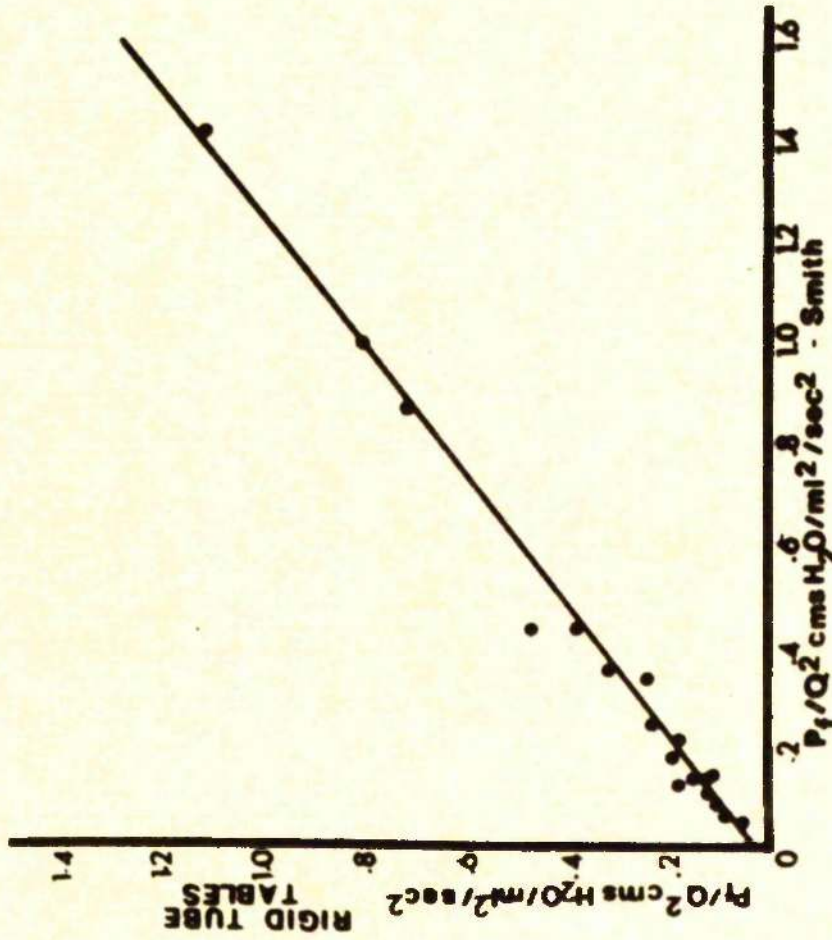


FIG 4.26

urine Figure 4.25.

Smith (1968) published the frictional resistances obtained from a series of investigations on male patients. The frictional resistance was determined using an open ended catheter inserted just beyond the external urethral meatus to measure the exit pressure. Using Smith's bladder pressure and urine flowrate data, the equivalent rigid tube frictional resistance was calculated using the rigid tube tables as determined in Chapter 3, and plotted against the frictional resistance as determined by Smith. The correlation between the two parameters is shown in Figure 4.26. The length of the rigid tube used for the calculations was 18 cm. The higher frictional resistance obtained by Smith may be due to the presence of the urethral catheter. The high degree of correlation suggests that the rigid tube theory is, therefore, a reasonable working model and that the resistance estimations made using the model are related to the values which would be determined clinically. The patient data taken from Smith (1968) included data from patients with and without apparent urethral obstruction and urethral strictures.

In those patients in whom abdominal pressure was measured simultaneously with the bladder pressure and urine flowrate, it was found that eight patients initiated micturition by the use of abdominal pressure whilst seven patients initiated micturition using intrinsic pressure alone. The intrinsic pressure is defined as the difference in the intravesical and abdominal pressures. Both abdominal and intrinsic pressure were involved in one patient.

Those patients using abdominal pressure for initiation of micturition also frequently used abdominal pressure during micturition. The flowrates also tended to be low. It would therefore seem that in the female subject, micturition need not be initiated by abdominal pressure.

The occurrence of "aftercontractions" were frequent, occurring in about 30 per cent of the female patients. During simultaneous bladder pressure, urine flowrate and abdominal pressure measurements, four patients exhibited secondary contractions. In three of these patients, the secondary contraction was not a result of abdominal pressure. The pressure rise was, therefore, due to increased detrusor activity, partial occlusion of the urethra due to muscular action resulting in an increased resistance or the possible transmission of energy from the urethra. It was also found that the occurrence of an aftercontraction was usually associated with a flowrate greater than 20 ml/sec. Out of the thirteen patients with aftercontractions, three patients obtained a peak flowrate between 14.5 and 19 ml/sec whilst ten patients developed a peak flowrate greater than 22.5 ml/sec. Of all the patients with flowrates greater than or equal to 22.5 ml/sec, 70 per cent of these patients exhibited aftercontractions. The occurrence of these aftercontractions therefore appears to be related to the magnitude of the peak urine flowrates. It is unlikely therefore that these pressure rises are due to increased detrusor activity. They may, therefore, be the result of some hydrodynamic interaction and this possibility is discussed in Chapter 6. The narrowing of

the urethra with a consequently increased resistance does not satisfactorily explain the pressure rise since the flowrate would be expected to be rapidly reduced.

Due to the distributions of bladder pressure, urine flowrate and rigid tube parameters, it is not possible to use the fluid dynamical analyses for diagnostic purposes. On the contrary, the condition of the patient tends to clarify the fluid dynamical data. When urethral obstruction can be diagnosed using rigid tube theory, the condition of the patient can often be determined from the size of the stream that the patient can develop. For this reason, it is felt that the rigid tube model is of little value diagnostically but may be of value in determining the efficacy of treatment in a given individual when performing pressure flow studies prior to and during treatment.

Recently electrical stimulation of the pelvic floor has been used in the treatment of incontinence Alexander, Rowan, Millar, Scott (1970), Alexander, Rowan (1968). The effect of electrical stimulation was investigated in three patients undergoing treatment using electrodes mounted on a vaginal pessary. The two tests were performed consecutively.

One patient with the pessary inserted but with no stimulus was found to develop a peak flowrate of 18.5 ml/sec and a corresponding bladder pressure of 64 cm H<sub>2</sub>O. On repeating the pressure flow study with the stimulus switched on, the peak flowrate was reduced to 13 ml/sec with a corresponding pressure of 68 cm H<sub>2</sub>O. This resulted in a change in the resistance from 0.187 to 0.403 and in the

equivalent rigid tube diameter from 2.8 to 2.3 mm. The parameter RN2 increased from 0.08 to 0.1. These changes suggest an increased urethral resistance to flow. A similar result was obtained in another patient in whom the resistance index changed from 0.024 to 0.031, the equivalent urethral diameter from 4.5 to 4.2 and the parameter RN2 from 0.047 to 0.05. These changes are not as significant as in the first patient and may reflect not only the effects of stimulation but also the individual variation in micturition dynamics. The flowrate profiles were changed however. In the latter case with the stimulus switched on, the flowrate profile was flattened and also widened with the micturition time rising from 18 seconds to 25 seconds. The data, therefore, indicates that there was an overall increased resistance to flow. In a third patient, the resistance index, equivalent diameter and RN2 changed from 2.33 to 1.17, 1.58 to 1.84, and 0.146 to 0.122 respectively on stimulation giving an opposite result to the previous two patients. The micturition time was also decreased. A pressure flow study was also performed on this patient prior to the insertion of the pessary. The resistance index, equivalent rigid tube diameter and RN2 were 2.9, 1.5 and 0.15 respectively. The insertion of the pessary would, therefore, seem to have decreased the resistance to flow.

One patient suffering from stress incontinence using a radio-frequency stimulator with electrodes implanted in the pelvic floor, Alexander and Rowan (1968), was also investigated prior to and after operation. In this instance, the resistance index, equivalent

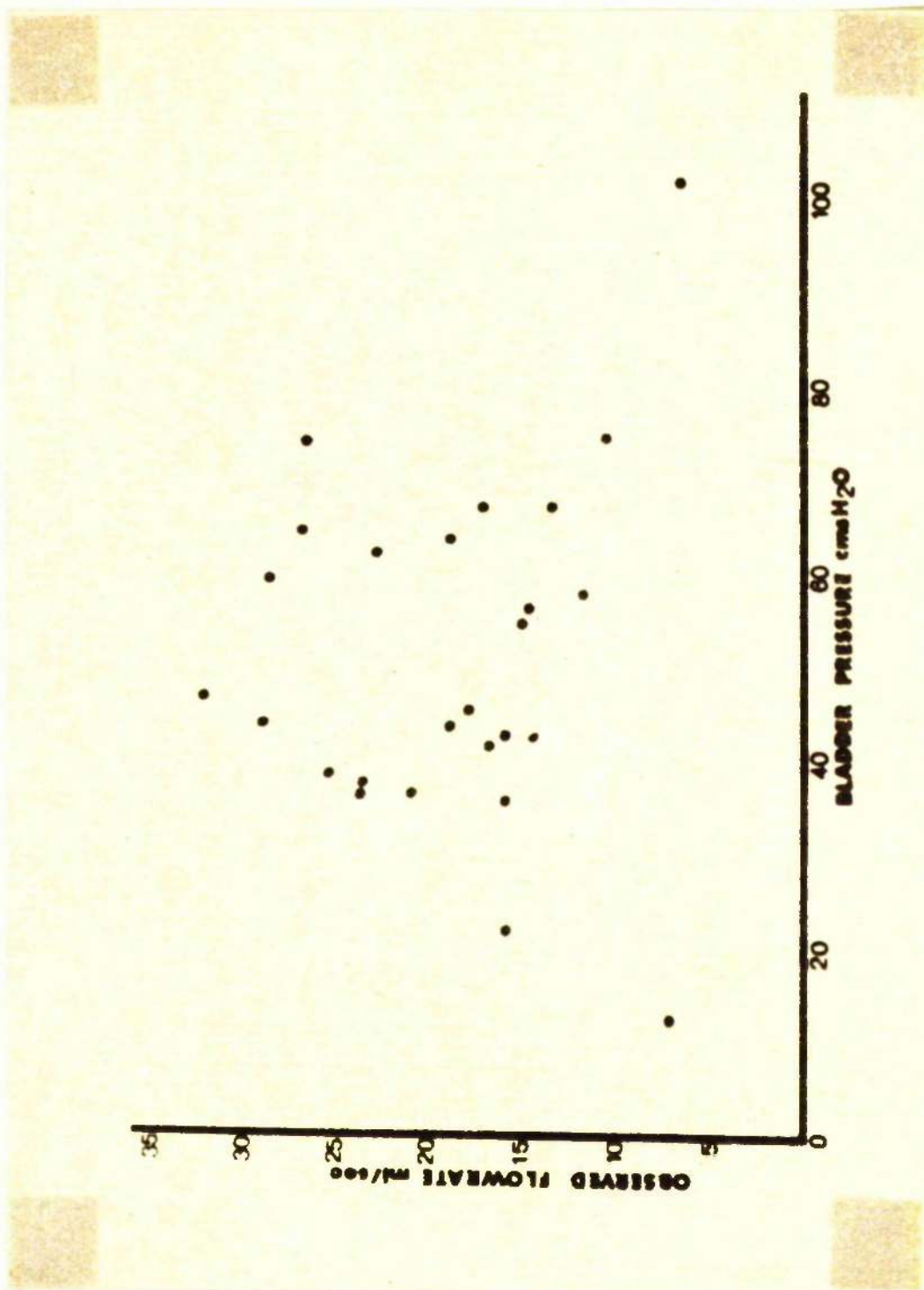


Fig. 4.27

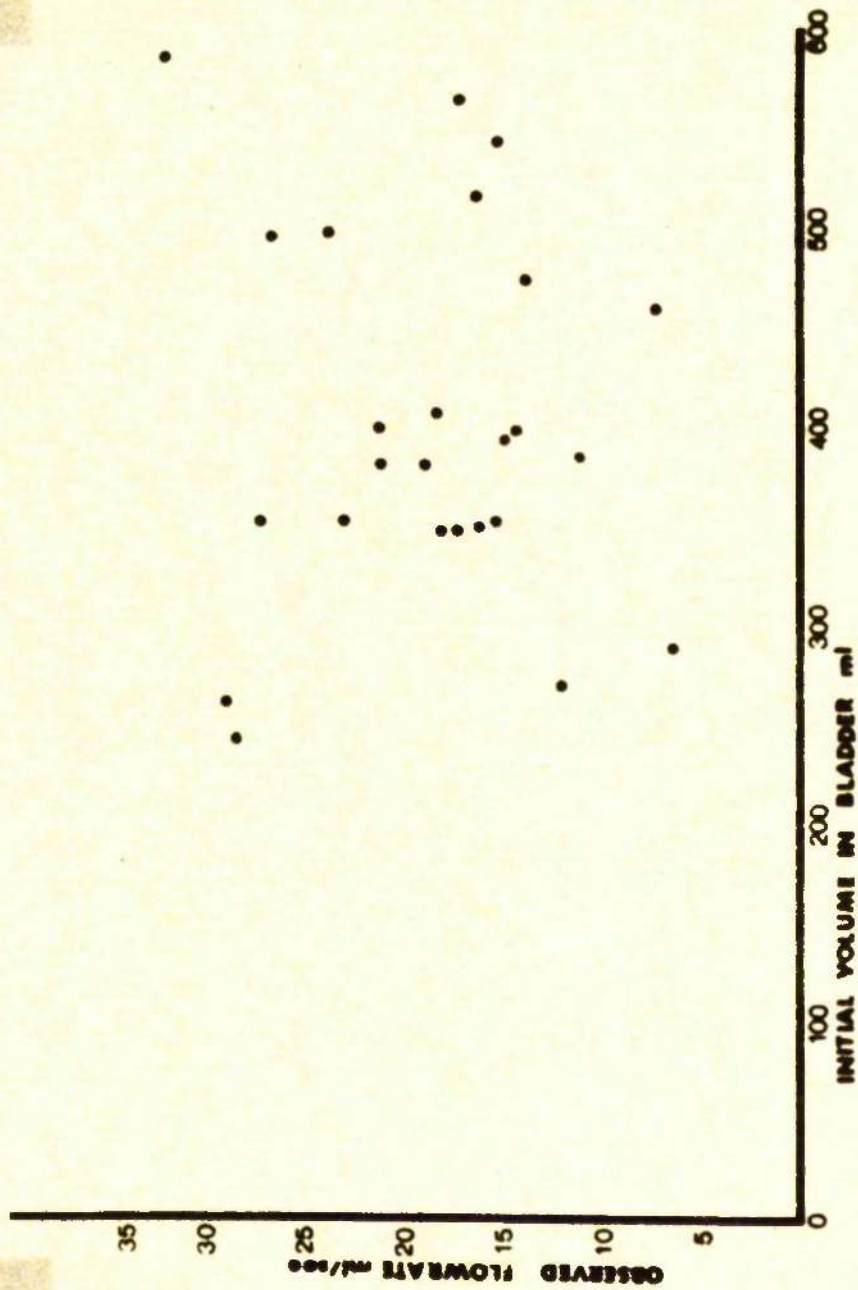


FIG 4.28

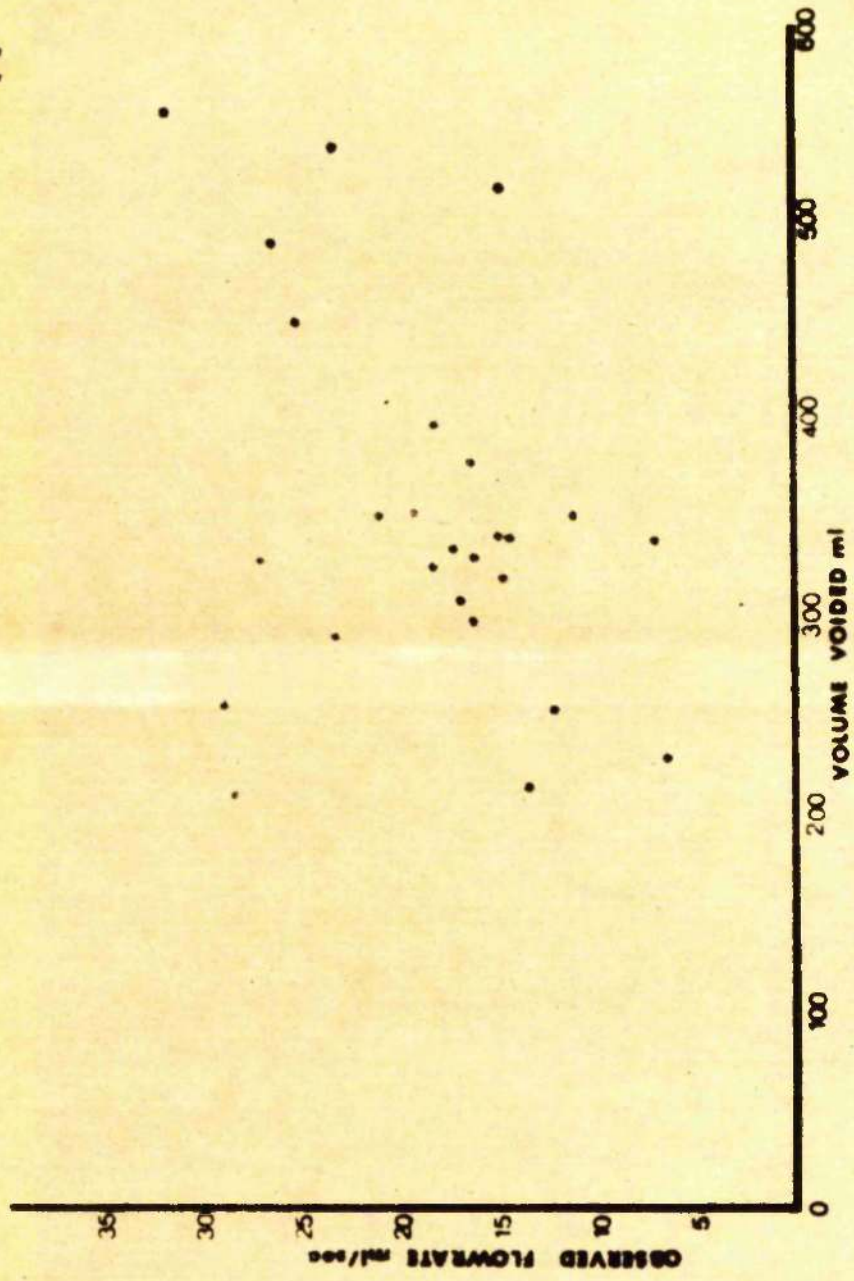


FIG 4.29

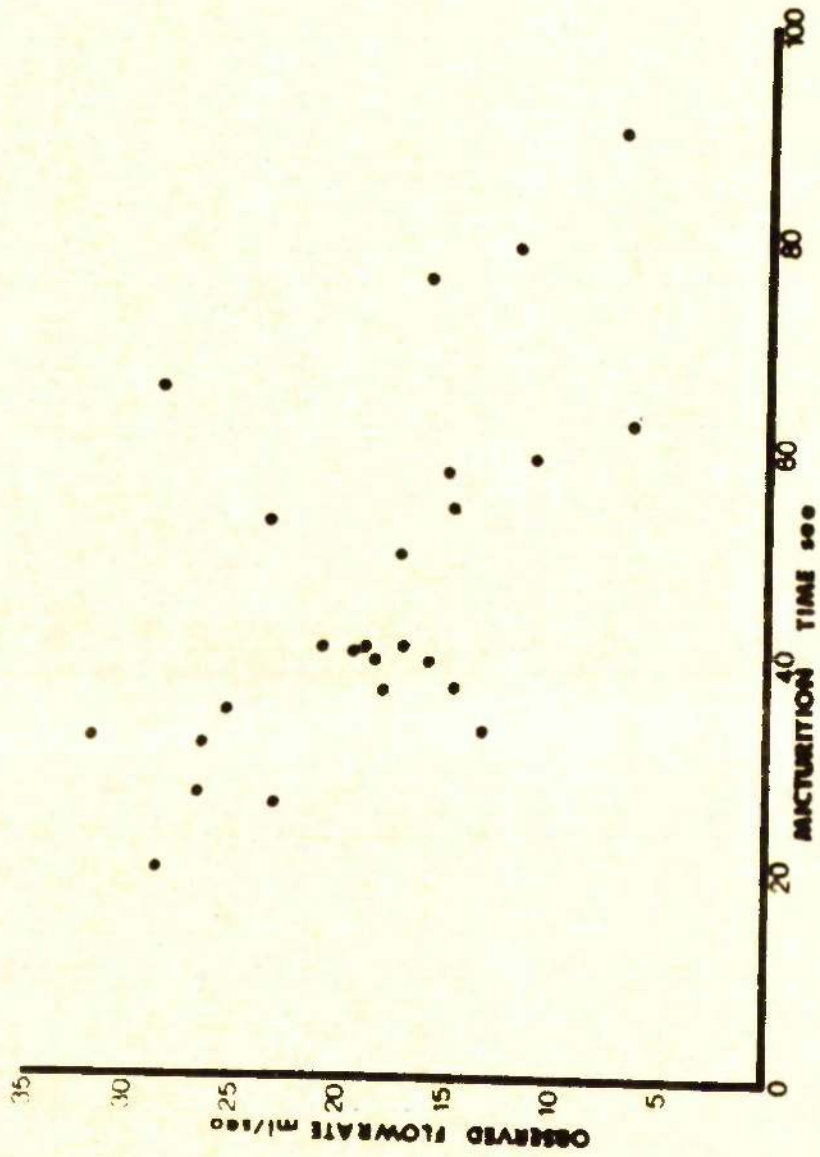


FIG 4.30

rigid tube diameter and RN2 changed from 0.115 to 0.083, 3.0 to 3.4 and 0.078 to 0.067 respectively on application of the stimulus. These results imply that the resistance to flow has decreased. The micturition time was again reduced from 47 seconds to 21 seconds. The volumes in the bladder prior to micturition were 347 ml and 380 ml and there was no change in the residual.

The patients had not been subjected to electrical stimulation prior to these studies and the results therefore indicate the initial reaction to electrical stimulation. Follow-up studies were not possible due to technical difficulties. The patient treated by the radicimplant received benefit from the treatment and therefore the long-term physiotherapeutic effect of the stimulation may not be reflected by the initial reaction.

#### 4.2 Multiple Correlation Analyses

In order to find out whether there was any relationship between the maximum urine flowrate, bladder pressure at maximum flowrate, initial volume in the bladder, volume voided and the micturition time in the group of patients suffering from incontinence, multiple correlation analysis was performed on these parameters. The peak flowrate was compared with each of these variables separately Figures 4.27, 4.28, 4.29 and 4.30. No correlation was found. The dependent variable used was the maximum urine flowrate. If  $y(k)$ ,  $x_j(k)$  refer to the  $k^{\text{th}}$  observation of the dependent variable and the  $j^{\text{th}}$  independent variable respectively, the multiple correlation analysis calculates the coefficients  $a_j$ , which are constants, for the best least squares fit of the set of equations

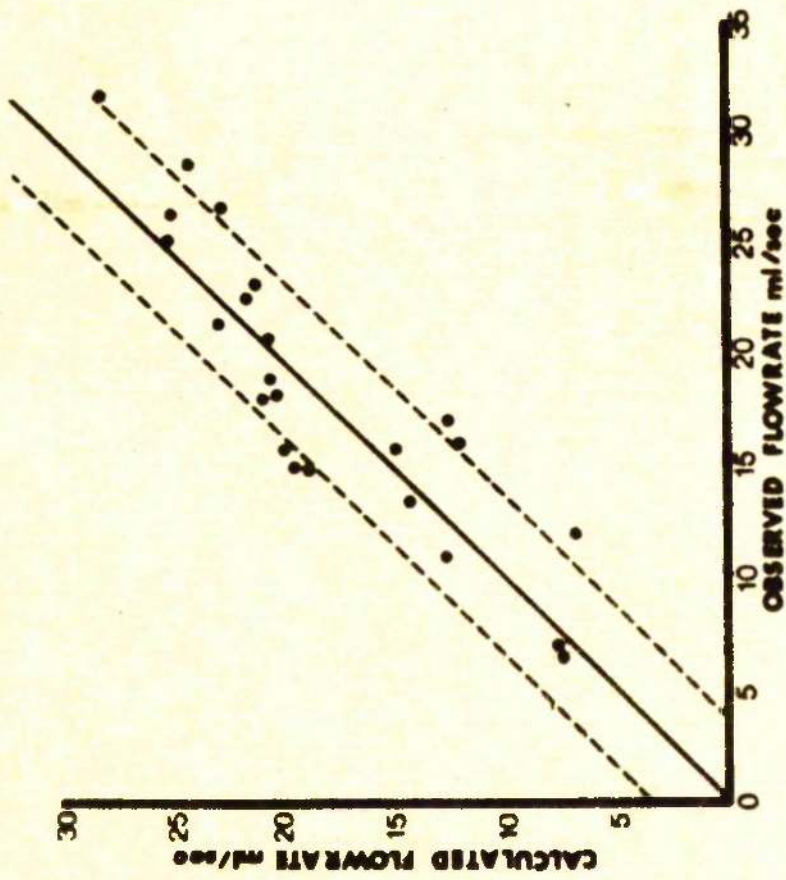


FIG 4.31

$$y(k) = a_0 + \sum_{j=1}^4 a_j x_j \quad (1)$$

$$y(1) = a_0 + \sum_{j=1}^4 a_j x_j \quad (2) \quad 4.2$$

$$\vdots \quad \vdots \quad \vdots \quad \vdots$$

$$y(N) = a_0 + \sum_{j=1}^4 a_j x_j \quad (N)$$

where  $N$  = the number of observations and the  $x_j$ ,  $j = 1, \dots, 4$ , are the independent variables.

Using the coefficients  $a_j$  and the values of  $x_j$  obtained from a clinical investigation in equation 4.2 the predicted value of  $y$ , that is,  $y_p$  can be determined. The pressure flow data obtained from twenty-nine female patients, using the isotope technique for the flowrate, were used in the calculation of the coefficients,  $a_j$ . The correlation coefficient between the predicted values  $y_p(k)$  and the observed values  $y(k)$  of the maximum urine flowrate was 0.87 and the standard deviation was 3.5 ml/sec.

The patient data used to determine the coefficients  $a_j$  were selected at random the only requirements being that:-

- (a) the micturition time was uniquely determinable, that is, there were no multiple voiding episodes;
- (b) there was no evidence of a cystocele which would result in the residual being abnormally large.

The graph of the predicted flow against the observed flow is shown in Figure 4.31. The correlation equation was found to be

$$y = 26.17 - 0.066 x_1 - 0.0128 x_2 + 0.0376 x_3 - 0.27 x_4 \quad 4.3$$

| OBSERVED FLOWRATE | CALCULATED FLOWRATE | FLOWRATE DIFFERENCE LESS THAN STANDARD DEVIATION |
|-------------------|---------------------|--|
| 230               | 231                 |  |
| 185               | 180                 |  |
| 135               | 140                 |  |
| 230               | 222                 |  |
| 200               | 180                 |  |
| 100               | 87                  |  |
| 201               | 170                 |  |
| 105               | 62                  |  |
| 50                | 132                 |  |
| 135               | 218                 |  |
| 145               | 44                  |  |
| 140               | -81                 |  |

FIG 4.32

where  $x_1$  = bladder pressure at peak flowrate - cm H<sub>2</sub>O,  $x_2$  = initial volume in the bladder - ml,  $x_3$  = volume voided - ml and  $x_4$  = micturition time - seconds.

Values of these parameters from patients not included in the set used to calculate the  $a_j$  were fed into equation 4.3 to calculate the predicted peak urine flowrate. Figure 4.32 shows the results obtained. The degree of correlation obtained in the majority of cases shows that there is some fundamental relationship between these variables from patient to patient and that the correlation determined by the defining group of patients was not fortuitous. Those patients who voided in multiple episodes did not fit the model.

From equation 4.3, it can be seen that:-

- (a) the maximum urine flowrate increases as the corresponding bladder pressure decreases, the other variables being kept constant;
- (b) the maximum urine flowrate increases as the initial volume decreases, the other variables being kept constant;
- (c) the maximum flowrate increases as the volume voided increases, the other variables being kept constant;
- (d) the maximum flowrate increases as the micturition time decreases, the other variables being kept constant.

Referring to implication (a), it is seen that this is reasonable since in order to void the same volume in the same time at a

larger flowrate, it would be required that the urethra was of a larger calibre, that is, a larger equivalent urethral diameter. This requires that the corresponding bladder pressure is reduced. Implication (b) suggests that the larger the initial volume in the bladder the less peaked the flowrate profile in time and that flowrates close to the peak flowrate would be maintained over a larger period of time (although it is required that the total micturition time remains constant). This is in accord with common experience. Results (c) and (d) are basic mass conservation laws. Thus not only does the model hold together numerically, but it does so also on physical grounds.

Equation 4.2 may be rewritten as

$$y = 26.17 - 0.066 x_1 - 0.0128 x_5 + 0.0243 x_3 - 0.27 x_4 \quad 4.4$$

where  $x_5$  = residual urine in ml.

The model, therefore, implies that the peak flowrate is reduced when the residual urine is elevated with the bladder pressure at peak flowrate, volume voided and micturition time being kept constant. The model, therefore, predicts a tendency towards reduced flowrates when

- (a) the micturition time is prolonged; or
- (b) the bladder pressure is elevated; or
- (c) the residual urine is high,

provided the other variables are within the normal range of values.

The effect on the residual volume is even more dramatic when the initial volume is kept constant rather than the volume voided.

Rearrangement of equation 4.2 gives:-

$$y = 26.17 - 0.066 x_1 + 0.0248 x_2 - 0.0376 x_5 - 0.27 x_4 \quad 4.5$$

Thus for the bladder pressure at the peak flowrate, initial volume in the bladder and micturition time remaining constant, the peak flowrate will be reduced by 3.76 ml/sec for each 100 ml residual in the bladder. In this situation, the flowrate increases with the initial volume in the bladder when the other variables in equation 4.5 are kept constant. This is because the volume voided is increased, for a given residual, so that according to the principle of mass conservation, the peak flowrate must increase assuming that the flowrate profile does not change.

Von Garrelts (1953) showed that in a given normal male the flowrate was approximately proportional to the volume voided at volumes greater than 200 ml although better correlation was obtained using the volume voided to the power 0.7. This relationship also held for a group of normal males. However, in these cases presumably the other parameters, such as the micturition time and bladder pressure, were not constant during the investigations.

Unfortunately, there is no pressure flow information available on another series of incontinent or normal adult females so that it is not as yet possible to determine whether or not the coefficients in the multiple correlation analysis will define different groups of patients, for example, incontinent patients from normals.

Recently, Krøigard (1970) published data obtained during pressure flow studies in young girls. Since there was no residual urine aspirated in these patients, the independent variables used in the multiple correlation analysis were the bladder pressure at peak

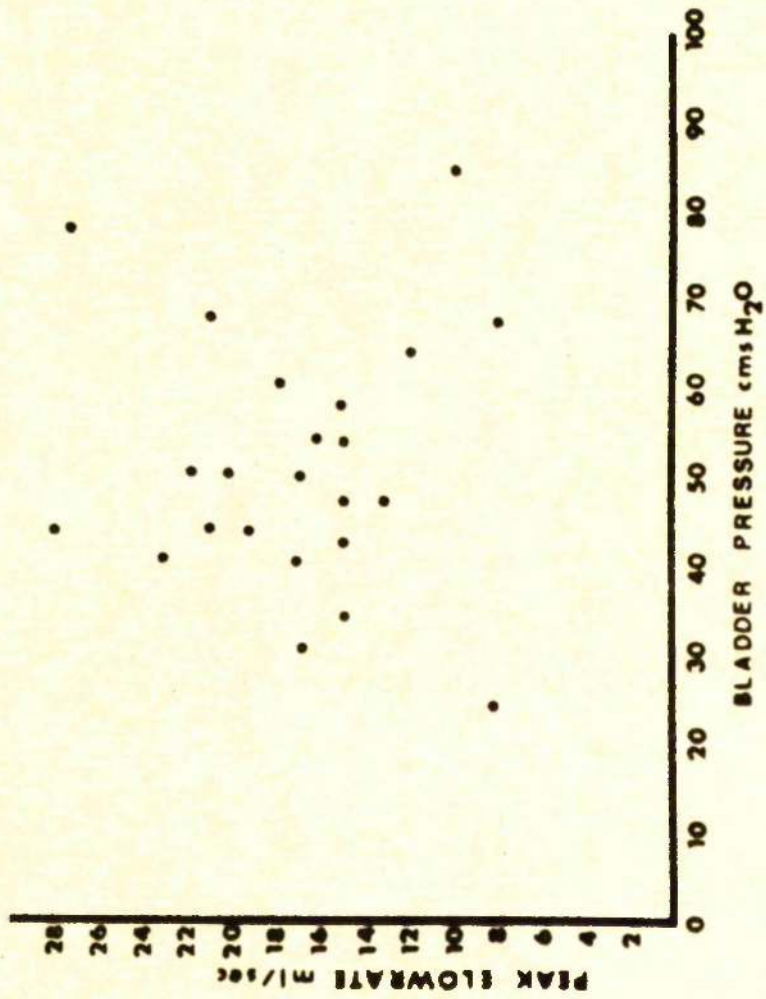


FIG 4.33

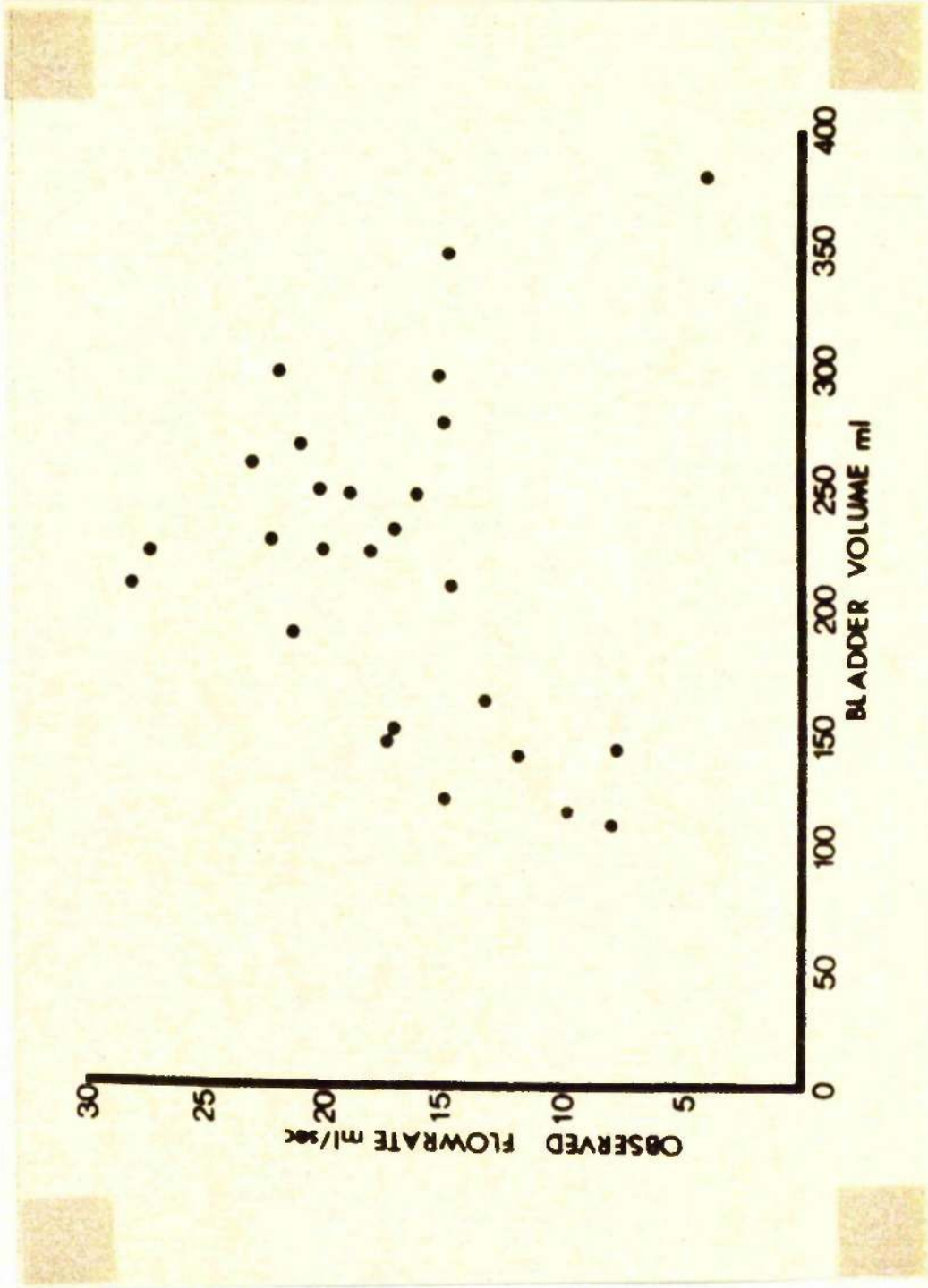


Fig. 4.34



Fig. 4.35

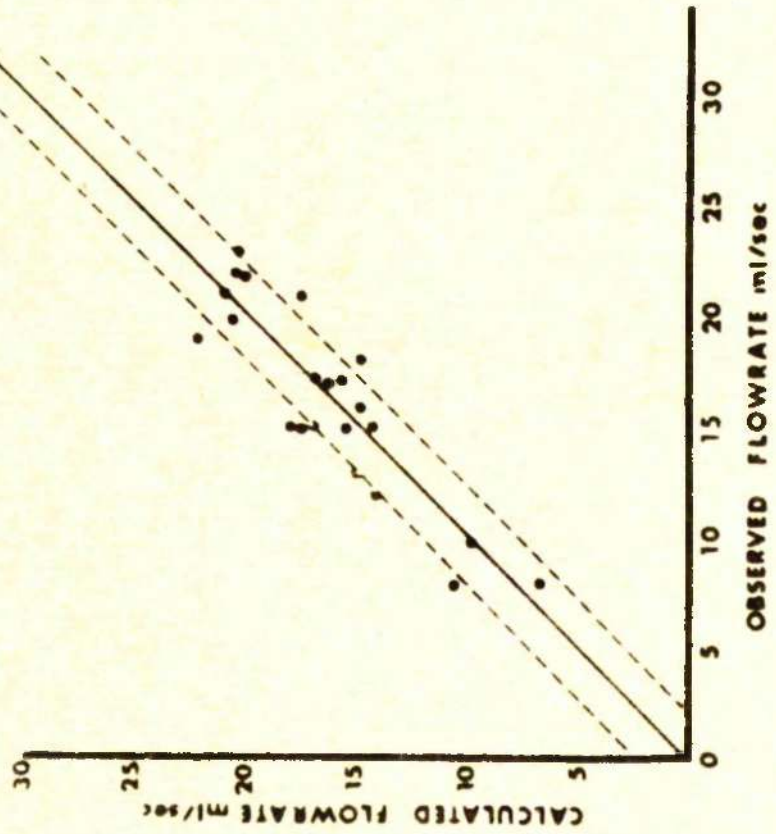


FIG 4.36

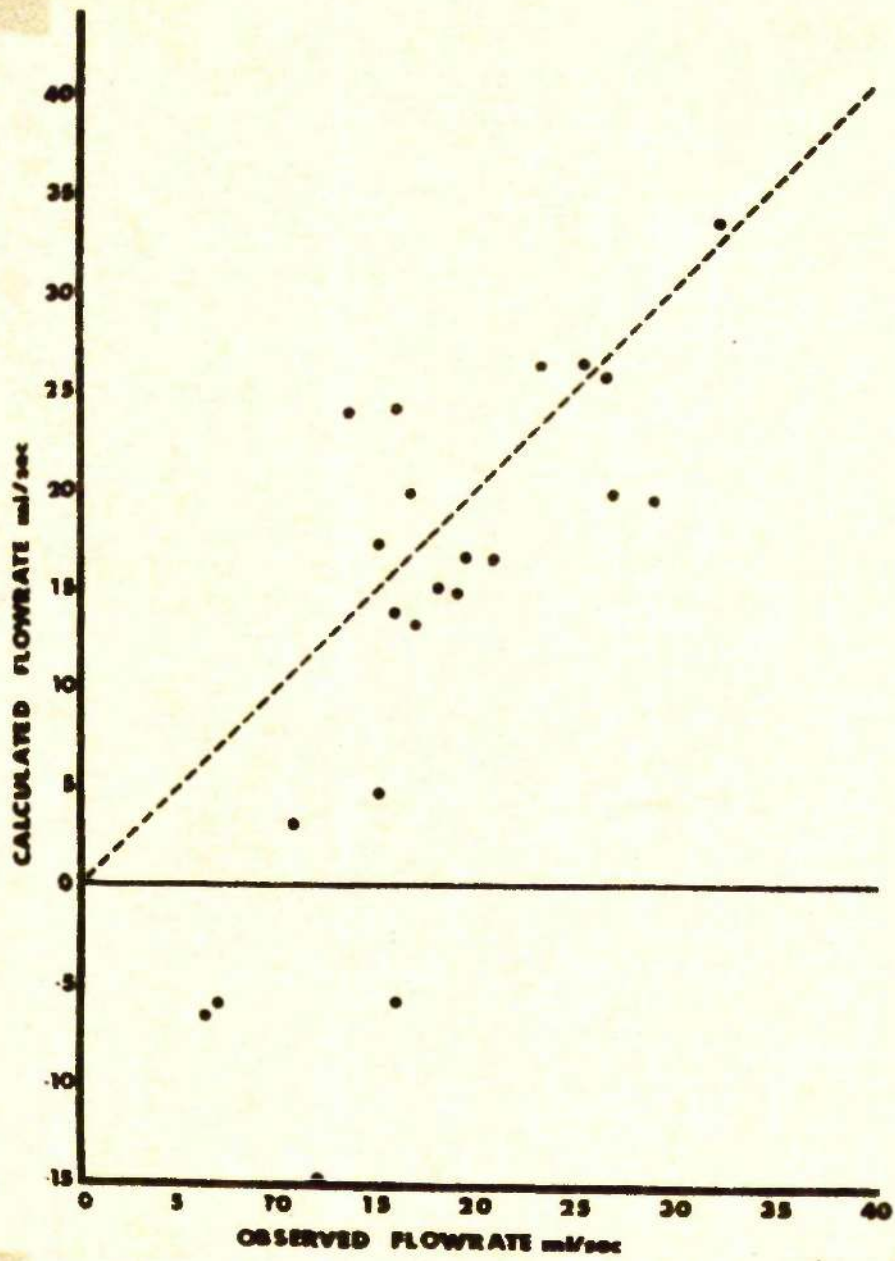


FIG 4.37

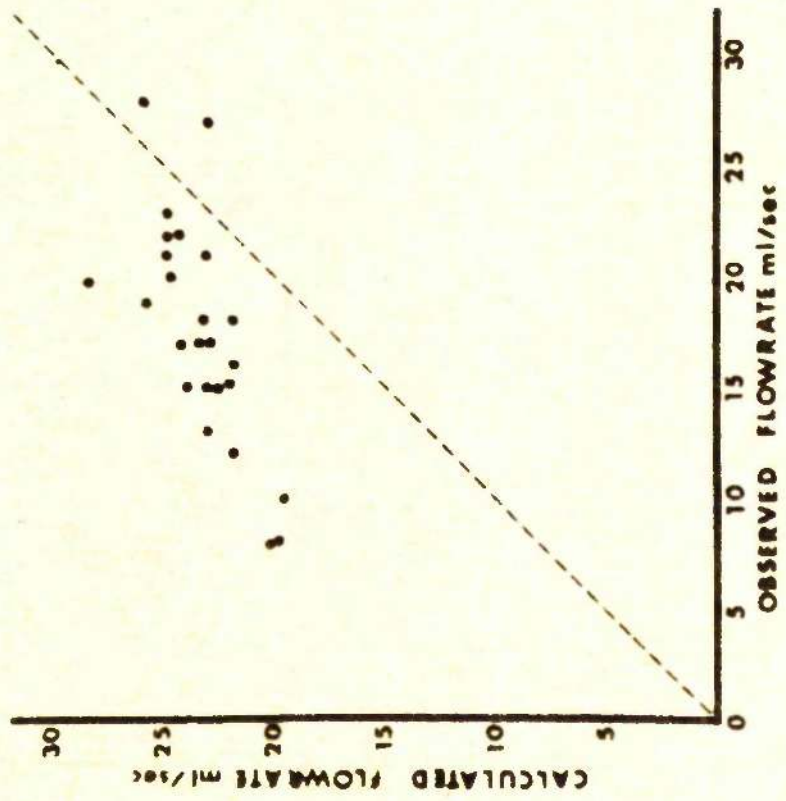


FIG 4.38

flowrate, initial volume in the bladder and the micturition time. The peak flowrate was plotted against each of the variables separately and are shown in Figures 4.33, 4.34 and 4.35. The peak flow determined from the analysis was also plotted against the observed flow Figure 4.36. The multiple correlation coefficient was 0.88 and the standard deviation 2.2 ml/sec. In order to determine whether or not the data obtained from the children defined a unique set with respect to the data obtained from the adult females in the first analysis, the adult patient data was used with the correlation coefficients determined using the children's data and the predicted peak flowrate calculated. The predicted flowrate was then compared with the observed flowrate Figure 4.37. Thirty per cent of the predicted flowrates deviated from the observed flowrates by more than two standard deviations as defined by the set of children's data. This suggests that the two sets of data define different groups of patients. This implication is also supported by calculating the predicted peak flowrate for children using the correlation coefficients determined by the adult data. The predicted peak flowrate was plotted against the observed flowrate Figure 4.38. In this case 50 per cent of the predicted peak flowrates deviated by more than two standard deviations as determined by the adults' set of data. It is possible that the residual urine was not zero in these patients, with this error amplifying any deviation from the adult model.

The frictional resistances and equivalent rigid tube diameters were calculated for the set of children's data, using a urethral length of 3 cm, from the tables previously discussed in Chapter 3.

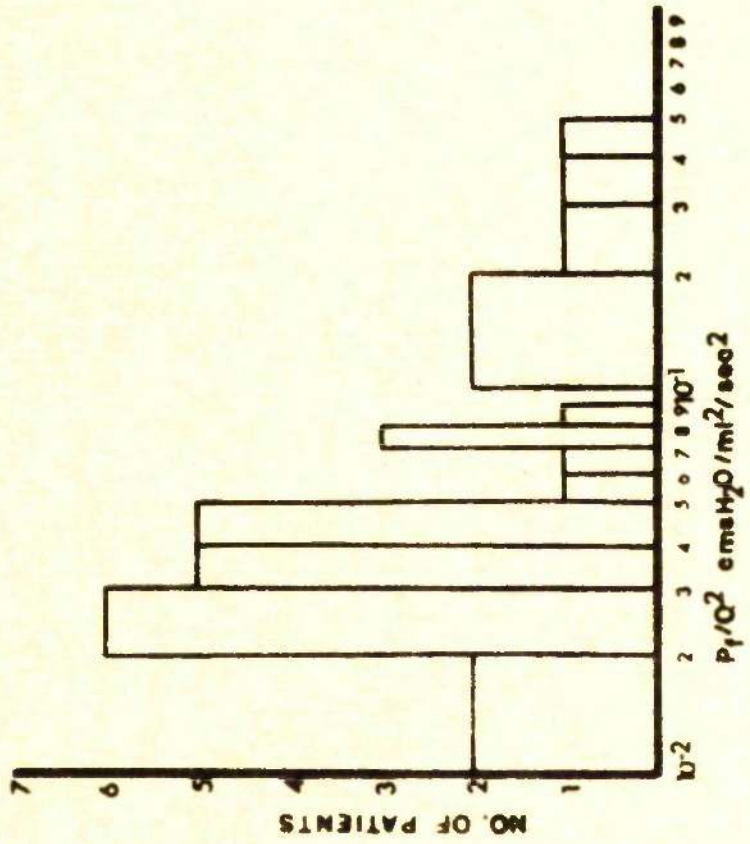


FIG 4.39

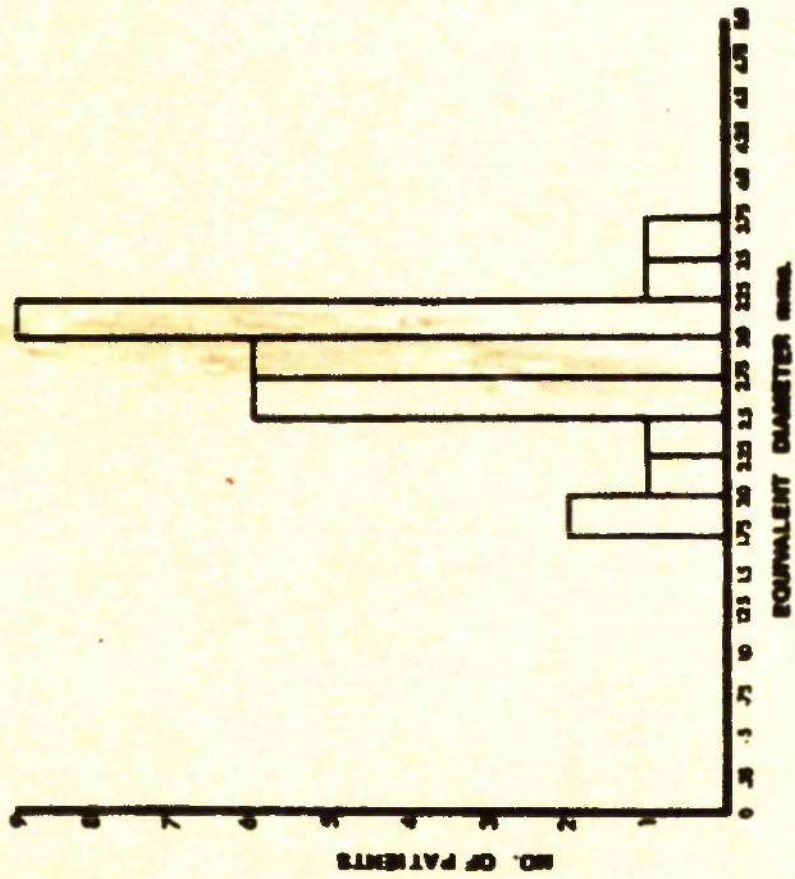


FIG 4.60

The distributions of these parameters are shown in Figures 4.39 and 4.40. From these distributions it would not be possible to separate out the children from the adults.

At the present stage, it is not possible to use this model as a basis for diagnosis since within the adult group of patients, the majority of flowrates are determinable to within a standard deviation of 3.5 ml/sec whilst 50 per cent of the children were indistinguishable from the adults. Once a much larger group of patients has been analysed, it may be possible to obtain more accurate values for the correlation coefficients which may permit the discrepancies between the observed and predicted flowrates to be used as a diagnostic basis, with, for example, predicted flowrates greater than observed flows implying a tendency towards increased resistance.

The correlation equation for the data from the children obtained by Krøigaard (1970) is -

$$y = 16.6 - 0.0625 x_1 + 0.0641 x_2 - 0.572 x_4$$

Comparison with the corresponding equation for the adult data shows that the correlation coefficients for the bladder pressure are very similar and that the main discrepancy between the two groups of data lies in the bladder volume and micturition time coefficients.

The order of significance of the variables in the group of data from the adult patients in accounting for the residual error sum of squares was, in descending order, the micturition time, volume voided, bladder pressure at peak flowrate and the initial volume in the bladder. In the data from Krøigaard's studies the order was initial volume in bladder (equivalent to the volume voided),

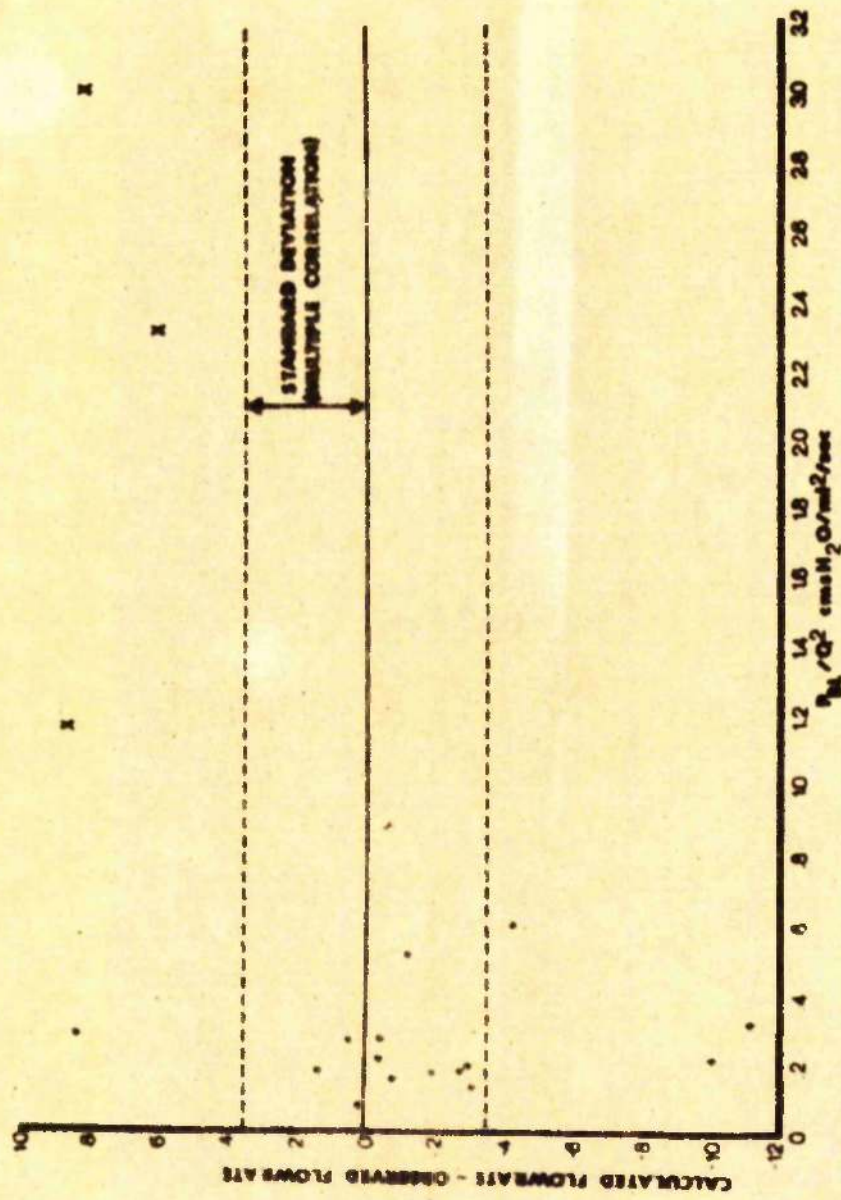


FIG 4.41

micturition time and the bladder pressure at peak flowrate. The multiple correlations for the variables in the group of adults lay between 0.796 and 0.849 except for the micturition time when it was 0.5. The group of children, however, gave multiple correlations of 0.879, 0.297 and 0.568 for the bladder pressure, initial volume in the bladder and micturition time respectively. The multiple correlations are comparable in the two groups except for the initial volume in the bladder for which the adult group showed a better correlation.

Using adult data not used to develop the multiple correlation model, the difference between the predicted peak flowrate and the observed peak flowrate was correlated with the resistance index Figure 4.41. The values marked with an X were points obtained from the same patient with and without an electric pessary inserted and with the pessary switched on and off. This was the patient discussed on page 4.12 where the pessary appeared to reduce the urethral resistance. Two of the patients with negative differences in excess of a standard deviation had multiple voiding episodes. The patients with a resistance greater than  $0.6 \text{ cm H}_2\text{O/ml}^2/\text{sec}^2$  developed a peak flow less than the predicted flow whilst three patients with flows less than the peak flowrate by more than one standard deviation had resistances less than  $0.6 \text{ cm H}_2\text{O/ml}^2/\text{sec}^2$ . Of the eleven patients whose predicted flow lay within one standard deviation of the observed flow only four values exhibited a positive difference. Eleven of the seventeen patients developed flowrates greater than the predicted flowrates. This correlates with the fact that the patients

were suffering from incontinence. The degree to which any predicted value differs from the observed value may be less marked at this stage since in the development of the model a non-homogeneous group of patients was used. The results, however, suggest that this type of analysis may eventually be of diagnostic value.

CHAPTER 5Elastic Tube Theory I5.1 Elastic Tube Theory

Since it is not possible to describe the time varying flow in the urethra using the rigid tube model, it is necessary to investigate fluid flow through highly distensible tubes. The urethra is such a tube but with time varying elastic properties along its length. The manner in which these properties change is not known. The urethra, therefore, as a first approximation, is considered to be a homogeneous elastic tube with time independent properties and a circular cross-section. During the main part of the flow in the urethra, it is expected that the elastic properties will not change significantly with time and that the significant changes in elasticity will occur at the beginning and end of micturition.

5.2 The Flow Equation

The equation of continuity may be written -

$$\frac{D(\rho Av)}{Dt} = 0$$

where  $\rho$  = density of the fluid,  $v$  = velocity of a stream tube and  $A$  = area of the stream tube.

Let  $ds$  = element of length. Then

$$\frac{\partial(\rho A ds)}{\partial t} + v \frac{\partial}{\partial s} (\rho A) ds = 0$$

$$\frac{\partial}{\partial t} (\rho A) ds + \rho A dv + v \frac{\partial}{\partial s} (\rho A) ds = 0$$

Therefore,

$$\frac{\partial}{\partial t} (\rho A) + \frac{\partial}{\partial s} (\rho Av) = 0$$

Thus, if  $v$  = the average velocity over the cross-section of the tube and  $A$  = the cross-sectional area of the tube at some point  $z$  at time  $t$ , then -

$$\frac{\partial Q}{\partial z} + \frac{\partial A}{\partial t} = 0 \quad 5.1$$

where  $Q = vA$  and  $\rho = \text{constant}$ , that is, the fluid is incompressible.

The general equations of fluid motion are (Schlichting (1955)) -

$$\frac{\partial \underline{v}}{\partial t} + (\underline{v} \cdot \text{grad}) \underline{v} = -\frac{1}{\rho} \text{grad} (p) + \nu \nabla^2 \underline{v}$$

where  $\underline{v} = (v_1, v_2, v_3)$  = velocity vector,  $p$  = pressure and  $\nu$  = kinematic viscosity.

If motion along the  $z$ -axis only of the elastic tube is considered, then using cylindrical co-ordinates  $(r, \theta, z)$

$$\frac{\partial u}{\partial t} + u \frac{\partial u}{\partial z} = -\frac{1}{\rho} \frac{\partial p}{\partial z} + \nu \nabla^2 u \quad 5.2$$

where  $u$  is the velocity along the  $z$ -axis.

In order to apply an averaging process across the cross-section of the tube, both sides of equation 5.2 are multiplied by  $2\pi r$  and integrated between 0 and  $R$  where  $R$  is the radius of the tube at the point  $z$ . Then -

$$\int_0^R 2\pi r \frac{\partial u}{\partial t} dr + \int_0^R 2\pi r u \frac{\partial u}{\partial z} dr + \frac{1}{\rho} \int_0^R 2\pi r \frac{\partial p}{\partial z} dr = \nu \int_0^R 2\pi r \nabla^2 u \quad 5.3$$

Therefore, denoting the left hand side of equation 5.3 by L.H.S. -

$$\text{L.H.S.} = 2\pi \int_0^R r \frac{\partial u}{\partial t} dr + \int_0^R r u \frac{\partial u}{\partial z} dr + \frac{1}{\rho} \int_0^R r \frac{\partial p}{\partial z} dr$$

If  $P$  and  $Q$  are two variables which are functions of  $x$ ,

then -

$$\overline{PQ} = \frac{\int_0^R PQ \, dx}{\int_0^R dx}$$

where  $\overline{PQ}$  = the average value of  $PQ$  between  $x = 0$  and  $x = R$ .

Hence,

$$\begin{aligned} \overline{Ar} &= \frac{\int_0^R Ar \, dr}{\int_0^R dr} \\ &= \frac{1}{R} \int_0^R Ar \, dr \end{aligned}$$

Therefore,

$$\text{L.H.S.} = 2\pi r \left( r \frac{\partial u}{\partial t} + r u \frac{\partial u}{\partial z} + \frac{1}{\rho} r p \right)$$

If  $A'$  is defined by the equation

$$\frac{R}{2} A' = \overline{Ar}$$

and similarly for  $u$ ,  $\frac{\partial u}{\partial z}$

$$\text{L.H.S.} = R^2 \left( \frac{u'}{t} + u \frac{u'}{z} + \frac{1}{\rho} p' \right)$$

In cylindrical co-ordinates -

$$\nabla^2 = \frac{\partial^2}{\partial r^2} + \frac{1}{r} \frac{\partial}{\partial r} + \frac{\partial^2}{\partial z^2}$$

Therefore, from equation 5.3

$$\text{R.H.S.} = 2\pi \mu \left[ \int_0^R r \frac{\partial^2 u}{\partial r^2} \, dr + \int_0^R \frac{\partial u}{\partial r} \, dr + \int_0^R r \frac{\partial^2 u}{\partial z^2} \, dr \right]$$

$$= 2\pi\nu R \left. \frac{\partial u}{\partial r} \right|_R + 2\pi\nu \frac{R^2}{2} \frac{\partial^2 u'}{\partial z^2}$$

On integration by parts

$$\text{R.H.S.} = 2\pi R \tau \Big|_R + \Delta\nu \frac{\partial^2 u'}{\partial z^2}$$

where  $\tau \Big|_R$  = shear stress at the wall, that is at  $r = R$ .

Hence the resulting equation is -

$$\frac{\partial u'}{\partial t} + u \frac{\partial u'}{\partial z} + \frac{\partial p'}{\partial z} = \frac{2}{R} \tau \Big|_R + \nu \frac{\partial^2 u'}{\partial z^2}$$

In order to relate the value  $u'$  to the average velocity, it is necessary to investigate the velocity distribution across the tube. Since the flow is basically turbulent (though not fully turbulent) in the tube, the flow profile is expected to be almost flat. If the velocity profile were flat then  $u' = \bar{u}$  = the average velocity. The deviation of  $u'$  from  $\bar{u}$  was estimated using the velocity distribution law for turbulent flow

(Schlichting (1955)). The law is:-

$$u = u_m \left(\frac{r}{R}\right)^{\frac{1}{n}}$$

for steady flow where  $u_m$  = the maximum velocity.

Assuming that -

$$u(z, r) = u_m(z) \left(\frac{r}{R}\right)^{\frac{1}{n}}$$

then

$$\begin{aligned} \bar{u} &= u_m \frac{1}{R} \int_0^R \left(\frac{r}{R}\right)^{\frac{1}{n}} dr \\ &= \frac{u_m(z)}{\left(1 + \frac{1}{n}\right)} \end{aligned}$$

and

$$\bar{u} \frac{\partial \bar{u}}{\partial z} = \frac{u_m(z) \frac{\partial u_m(z)}{\partial z}}{\left(1 + \frac{1}{n}\right)^2}$$

Also

$$\begin{aligned} u' &= \frac{2}{R} \int_0^R u r \, dr \\ &= \frac{2}{R^2} u_m \int_0^R \frac{r \left(1 + \frac{1}{n}\right)}{1 + \frac{1}{n}} \, dr \\ &= \frac{2u_m}{2 + \frac{1}{n}} \end{aligned}$$

Therefore,

$$\frac{u' - \bar{u}}{u'} = \frac{1}{2(n+1)}$$

For  $n = 9$ , the difference is of the order of 5 per cent.

Similarly

$$u \frac{\partial u'}{\partial z} = \frac{u_m \frac{u_m}{z}}{\left(1 + \frac{1}{n}\right)}$$

and

$$\frac{u \frac{\partial u'}{\partial z} - \bar{u} \frac{\partial \bar{u}}{\partial z}}{u \frac{\partial u'}{\partial z}} = \frac{1}{n+1}$$

For  $n = 9$  the error is of the order of 10 per cent.

These calculations give an approximate indication of the error involved in the equations. Since the female urethra is short, approximately 3 cm, the velocity profile will be much flatter than

the velocity profile used. The error will, therefore, in general be much less. The equations may be further simplified by ignoring the term  $\frac{\partial^2 u}{\partial z^2}$ . In the model used, the flow and urethral profiles are continuous functions so that  $\frac{\partial^2 u}{\partial z^2}$  will be small compared to  $\frac{\tau}{R}$ .

The resulting fluid dynamical equations are, therefore

$$\frac{\partial Q}{\partial z} + \frac{\partial A}{\partial t} = 0 \quad 5.4$$

$$\frac{\partial \bar{u}}{\partial t} + \bar{u} \frac{\partial \bar{u}}{\partial z} = -\frac{1}{\rho} \frac{\partial p}{\partial z} + \frac{2\tau}{R} \quad 5.5$$

Since  $Q = \bar{u} A$ , equation 5.5 may be written:-

$$\frac{\partial Q}{\partial t} + \frac{Q}{A} \frac{\partial Q}{\partial z} - \frac{Q}{A} \frac{\partial A}{\partial t} - \frac{Q^2}{A^2} \frac{\partial A}{\partial z} + A \left( \frac{1}{\rho} \frac{\partial p}{\partial z} - \frac{2\tau}{R} \right) = 0 \quad 5.6$$

Since these are three dependent variables  $Q$ ,  $A$  and  $p$ , another equation describing the elastic property of the tube is required, that is, an equation relating the pressure  $p$  and the area  $A$ . This equation is assumed to be of the form -

$$p = \gamma \times H(A, z, t) \quad 5.7$$

where  $\gamma = \text{constant}$  and  $H$  is some function of  $A$ ,  $z$  and  $t$ .

The set of equations 5.4, 5.6 and 5.7 form a set of quasi-linear partial differential equations for the variables  $Q$ ,  $p$  and  $A$  in the two independent variables  $z$  and  $t$ . There are two main methods of solving these equations numerically:-

- (a) finite difference techniques
- (b) method of characteristics.

In the first method extreme care has to be taken since the algorithms used tend to become unstable. The equations are more

conveniently solved using the method of characteristics.

### 5.3 Method of Characteristics

A detailed account of the theory of characteristics is given by Berezin and Zhidkov (1965). Consider the set of  $n$  quasilinear partial differential equations for the  $n$  dependent variables  $u_1 \dots u_n$  in two independent variables  $x$  and  $y$ .

$$AU_x + BU_y = C \quad 5.8$$

where

$$U = \begin{pmatrix} u_1 \\ u_1 \\ \vdots \\ u_n \end{pmatrix}$$

$$U_x = \begin{pmatrix} \frac{\partial u_1}{\partial x} \\ \frac{\partial u_2}{\partial x} \\ \vdots \\ \frac{\partial u_n}{\partial x} \end{pmatrix}$$

and

$$U_y = \begin{pmatrix} \frac{\partial u_1}{\partial y} \\ \frac{\partial u_2}{\partial y} \\ \vdots \\ \frac{\partial u_n}{\partial y} \end{pmatrix}$$

and  $A$  and  $B$  are the matrices of the coefficients of  $U_x$  and  $U_y$  respectively. It is assumed that  $U$  is known in some region  $R$ .

Suppose that  $C$  is a differentiable curve in  $R$  where  $C = C(x, y, u_i)$ .

Let  $p_i = \frac{\partial u_i}{\partial x}$  and  $q_i = \frac{\partial u_i}{\partial y}$ . Then

$$du_i = p_i dx + q_i dy$$

$$dU = P dx + Q dy$$

where

$$P = \begin{pmatrix} p_1 \\ p_2 \\ \vdots \\ p_n \end{pmatrix} \text{ and } Q = \begin{pmatrix} q_1 \\ q_2 \\ \vdots \\ q_n \end{pmatrix}$$

Therefore,

$$AP + BQ = C$$

$$(A dy - B dx) P = C - B dU$$

In order that  $P$  can be determined knowing  $U$ , it is required that  $\Delta = |A dy - B dx| = 0$  since otherwise  $P$  and  $Q$  are also determined. If  $\Delta = 0$ , the system admits an infinite number of solutions. Therefore,

$$|A \lambda - B| = 0 \quad 5.10$$

where  $\lambda = \frac{dy}{dx}$ .

This implies  $n$  values of  $\lambda$ .

Since this requirement necessitates that  $P, Q$  are not determined on  $C$  (the characteristics of the set of equations), discontinuous solutions to the equations may be allowed on  $C$ . Thus once the  $\lambda^{(i)}$  ( $i = 1, n$ ) are determined from equation 5.10,  $dU$  can be determined from equation 5.9.



#### 5.4 Solution of the Flow Equations

Using equations 5.4 and 5.6 it is found that the characteristic directions are given by:-

$$\lambda_+ = \frac{Q}{A} + \sqrt{A \frac{dp}{dA}}$$

$$\lambda_- = \frac{Q}{A} - \sqrt{A \frac{dp}{dA}}$$

Let  $C = \sqrt{A \frac{dp}{dA}}$  = critical velocity characterised by the elastic properties of the tube. The characteristic directions are, therefore, real (provided  $\frac{dp}{dA} \geq 0$ ) and distinct unless  $\frac{Q}{A} = \sqrt{A \frac{dp}{dA}}$ . The analysis becomes unstable as  $\frac{Q}{A}$  approaches C. The critical flowrate  $Q_{crit}$  is defined as  $Q_{crit} = A C$

Considering Figure 5.1 and using equation 5.9

$$(A\lambda_+ - B) P dx = C - B (U(P) - U(J)) \quad 5.11$$

and

$$(A\lambda_- - B) P dx = C - B (U(P) - U(K)) \quad 5.12$$

Supposing that the solution to the partial differential equations is known or specified at specific points on the line  $x = x_0$ , for example, at the mesh nodes, then if the solutions are continuous, the  $u_i(J)$  can be determined by first order interpolation as in Masseau's method (Berezin and Zhidko (1965)).

$$u_i(J) = u_i(A) - \frac{(u_i(C) - u_i(A))}{\Delta t} t$$

where  $u_i(A)$  and  $u_i(C)$  are known. Since

$$\lambda_- = \frac{\Delta x}{(\Delta t - \delta t)}$$

and  $\Delta x$  and  $\Delta t$  are specified,  $u_i(J)$  can be determined. The  $\lambda_+$  and  $\lambda_-$  are evaluated at C. Substituting  $U_i(J)$  and  $U_i(K)$  into the

two equations 5.11 and 5.12, the  $u_i$  (P) can be calculated by solving the two simultaneous equations. This procedure is extended along the line  $x = X_0$  for each node. If the boundary data is known on the line  $x = X_0 \forall t : t \in [\bar{0}, T_{\text{final}}]$ , then the solution on  $X = X_0 + \Delta x$  can only be determined for each  $t : t \in [\Delta t, T_{\text{final}} - \Delta t]$ . Thus, the solution on  $x = X_{\text{final}}$ , where  $X_{\text{final}} = N\Delta x$  can be determined for  $t : t \in [T_1, T_2]$  where  $T_1 = N\Delta t$  and  $T_2 = T_{\text{final}} - N\Delta t$ .

### 5.5 Pressure-area Relationship

Many biological elastic tissues have properties similar to rubber and so the pressure-area law for a Mooney-Rivlin material, which approximates the properties of rubber, was investigated (Green and Zerna(1968)). Let the deformed state be represented by the curvilinear co-ordinates  $(r, \theta, Z)$ . Then in Cartesian co-ordinates  $(y_1, y_2, z)$

$$y_1 = r \cos \theta, \quad y_2 = r \sin \theta, \quad z = Z$$

and for the natural state

$$x_1 = \sigma \cos \theta, \quad x_2 = \sigma \sin \theta, \quad z = Z$$

where  $(\sigma, \theta, Z)$  are the co-ordinates of the natural state, with radial deformation only being considered. In the tensor notation of Green and Zerna(1968)

$$C_{ij} = \frac{\partial x^r}{\partial \theta^i} \frac{\partial x^s}{\partial \theta^j} \delta_{rs}$$

$$G_{ij} = \frac{\partial y^r}{\partial \theta^i} \frac{\partial y^s}{\partial \theta^j} \delta_{rs}$$

Hence,

$$C_{ij} = \begin{pmatrix} \left(\frac{\partial \sigma}{\partial r}\right)^2 & 0 & 0 \\ 0 & \sigma^2 & 0 \\ 0 & 0 & 1 \end{pmatrix}$$

and

$$G_{ij} = \begin{pmatrix} 1 & 0 & 0 \\ 0 & r^2 & 0 \\ 0 & 0 & 1 \end{pmatrix}$$

The condition for incompressibility (Green and Zerna(1968)) implies

$$\begin{vmatrix} \left(\frac{\partial \sigma}{\partial r}\right)^2 & 0 & 0 \\ 0 & \sigma^2 & 0 \\ 0 & 0 & 1 \end{vmatrix} = \begin{vmatrix} 1 & 0 & 0 \\ 0 & r^2 & 0 \\ 0 & 0 & 1 \end{vmatrix} \quad 5.12$$

If the inner diameter =  $d_1$ , and the outer diameter =  $d_2$  in the deformed state and the inner diameter =  $d_{01}$  and the outer diameter =  $d_{02}$  in the natural state, then from equation 5.12

$$\left(\sigma \frac{d\sigma}{dr}\right)^2 = r^2$$

On integration

$$\sigma^2 - r^2 = \text{constant}$$

therefore,

$$r^2 - \sigma^2 = d_1^2 - d_{01}^2 = D^2$$

The components of the stress tensor (Green and Zerna(1968))

are

$$\tau^{11} = \frac{\sigma^2}{r^2} \mathbb{I} + \left(1 + \frac{2}{r^2}\right) \psi + p$$

$$\tau^{22} = \frac{1}{2} \mathbb{I} + \left(\frac{1}{r^2} + \frac{1}{2}\right) \psi + \frac{p}{r^2}$$

$$\tau^{33} = \mathbb{I} + \left(\frac{2}{r} + \frac{r^2}{2}\right) \psi + p$$

$$\tau^{ij} = 0 \text{ for } i \neq j$$

These results were obtained from the equations

$$\tau^{ij} = \Phi g^{ij} + \psi B^{ij} + p G^{ij}$$

$$B = g^{rs} G_{rs} g^{ij} - g^{ir} g^{is} G_{rs}$$

where  $\Phi, \psi$  are defined by

$$\Phi = 2 \frac{w}{I_1}, \quad \psi = 2 \frac{w}{I_2}$$

and  $w =$  strain energy density and  $I_1, I_2$  are the first and second strain invariants.

The equations of motion are

$$\tau^{ik},_{,i} + \Gamma_{ir}^i \tau^{rk} + \Gamma_{ir}^k \tau^{ir} = f$$

where the  $\Gamma_{jk}^i$  are the Christoffel symbols for the co-ordinate transformation and

$$\Gamma_{22}^1 = -r \quad \text{and} \quad \Gamma_{12}^2 = \Gamma_{21}^2 = \frac{1}{r}$$

The radial equation reduces to

$$\frac{\partial \tau^{\rho\rho}}{\partial r} + \left(\frac{\sigma^2}{r^2} - \frac{r^2}{\sigma^2}\right) \frac{\Phi}{r} + \left(\frac{\sigma^2}{r^2} - \frac{r^2}{\sigma^2}\right) \frac{\psi}{r} = f$$

If  $\gamma = \psi + \Phi$ , then integration through the wall of the tubes gives

$$\tau^{\rho\rho}(\rho, t) = \gamma \int^{\rho} \left[ \frac{r^2 - D^2}{r^3} \right] dr + \int^{\rho} f dr + h(t)$$

where  $h(t) =$  function of time only and  $\gamma =$  constant.

If

$$\tau^{\rho\rho}(a_1, t) = -p_1(t)$$

$$\tau^{\rho\rho}(a_2, t) = -p_2(t)$$

then integration gives

$$\Delta p(t) = p_1(t) - p_2(t)$$

$$= \left[ \log \left[ \frac{1 - \frac{D^2}{d_2^2(t)}}{1 - \frac{D^2}{d_1^2(t)}} \right]^{\frac{1}{2}} + \frac{D^2}{2d_1^2(t)} - \frac{D^2}{2d_2^2(t)} \right] \quad 5.13$$

This equation assumes that the parameter  $D$  does not change with the deformation. Equation 5.13 relates the transmural pressure  $\Delta p(t)$  and the corresponding area in a Mooney material when the pressure is a function of time. This is the equation obtained by Green and Zerna for steady state conditions.

#### 5.6 Numerical Solution of the Pressure Flow Equations

If continuous solutions of the set of equations 5.3, 5.5 and 5.13 are considered, then the solution is unique (Courant and Hilbert (1961)). Since the pressure decreases along the elastic tube towards the exit then, ignoring end effects, the pressure at the exit from the tube will be approximately atmospheric. The exit area should, therefore, remain approximately constant =  $A_0$  where  $A_0$  is the equilibrium area of the tube (the small pressure required to prevent the tube from collapsing under its own weight is neglected).

Using the techniques described in Chapter 2, the urine flowrate may be determined. The boundary conditions used are, therefore,

$$\begin{aligned} \text{(a)} \quad A(l, t) &= A_0 & t : t & \in [0, T_{\text{final}}] \\ \text{(b)} \quad Q(l, t) &= Q_0(t) & t : t & \in [0, T_{\text{final}}] \end{aligned}$$

where  $l$  = length of the tube and  $Q_0(t)$  is the measured flowrate profile.

A digital computer programme was written to solve equations 5.3, 5.5 and 5.15 with the above boundary conditions. The programme is listed in Appendix I. The equations were transformed using the transformation  $z \rightarrow 1 - z$  and the variables  $Q$ ,  $\Delta$  and  $p$  calculated going in the direction from the external urethral meatus towards the bladder neck. Using the programme, it is possible to calculate:-

$$(a) \quad \Delta (x_1, t)$$

$$(b) \quad p (x_1, t)$$

$$(c) \quad Q (x_1, t)$$

throughout the length of the tube.

In order to check the accuracy of the digital computer programme, in equation 5.15 was made very large so that the elastic tube was effectively rigid, and the bladder pressure calculated for constant flowrates in the range 1 to 50 ml/sec. The bladder pressure was determined from the bladder neck pressure calculated by the computer programme and the flowrate using Bernoulli's equation

$$P_{BL} = P_{BN} + \frac{Q^2}{2gA_{BN}^2}$$

where  $P_{BL}$  = bladder pressure cm  $H_2O$ ,  $P_{BN}$  = bladder neck pressure cm  $H_2O$ ,  $Q$  = flowrate ml/sec and  $A_{BN}$  = area at the bladder neck  $cm^2$ .

Any deviation between the values calculated using the elastic tube programme and the values determined from the rigid tube tables (Chapter 3) was less than 0.001 per cent.

The widest part of the urethra is frequently at the bladder neck and may be a factor of two to three times the diameter of the

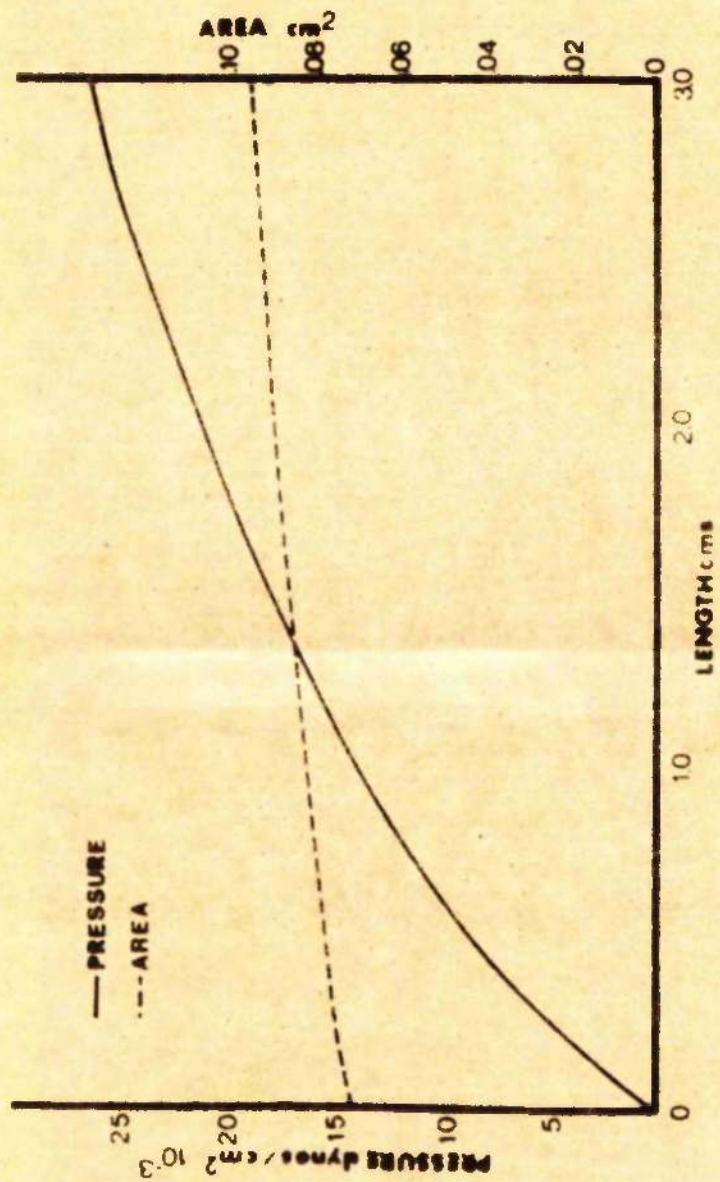


FIG 52

narrowest section of the urethra in the female, as observed using micturition cystography. The narrowest diameter is normally of the order of 2.5 to 3.5 mm. Using these figures and the fact that the average bladder pressure at a peak flowrate of 15 ml/sec is in the region of 50 cm  $H_2O$ , the elasticity constant  $\delta$  is required to be of the order of 20 to 40 cm  $H_2O$ . This value of  $\delta$  implies a critical flowrate at the urethral meatus which is sometimes less than the flowrate observed. Since continuous flow is being considered, the value of  $\delta$  has to be increased in order that the flow cannot try to go from a subcritical flow state to a supercritical flow regime, that is, the velocity of the flow passes through the critical velocity  $C$ .

Using the elastic tube programme, the value of  $\delta$  required to render the flow just subcritical at the exit was calculated and the bladder pressure and area profile determined. The area at the bladder neck was found to be only approximately 30 per cent larger than the exit area for flowrates between 10 and 20 ml/sec. It was, therefore, impossible to obtain physiological bladder neck diameters.

Figure 5.2 shows the profiles of the area and pressure calculated for a flowrate of 20 ml/sec and an exit diameter of 3 mm. The critical flowrate at the exit determined by was 24 ml/sec. Similar results for a flowrate of 15 ml/sec were obtained.

The result, therefore, implies that --

- (a) The concept of a homogeneous elastic tube with the exit pressure equal to atmospheric pressure is not practicable.

(b) the area at the external meatus is greater than its equilibrium value, that is, the exit pressure is greater than atmospheric pressure.

(c) Supercritical flow may possibly occur.

The possibility (b) is doubtful since the measurement of urethral pressure profiles during micturition suggest an exit pressure equal to atmospheric pressure (Scott, Clayton (1966)).

The two main possibilities are (a) and (c). The latter possibility is discussed in Chapter 6. If the urethra at the bladder neck is assumed to be highly elastic, then in order for the flowrate to remain subcritical throughout the urethra the tube must become less elastic towards the external meatus. The urethral pressure at the exit would still be atmospheric. This would permit larger areas at the bladder neck to occur since most of the static pressure fall would take place in the less elastic narrower section of the tube where the critical flowrate would be much larger than the physical flowrate. Experiments with dog urethras (Chapter 6) however imply that the female urethra is approximately uniformly distensible throughout its length. It is possible that continuous flow may not necessarily occur and that the high degree of elasticity required to produce the large distensions may occur in conjunction with supercritical flow and the resulting discontinuities. The urethra may not in practice be highly distensible throughout its length due to muscular attachments. This may permit the occurrence of flowrates which would otherwise imply discontinuous flow.

If the urethral elasticity profile were known, then since

$$\frac{\partial p}{\partial z} = \gamma \frac{\partial H}{\partial z} + \frac{p}{\gamma} \frac{\partial \gamma}{\partial z}$$

the urethral profile could be computed by using the transformation

$$2 \frac{L \cdot \tau_R}{R} \rightarrow 2 \frac{L \cdot \tau_R}{R} - \frac{p}{\gamma} \frac{\partial \gamma}{\partial z}$$

in equation 5.5.

Due to the unexpected result that it is not possible to determine bladder neck areas of physiological dimension, the time dependent flowrate data from patients with no abdominal pressure interaction computed by the elastic tube programme differ very little from the results obtained from the rigid tube theory. Using a flowrate of 20 ml/sec, the rigid tube theory implies a bladder pressure of 54.4 cm H<sub>2</sub>O at an equivalent rigid tube diameter of 3mm. The elastic tube theory with the exit diameter equal to 3 mm and a value for  $\gamma$  giving a critical flowrate of 24 ml/sec implies a value of 49.3 cm H<sub>2</sub>O.

The phase relationship between the bladder pressure and the urine flowrate was investigated by feeding a sinusoidal flowrate into the elastic tube programme as boundary data at the exit. The phase difference between the two variables was negligible (less than 0.005 radians), within the accuracy of the theory, for flowrates up to 30 ml/sec and frequencies up to 0.25 cycles/sec. This agrees with Womersley (1958) who investigated oscillatory flow in tubes with low distensibility.

If one considers the steady flow of a liquid through an elastic tube in which, as before, the velocity profile is assumed

flat, then (Landau and Lifshitz).

$$\frac{d \Sigma}{dz} = \frac{d}{dz} \left[ A \rho v \left( w + \frac{1}{2} v^2 \right) \right] - \bar{\Phi}$$

where  $\Sigma$  = energy flux through the area  $A$ ,  $w$  = specific enthalpy of the fluid and  $-\bar{\Phi}$  = the energy flux lost due to the change in state.

Since

$$dw = T ds + \frac{1}{\rho} dp$$

where  $ds$  = specific entropy

$$\begin{aligned} T \frac{ds}{dz} &= \frac{dw}{dz} - \frac{1}{\rho} \frac{dp}{dz} \\ &= \frac{1}{\rho^3} \frac{Q^2}{A^2 C^2} \frac{dp}{dz} - \frac{1}{\rho} \frac{dp}{dz} - \frac{1}{Q} \bar{\Phi} \end{aligned}$$

where  $C$  = critical velocity at the area  $A = \frac{1}{\rho} A \frac{dp}{dA}$  and  $Q = \rho A v$ .

If

$$Q_{\text{crit}} = \rho A C$$

then

$$T \frac{ds}{dz} = \frac{1}{\rho} \left[ \frac{Q^2}{Q_{\text{crit}}^2} - 1 \right] \frac{dp}{dz} - \frac{1}{Q} \bar{\Phi}$$

In order that the change in entropy is not negative, the following conditions must be satisfied (assuming that  $\bar{\Phi} \approx 0$ )

(a) for  $Q \geq Q_{\text{crit}}$  the pressure  $p$  must increase with  $z$ ,

$$\text{that is, } \frac{\partial p}{\partial z} \geq 0$$

(b) for  $Q \leq Q_{\text{crit}}$  the pressure  $p$  decreases with  $z$ ,

$$\text{that is, } \frac{dp}{dz} \leq 0.$$

Also

$$\frac{d^2 s}{dz^2} = - \frac{2Q^2}{Q_{\text{crit}}^3} \frac{dQ_{\text{crit}}}{dz} = \frac{1}{Q} \frac{d\bar{\Phi}}{dz}$$

Since  $\frac{dQ_{\text{crit}}}{dA} > 0$  for the elastic material used (Mooney-Rivlin)

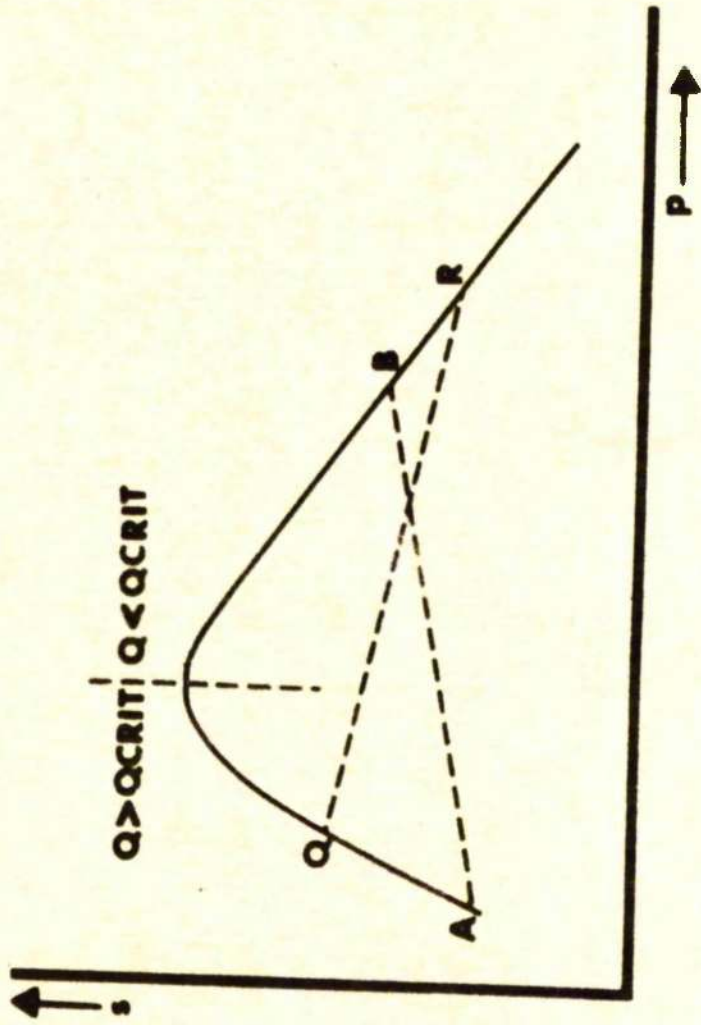


FIG 53

then at  $Q = Q_{\text{crit}}$

$$\frac{d^2 s}{dz^2} \leq 0$$

Hence, since

$$\frac{ds}{dz} = \frac{ds}{dA} \frac{dA}{dz}$$

the shape of the  $s - z$  curve for a given flowrate  $Q$  is as shown in Figure 5.3.

From these curves, it can be seen that if the flowrate is subcritical, then the pressure must decrease towards the exit and that for supercritical flow the pressure increases downstream. It would also appear that it could be possible, with reference to Figure 5.3, for a transition to occur from the supercritical state A to the subcritical state B or from the subcritical state R to the supercritical state Q without contravening the entropy requirements.

To investigate the occurrence of discontinuities, the equations of continuity and of conservation of momentum are used. States 1 and 2 are just upstream and just downstream from the discontinuity respectively.

$$A_1 v_1 = A_2 v_2$$

that is,

$$B v_1 = v_2 \quad 5.14$$

where  $B = \frac{A_1}{A_2}$  and

$$A_1 \left( p_1 + \frac{1}{2} v_1^2 \right) = A_2 \left( p_2 + \frac{1}{2} v_2^2 \right)$$

that is,

$$B \left( p_1 + \frac{1}{2} v_1^2 \right) = p_2 + \frac{1}{2} v_2^2 \quad 5.15$$

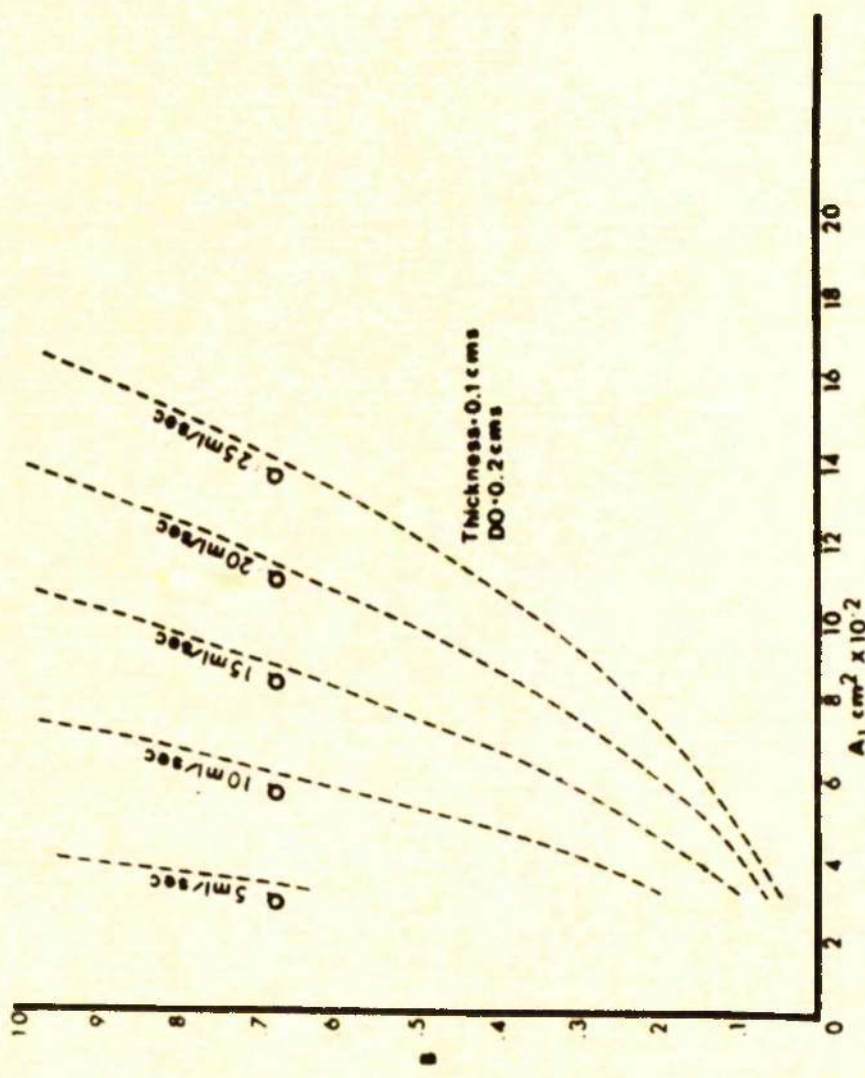


FIG 54

If

$$E_1 = p_1 + \frac{1}{2} v_1^2 \quad \text{and} \quad E_2 = p_2 + \frac{1}{2} v_2^2$$

then using 5.14 and 5.15

$$E_1 - E_2 = \frac{(1-B)}{2B^2} [(2B-1)E_2 + E_2]$$

Therefore, if  $B > 1$  then  $E_1 - E_2 < 0$ . This is not allowed due to energy conservation. Therefore, energy conservation requires that  $B < 1$  that is, referring to Figure 5.3, the transition from R to Q is not allowed. This also requires that if a discontinuity is to occur, the flow must be supercritical on entry, or else the elastic properties of the tube must suddenly change in such a way that the critical flowrate defined by the elastic property is sufficiently reduced to make the existing flow supercritical. Therefore, if a discontinuity occurs, the area on the bladder neck side of the discontinuity will be less than the area on the other side, that is, the area expands across the discontinuity. The condition  $B = 1$  requires that  $v_1 = v_2$  and  $p_1 = p_2$  so that there is no physiological discontinuity.

Given that discontinuities may occur during micturition, it is necessary to investigate magnitude of the parameter B. Using the equations 5.14 and 5.15 expressing the conservation of mass and momentum flux and the pressure-area law 5.13 the roots B of the equation

$$B(p_1 + v_2) = p_2 + B^2 v_1^2 \quad 5.16$$

can be determined given  $p_1$ ,  $Q = v_1 A_1 = v_2 A_2$  and . The Newton Raphson iterative technique was used to determine the roots of the equation 5.16, only those roots less than 1.0 but positive being

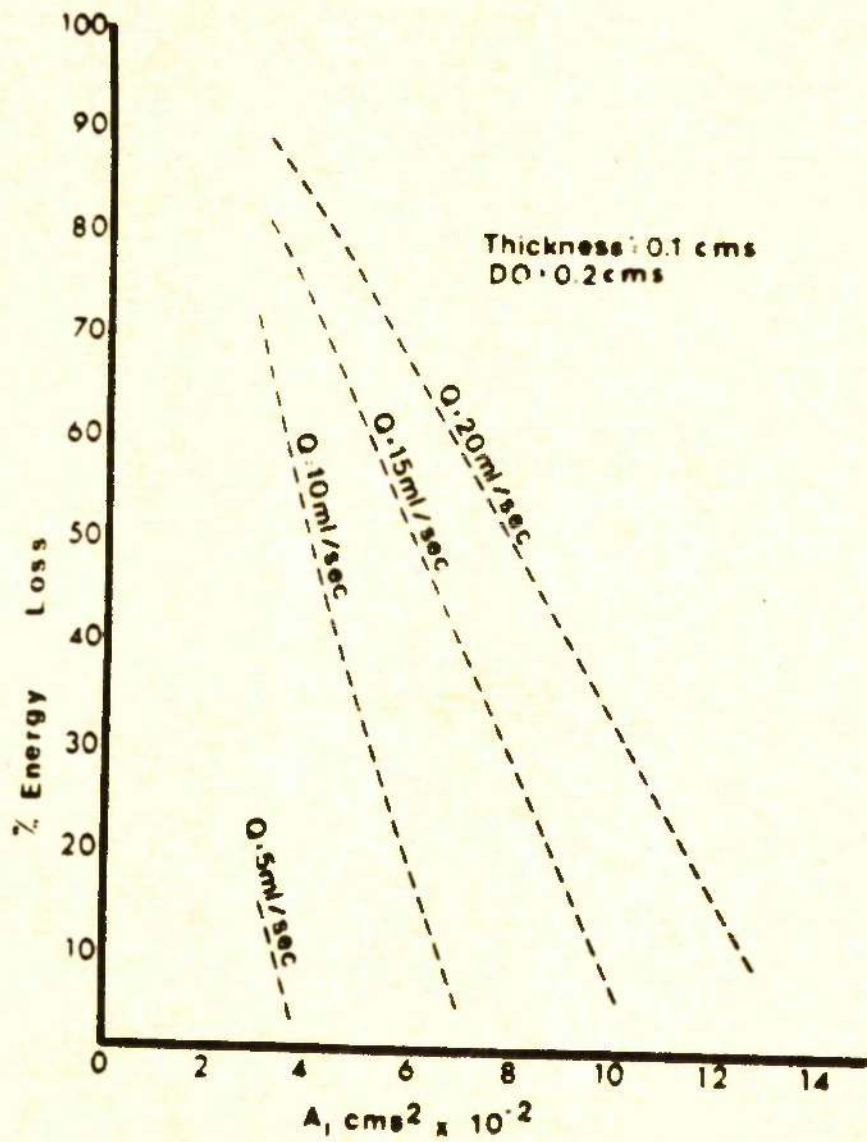


FIG 55

accepted. The variation of B with  $A_1$  is shown in Figure 5.4. The nearer  $A_1$  approaches the equilibrium area under supercritical flow, the larger the discontinuity (that is, the smaller the value of B) for a given flowrate  $Q$ . Also the more elastic the material the greater the discontinuity.

The energy loss across the discontinuity was also calculated as a function of  $A_1$  by calculating  $p + \frac{1}{2} \frac{Q^2}{A^2}$  behind and in front of the discontinuity. The variation of the energy loss with  $A_1$  is shown in Figure 5.5. The percentage energy loss may therefore be a significant fraction of the bladder pressure.

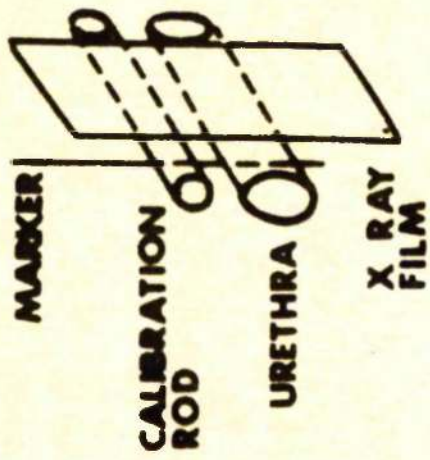
CHAPTER 6Elastic Tube Theory II

In order to investigate the elasticity of the urethra experiments were performed on excised dog urethras. These specimens were obtained from the dogs immediately upon death. All specimens were investigated within fifteen hours of excision, some, however, being studied within three hours. No significant difference was found in the same specimens studied at three hours and fifteen hours. The specimens were stored at 3°C. The purpose of this study was two fold:-

1. to determine the pressure-area law for the urethra;
2. to calculate the critical flowrate as a function of area.

The urinary bladder and urethra were excised as a whole from the dog and the bladder completely emptied. A fine cannula was inserted for approximately 3 mm from the urethral meatus and then firmly secured by tightly tying a thread round the meatus clamping it to the cannula. The urethra was straightened, keeping the stretch to a minimum.

A water manometer was connected to the cannula via a three-way tap. The bladder and urethra were gradually filled with a solution of Eypaque until the urethra attained its equilibrium diameter, that is, there was just sufficient pressure to overcome the weight of the urethra which was tending to collapse it. The specimen was positioned 100 cm from an X-ray generator. An X-ray photographic plate was then placed 2 cm from the urethra but on the opposite side of it from the X-ray generator as in Figure 6.1. A circular rod



X RAY  
GENERATOR

FIG 6.1

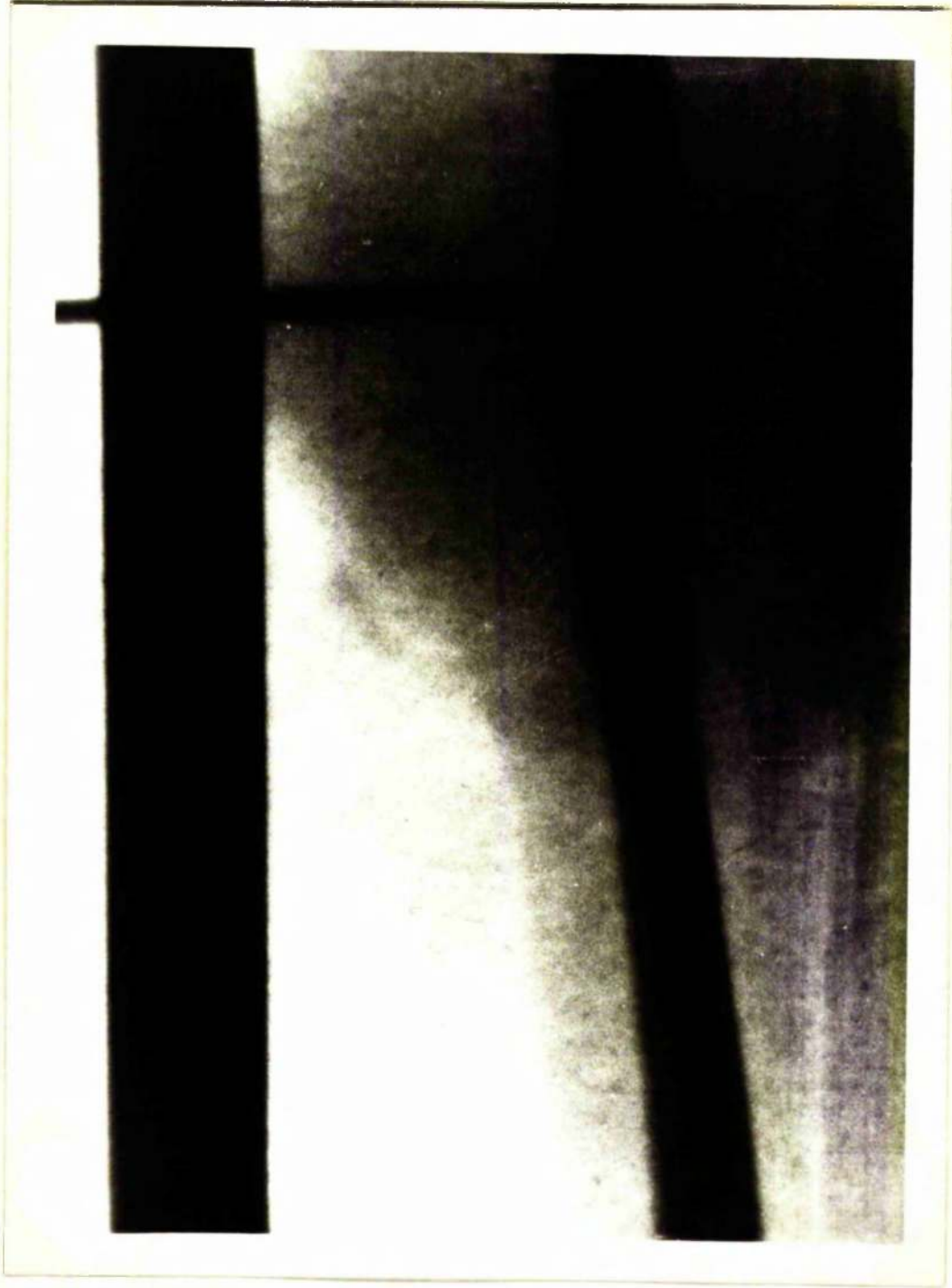


Fig. 6.2

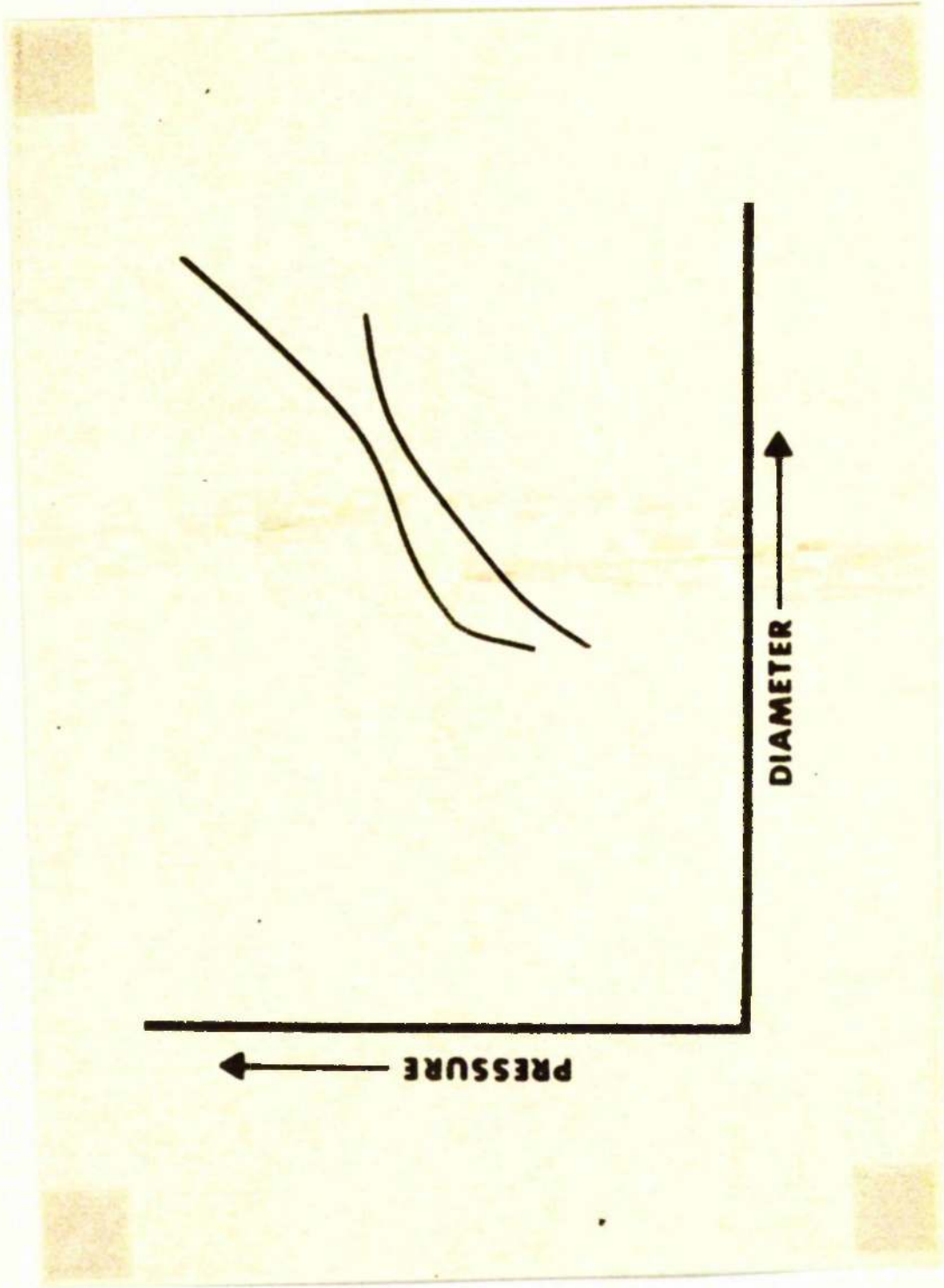


Fig. 6.3

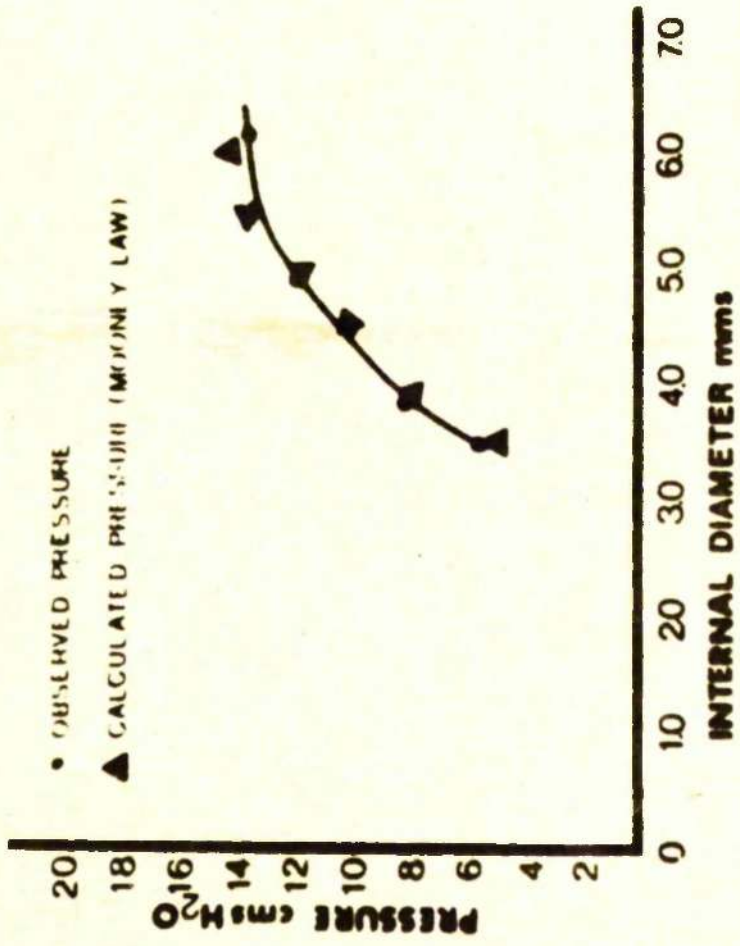


FIG 64

of known diameter was positioned in the same plane as the urethra. In order to have some constant reference position, a fine wire was suspended vertically marking the position of interest. The assembly was then X-rayed and recorded on the photographic plate. The bladder and urethra were then filled with more Eypaque via the cannula, thus increasing the pressure within the urethra. Once this pressure had stabilised, that is, any viscoelastic effects had decayed, the pressure was measured and the assembly X-rayed. This was repeated at different pressures. A typical X-ray photograph is shown in Figure 6.2.

The X-ray photographs were then enlarged and the urothral diameters on the enlargements measured at the reference position using Vernier calipers. The diameter on the enlargement of the calibration rod was also determined and so the actual diameter of the urethra could be determined at each pressure step.

Figure 6.3 shows the two types of pressure-area curves obtained.

In many of the urethras excised little distension from the equilibrium position occurred as the intra-urethral pressure was increased, thus behaving as a rigid tube. Those urethras which behaved like rigid tubes also did so immediately after excision.

The correlation between the observed pressure-area law and the Mooney-Rivlin law was investigated. The equilibrium diameter was measured to the nearest 0.5 mm and the average thickness taken as 0.2 mm. The fit was good for those urethras which did not exhibit the flattening of the pressure-area law with the subsequent secondary rise, Figure 6.4. These urethras deviated significantly from

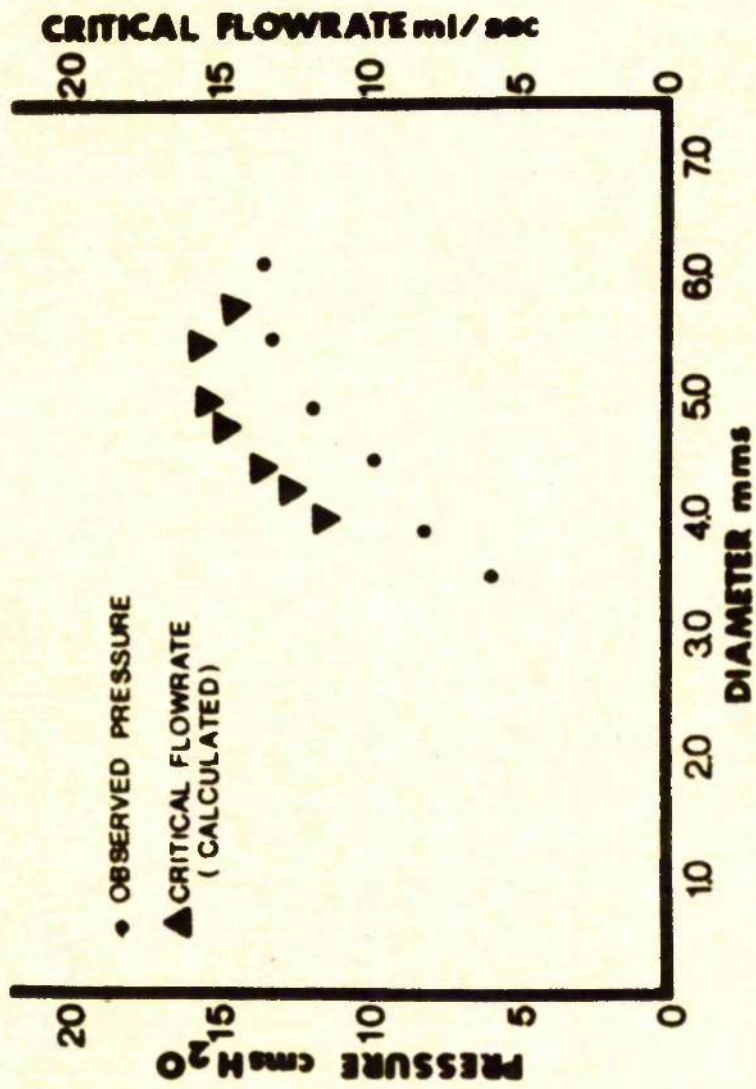


FIG 6.5

the theoretical law used. The elastic constant  $EK$  ranged from 20 cm H<sub>2</sub>O upwards.

It was possible to calculate the critical flowrate defined by the observed pressure-area laws for the urethras investigated using the formula (Chapter 5).

$$Q_{\text{crit.}} = L \sqrt{E \frac{dP}{dA}}$$

It can be seen that for urethras exhibiting little distension/unit pressure the value of  $Q_{\text{crit.}}$  tended towards infinity. In other urethras the critical flowrate near the equilibrium diameter ranged from 5 ml/sec upwards. The critical flowrate was lower at smaller diameters for a given urethra. It is probable that the critical flowrates would be even less at smaller deviations from the equilibrium diameters than those obtained in the investigations. Figure 6.5 shows the general behaviour of the critical flowrate as a function of diameter. Thus in some of the urethras investigated, the critical flowrates at small deviations of the urethral diameter from the equilibrium diameter were much less than the peak urine flowrates observed in the human.

These results apply to that part of the dog urethra approximately 1 cm from the bladder neck. It was found that the greater the distance from the bladder neck the less elastic the tissue. This difference in the elastic property was much more pronounced in the male urethra.

Since the urethras in these investigations were excised, the elastic properties will reflect those of the relaxed urethra.

It has been shown in Chapter 5 that it is not possible for the

flow in the urethra to be subcritical with a subsequent change to supercritical flow. However, if subcritical flow were to exist with respect to the existing elastic properties any sudden change in these elastic properties of the urethra at some point may render the existing flowrate supercritical with respect to the new elastic properties. In order for this to happen the urethra would have to become more elastic.

It has been observed that on initiation of micturition the pelvic floor relaxes with the subsequent descent of the bladder neck resulting in a shortening of the urethral length, and relaxation of the urethral striated muscle, Mueller (1965). Woodburne (1968) found a high density of elastic fibres in the urethra near the bladder neck.

It is expected, therefore, that as the pelvic floor relaxes and the urethra shortens, the elasticity of the urethra especially in the region of the bladder neck will change. It is possible that at this stage in micturition discontinuous flow may occur. Many investigations have shown that stress incontinence is due to either a weak pelvic floor or reduced ability of the urethral closure forces, Emborning (1961), Lund, Fristan, Ramsey, Watson (1957), Jeffcoate and Roberts (1952).

Due to these elastic properties in patients suffering from incontinence it is possible that in some cases the flowrate during micturition may attain large values prior to the complete relaxation of the striated muscle and maximum shortening of urethra. This means that once the new more elastic properties occur, the flowrate

may already be greater than the critical flowrate defined by the tissue. This will result in supercritical flow. Supercritical flow may also be expected to occur in young girls with highly elastic urethras.

It is possible, therefore, for three main types of flow to occur in the urethra:-

1. subcritical flow;
2. trans-subcritical flow;
3. supercritical, discontinuous flow.

In the first type of flow, entropy requires that the pressure decreases downstream in subcritical flow. It is expected that the flow profile will be determined by the elasticity-rigidity profile of the urethra such that pressure mismatches do not occur. Any area variation in this type of flow must, therefore, be due to local elasticity variations, equilibrium diameter variations or the existence of rigid sections. This suggests that in the normal subject with no urethral fibrosis or stricture, the diameter should be minimum at the external meatus. This is often the case in the female, Nordenström (1952), Krøigaard (1970), Hoffman and Ulrich (1966). It would also be expected that the diameter determined by a single urethral stricture, exhibiting the narrowest urethral diameter would be propagated downstream with little increase since the pressure will not recover. The string urethra as observed by Whittaker (1968) may, therefore, be due to a stricture in the posterior urethra.

Griffith (1969) discussed the flow profile which would occur

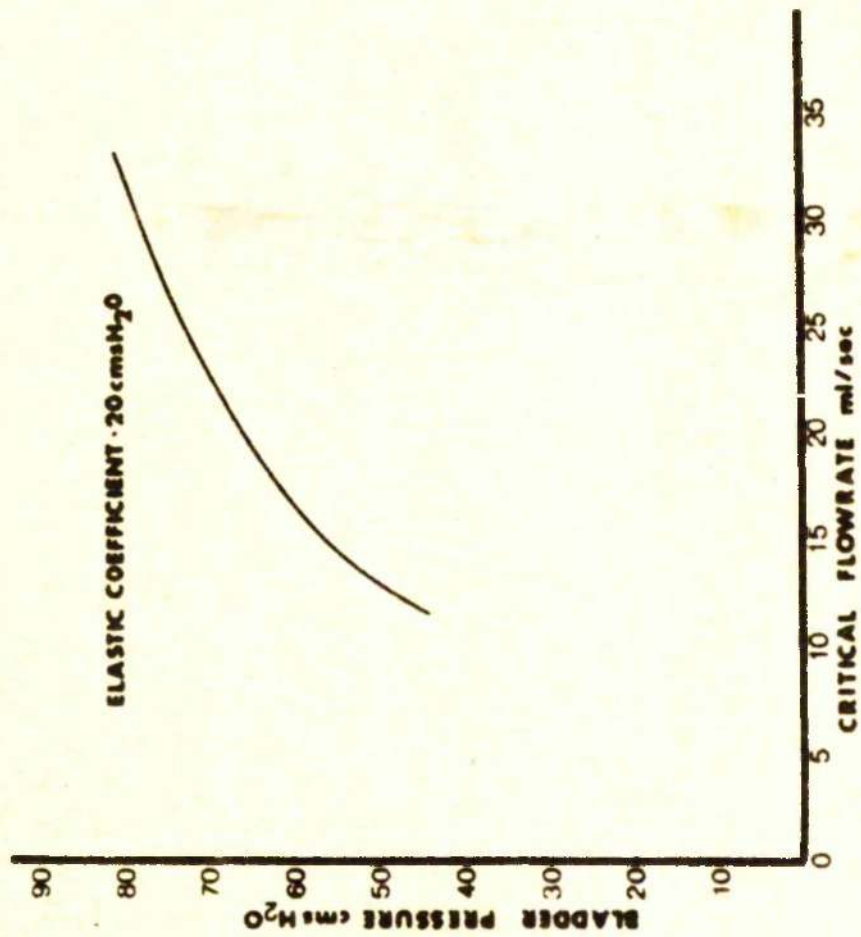


FIG 6.6

due to a short constriction in the mid-urethra. The equilibrium diameter was considered to increase downstream from the constriction. Griffith suggested that beyond the constriction, at which critical flow occurred, the pressure was atmospheric along the remainder of the urethra unless a critical pressure was exceeded in which case supercritical flow occurred just beyond the constriction with the pressure and radius both decreasing downstream.

The second type of flow was defined separately since in this type of flow, the elastic properties may limit the maximum flow-rate obtainable. Although the flow is always subcritical, the frictional loss along the tube will decrease the static pressure thus tending to decrease the area, assuming the tube is homogeneous.

If the flowrate tends towards the critical flowrate defined by the elastic property at the diameter, the tube will be unable to decrease. This is due to the fact that the critical flowrate decreases as the diameter decreases so that for the diameter to decrease would render the flow supercritical. This would contravene the entropy requirements. Thus a homogeneous elastic tube would attain its minimum diameter before the external rectus and this would be maintained downstream. Any attempt to increase the flowrate would require an increase in bladder pressure to increase the urethral diameter so that the critical flowrate could be increased.

Figure 6.6 shows the variation of bladder pressure required to produce a flowrate just less than the critical flowrate, including

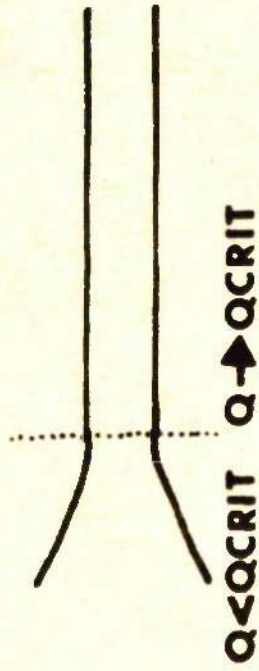
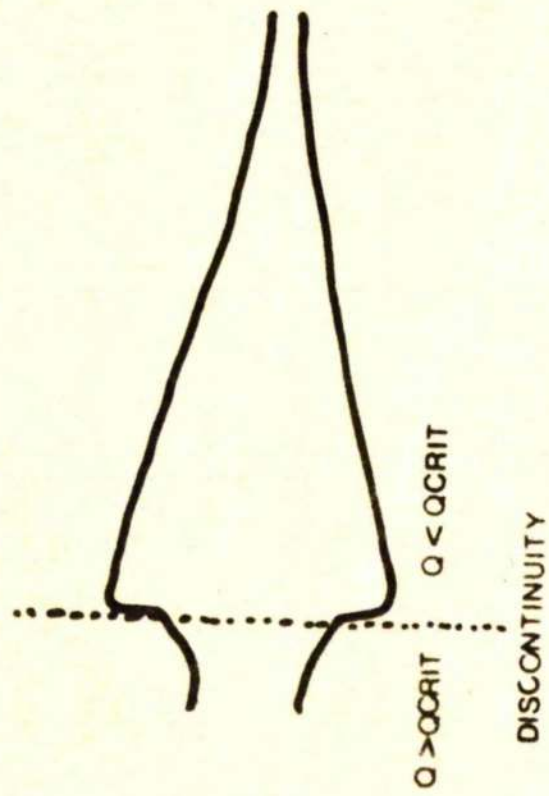


FIG 6.7



**FIG6.8**

frictional loss. This was determined using the rigid tube model for the calculation of the frictional loss. The theoretical elastic tube used had a thickness of 2 mm and an equilibrium diameter of 2.5 mm. The type of tube profile obtained under these flow conditions is shown in Figure 6.7. The diameter will be approximately constant from the point at which the flowrate tends towards the critical flowrate. If the bladder pressure does not increase, then the flowrate will decrease, forcing the diameter to increase due to energy conservation. This will increase the critical flowrate.

The third possibility, that supercritical flow can occur depends upon the possibility of a sudden change in the elastic properties of the tube. The basic shape obtainable under these circumstances is shown in Figure 6.8. From the equations defining the pressure-area law in a Mooney material, it can be shown that the critical flowrate tends towards a finite value greater than zero as the diameter tends towards the equilibrium diameter. Hence it is impossible using a Mooney material for the flow to be supercritical on initiation of micturition. In the proximal part of the urethra before the discontinuity the area increases downstream. After the discontinuity, the area decreases downstream since the flow is now subcritical. In Chapter 5 it was shown that only an increase in diameter at the discontinuity was permissible. It is possible theoretically that the flow could be supercritical over the whole length of the tube in which case the external meatus would be the point of maximum diameter, with the

corresponding increase in static pressure. Hence there would be a pressure mismatch at the exit. It is doubtful if this will ever occur in practice since the urethra is not homogeneous.

At low flowrates prior to the formation of a discontinuity, subcritical flow occurs throughout the whole urethra. A discontinuity may eventually occur but as the flowrate subsequently decreases to values smaller than the critical flowrate, subcritical flow throughout the urethra will recur. The area change at the discontinuity would, therefore, disappear.

Clayton et al (1966) showed in their paper diagrams of the shapes of the urethra in young female children encountered during their investigations. One of these shapes, similar to the one shown in Figure 6.8, has perplexed many urologists and radiologists. This urethral shape has also been observed by Nordenström (1952), Fisher and Forsythe (1954), Murphy, Schenberg, Tristan (1963) and Earrows (1965).

King (1969) observed posterior urethral narrowing with subsequent dilatation in young boys. He could find no evidence of urethral valves in some of these children and it was presumed that the dilatation was due to weakness of the urethral musculature. These relative narrowings, however, do not necessarily remain at a constant calibre during micturition, Krøigeard (1970). Hence it is unlikely that some of these profiles are due to a stricture.

In 1968, Whittaker and Johnston also reported observations of the above shapes in young girls during micturition. These investigations, however, made the important point that on repeated

investigations, the urethra assumed different shapes. This implies that these shapes, at least in those subjects investigated by Whittaker and Johnston, were not due to anatomical reasons but were due to the fluid dynamical/physiological interactions.

It is suggested that these inexplicable shapes may be due to discontinuous fluid dynamical phenomena. Since the region of the urethra at the bladder neck experiences probably the largest time varying change in elastic property during micturition, it is expected that the discontinuity will occur in this region. This is in accord with the position of the apparent discontinuity in the X-ray photographs of Whittaker and Johnston.

In order to obtain critical flow and the resulting discontinuity, it will be necessary for the flowrate to increase rapidly to some value which although subcritical with respect to the initial elastic state, will be in excess of the critical flowrate defined by the resulting elastic property. The inability to establish the required high flowrates prior to the change in elasticity will result in only subcritical flow being established. This may account for the variability in the urethral profile as reported by Whittaker and Johnston. If subcritical flow occurred and the urethra at the bladder neck was highly distensible, then funnelling could result. This has been observed by Nordenström (1952) and Hoffman and Ulrich (1966).

Shopfner (1970) believes that the bladder neck narrowing is due to the position of the trigonal plates. He observed that this apparent obstruction was most apparent at mid-voiding but

frequently disappeared at low flowrates. This does not explain why Whittaker and Johnston (1968) obtained different urethral shapes in their patients on different voidings. The course of events observed by Shopfner in young children agree well with the theoretical predictions of supercritical flow.

From the theoretical calculations in the previous chapter, it can be seen that the magnitude of the discontinuity (defined as the ratio of the area prior to the discontinuity to the area just distal to it) will be in the range 0.1 to 1.0. The ratio of the areas at the point of possible discontinuity in the X-rays published by Whittaker and Johnston (1968) is of the order of 0.5. One notable point is the significant energy loss which would occur at a discontinuity. This would result in a higher resistance compared to the same flow under subcritical conditions. It is rather a paradox that if such discontinuities exist then the resultant resistance is due to a highly elastic urethra and not as a result of a physical obstruction.

Whittaker and Johnston (1968) discussed one patient who had a very large resistance and a urethral profile as shown in Figure 6.8. On the subsequent investigation, the resistance was reduced by a factor of six and the urethral profile was of a normal convergent shape. This increase in resistance due to the discontinuous urethral profile supports the concept of supercritical flow since there would be a large pressure loss at the discontinuity under supercritical flow. The energy loss at the area change during subcritical flow would be due to turbulent losses and would be much

smaller.

It has also been observed by several investigators, Smith (1968), Krøigaard (1970), Hodgkinson and Morgan (1969), that there is not infrequently a rise in the intravesical pressure once the flowrate is starting to fall. Hodgkinson and Morgan (1969) could not correlate this pressure rise with abdominal pressure. Occasionally, a "secondary rise" in bladder pressure occurs after the flow has ceased, Krøigaard (1970). Certainly in the latter case, the rise in intravesical pressure is not due to fluid dynamical reasons. It has been suggested that the rise in general is due to the stricted musculature of the urethra forcing it to close hence increasing the resistance to flow, Zinner and Paguin (1963). It would, therefore, be expected that there would be a rapid fall in the flowrate with the detrusor muscle still contracting and creating this rise in pressure. This does not fully explain the case where the flowrate does not rapidly fall to zero. It is possible that the existence of supercritical flow may account for this phenomenon. If supercritical flow occurs at some stage in micturition the flow will eventually return to subcritical flow throughout the urethra, due either to reverse change in the elastic properties or reduction of the flowrate. At this point the flowrate does not change discontinuously but would result in energy being transferred upstream due to the change in the profile, that is, the energy loss due to the discontinuity would be partially recovered. Subcritical flow would then occur throughout the urethra.

It is well known from the theory of supersonic gas flow that

if the stream velocity of the gas in a rigid tube is greater than the velocity of sound in the gas, then any disturbance downstream propagated at the velocity of sound will be propagated downstream only (Landau and Lifshitz). The analogous situation also applies to flow in elastic tubes. From the theory of characteristic equations discussed in Chapter 5, it was shown that -

$$\frac{dx}{dt} = v \pm c$$

where  $v$  = velocity of the stream and  $c$  = critical velocity of the elastic material.

Hence it can be seen that for  $v < c$  the disturbances, which are propagated along the characteristic directions, are propagated both upstream and downstream.

When  $v > c$ , the characteristic directions are both downstream. If we consider a homogeneous elastic tube, then any disturbance downstream from a discontinuity will not be propagated up to the entry point if the flow is supercritical on entry. This is because any small disturbance will not force the tube area to become less than the area at which the flow would become supercritical. If the tube were to develop a constriction downstream due to the elastic properties suddenly becoming less elastic, then this may result in such a large frictional loss, that the total resistance to flow will be so high that the flowrate would decrease. If a constriction exists prior to flow, then this will control the rate at which the flowrate pattern is established and limit the maximum flowrate obtained. This may prevent the formation of supercritical flow. Thus, although small perturbations will not be reflected upstream beyond

the discontinuity, that is, the bladder pressure will not reflect pressure changes, they may control the flowrate and, therefore, the magnitude of the discontinuity.

Considering Bernouilli's law and with reference to Figure 6.8,

$$P_{BL}(t) = p(L_1) + \frac{Q^2(t)}{2A_1^2(t)}$$

Thus -

$$\begin{aligned} \frac{dP_{BL}(t)}{dt} &= \frac{\partial p}{\partial L_1} \frac{dL_1}{dt} - \frac{c^2}{L_1^3(t)} \frac{dA_1(t)}{dt} + \frac{Q}{A_1^2} \frac{dQ(t)}{dt} \\ &= \frac{v_{crit.}^2(L_1)}{L_1} \frac{dL_1}{dt} - \frac{c^2}{L_1^3(t)} \frac{dL_1(t)}{dt} + \frac{c}{L_1^2} \frac{dL_1(t)}{dt} \\ &= \frac{1}{L_1^3} \sqrt{c_{crit.}^2(L_1) - c^2(t)} \frac{dL_1(t)}{dt} + \frac{Q}{A_1^2} \frac{dQ(t)}{dt} \end{aligned} \quad 6.1$$

Therefore -

$$\frac{dP_{BL}}{dt} - \frac{2(P_{BL} - p)}{c} \frac{dQ}{dt} = \frac{1}{L_1^3} \sqrt{c_{crit.}^2(L_1) - c^2(t)} \frac{dL_1(t)}{dt}$$

Hence -

$$\left. \frac{P_{BL}}{L_1} \right|_{Q = \text{const.}} = \left[ \frac{Q_{crit.}^2 - Q^2}{L_1^3} \right] \quad \text{and}$$

$$\frac{P_{BL}}{c L_1} = \text{const.} = \frac{c}{A_1^2}$$

It can be seen that for  $Q = \text{constant}$  -

1.  $c < c_{crit.}(L_1)$  implies -

(a)  $A_1(t)$  increases as  $P_{BL}(t)$  increases;

(b)  $A_1(t)$  decreases as  $P_{BL}(t)$  decreases.

2.  $Q > Q_{crit.}(A_1)$  implies -

(a)  $A_1(t)$  increases as  $P_{BL}(t)$  decreases;

(b)  $A_1(t)$  decreases as  $P_{BL}(t)$  increases.

Also, if  $A_1 = \text{constant}$  it can be seen that, under both supercritical flow and subcritical flow, the flowrate increases as the bladder pressure increases and vice versa.

The conditions implied by 1. are within normal experience. However, the implication of 2. is most profound.

Referring to the situation discussed on Page 12 where the flowrate decreases but is still supercritical on entry to the tube, since the bladder pressure does not fall it can be seen that area  $A_1$  must increase.

The coefficient B relating the area distal to the discontinuity to  $A_1$ , will, therefore, increase as can be seen from Figure 5.4 Thus the jump in the magnitude of the ratio of the areas will decrease.

This phenomenon of a high bladder pressure with a reduction of  $A_1$  in supercritical flow may explain the observations in many patients with prostatic or bladder neck hypertrophy. Large peak flows develop quickly simultaneously with high bladder pressures. Although the bladder pressure remains high, the flowrate quickly falls. These pressure flow relationships have been observed by Von Garrelts (1958) in patients with prostatic hypertrophy. The early closure of the bladder neck correlates with the large residual

urine normally found in these patients.

This may be explained if it is assumed that supercritical flow occurs. In these cases, the bladder pressure is very high, but often sustained. If it is assumed, therefore, that the bladder pressure is approximately constant, then from equation 6.1 -

$$\frac{dQ}{dA_1} = - \frac{\sqrt{C_{crit.}^2 - Q^2}}{A_1 Q}$$

Hence if  $Q > C_{crit.}$ , then, as the flowrate decreases the area  $A_1$  at the bladder neck decreases. This may, therefore, result in a collapse of the urethra. If the bladder pressure does not remain constant and the flowrate increases but is supercritical, the bladder pressure will increase. This results in the area  $A_1$  decreasing with possibility of collapse. The bladder neck would not collapse if the supercritical flow decreased simultaneously with a decrease in the bladder pressure. This would, in fact, tend to open up the bladder neck.

Notice, however, that if  $Q < C_{crit.}$ , then if the flowrate decreases the area  $A_1$  will increase.

The theory of supercritical flow explains many phenomena observed in the investigation of the hydrodynamics of the lower urinary tract. It is necessary in future work to perform simultaneous pressure flow cineradiographic investigations in order to relate the hydrodynamic variables with the urethral geometrical profiles throughout micturition. It is also necessary to

distinguish between profiles resulting from discontinuous flow and those due to variations in the elasticity profile of the urethra. This may be possible by making the patient empty his bladder against a high resistance which will prevent a high flow from being established quickly and thus also discontinuous flow.

A P P E N D I X I

LIST(LP)S  
PROGRAM(PF32)  
OUTPUT(HELP)  
INPUTS(FCR)  
END

002

|    |  |      |
|----|--|------|
|    | DIMENSION Q(2,300),QIN(300),A(2,300),QOUT(300),AIN(300),     | 006  |
|    | 1TO(300),TO(300),IDENT(160),ARRAY(10,10),RHS(70),PBLOUT(300) | 007  |
|    | 2,JTRANS(300)  | 008  |
|    | COMMON JO,AQ,JT,JMAX,JM,DELX,DELT,EK,THETA,QIN,A,Q,ARRAY,RHS | 004  |
|    | 1,JTRANS,EMOD  | 005  |
|    | EXTERNAL H   | 009  |
| 03 | FORMAT(5(4X,E11.4))  | 010  |
|    | THICK=0.3  | 011  |
| 02 | FORMAT(80A1)   | 012  |
| 00 | CONTINUE   | 034  |
|    | READ(5,1) JMAX   | 013  |
| 1  | FORMAT(I3)   | 014  |
| 05 | FORMAT(1H,5(E10.3,4X))                                       | 015  |
| 07 | FORMAT(1H,7/3H X#,E10.4)                                     | 016  |
|    | READ(5,3004) AAMB,QDEF                                       | 0171 |
| 04 | FORMAT(2F0.0)  | 0172 |
|    | WRITE(6,603) AAMB  | 0173 |
|    | READ(5,602) (IDENT(I),I=1,160)                               | 017  |
|    | WRITE(6,602) (IDENT(I),I=1,160)                              | 018  |
| 01 | FORMAT(1H1)  | 019  |
|    | I=1  | 020  |
| 02 | FORMAT(E4.1)   | 021  |
| 00 | READ(5,82) QIN(I)  | 022  |
|    | IF(QIN(I)=99.0) 81,83,83                                     | 023  |
| 01 | I=I+1  | 024  |
|    | GOTO 80  | 025  |
| 03 | JM=J+1   | 026  |
|    | IFLAG=1  | 027  |
|    | IALPHA=1   | 028  |
|    | WRITE(6,28) (QIN(J),J=1,24)                                  | 029  |
|    | DO 1003 IJK=1,10   | 030  |
|    | RHS(IJK)=0.0   | 031  |
|    | DO 1003 IJL=1,10   | 032  |
| 03 | ARRAY(IJK,IJL)=0.0   | 033  |
|    | WRITE(6,60) JM,JMAX  | 035  |
| 04 | FORMAT(1H,3(E10.3,4X))                                       | 036  |
|    | TOO=2.0  | 037  |
| 00 | FORMAT(4H JM=,I3,6H JMAX=,I3)                                | 038  |
| 01 | FORMAT(3H, E9.2)   | 039  |
| 02 | FORMAT(1H,8(E11.4,2X))                                       |      |
| 01 | FORMAT(1H, F10.3//)  | 041  |
| 02 | FORMAT(E10.1)  | 042  |
| 1  | FORMAT(I1)   | 043  |
| 04 | FORMAT(E7.1)   | 044  |
| 05 | FORMAT(24E3.1)   | 045  |
| 01 | FORMAT(2I5)  | 046  |
| 02 | FORMAT(12E6.2)   | 047  |
| 03 | FORMAT(15A1)   | 048  |
| 09 | FORMAT(2E9.3)  | 049  |
|    | READ(5,11) ISEL  | 050  |
|    | READ(5,12) EK  | 051  |
|    | EK=EK*981.0  | 052  |
|    | ISEL=ISEL+1  | 053  |
| 03 | FORMAT(1H,7/4H AQ=,E10.3//)                                  | 054  |
|    | READ(5,24) D,EL  | 055  |
| 08 | FORMAT(5H QIN=,E9.2)   | 056  |
|    | AQ=(3.142*D**2)/4.0  | 057  |
|    | EK=EK*10.0/9.0   | 058  |

|    |                                      |      |
|----|--------------------------------------|------|
|    | DELTA=FLOAT(JM)/FLOAT(JMAX)          | 060  |
|    | DELX=4.0*EL*DELTA/FLOAT(JM)          | 061  |
|    | WRITE(6,29) DELX,DELTA               | 062  |
|    | TQ(1)=0.0                            | 063  |
|    | DO 70 KI=1,JMAX                      | 064  |
|    | TQ(KI+1)=TQ(KI)+1.0                  | 065  |
| 70 | TO(KI+1)=TO(KI)+DELTA                | 066  |
|    | CALL FA(QOUT)                        | 067  |
|    | WRITE(6,3003) (QOUT(ITL),ITL=1,JMAX) | 068  |
|    | DO 300 ITL=1,JMAX                    | 069  |
| 0  | QOUT(ITL)=ABS(QOUT(ITL))             | 070  |
|    | WRITE(6,601)                         | 071  |
| 9  | FORMAT(6H DELX=,E9.2,6H DELTA=,E9.2) | 072  |
|    | THETA=DELX/DELTA                     | 073  |
|    | TO(1)=0.0                            | 074  |
| 3  | FORMAT(1H ,E9.2)                     | 075  |
|    | D=0-0.05                             | 0751 |
|    | DO 250 IDIAM=1,4                     | 0752 |
|    | D=D+0.05                             | 0753 |
|    | ISTEP=IMAX/11                        | 076  |
|    | AO=(3.142*D**2)/4.0                  | 089  |
|    | QBOUND=0.0                           | 090  |
|    | ABOUND=AO                            | 091  |
|    | Q(1,1)=QBOUND                        | 092  |
|    | Q(2,1)=QBOUND                        | 093  |
|    | A(1,1)=ABOUND                        | 094  |
|    | A(2,1)=ABOUND                        | 095  |
|    | AEXIT=AAMB*AO                        | 096  |
|    | CALL VEL(AEXIT,AO,EK,THICK,F)        | 0961 |
|    | FMOD=F                               | 0962 |
|    | B=(FMOD*AEXIT)**0.5                  | 0963 |
|    | QCRIT=B*AEXIT                        | 0964 |
|    | RA=QCRIT/QDEF                        | 0965 |
|    | SRA=RA*RA                            |      |
|    | REK=1.5*EK/SRA                       | 1    |
|    | CALL VEL(AEXIT,AO,REK,THICK,F)       | 2    |
|    | B=(F*AEXIT)**0.5                     | 3    |
|    | QCRIT=AEXIT*B                        | 4    |
|    | IF(QDEF.GE.QCRIT) STOP 55            | 5    |
|    | EK=REK                               | 6    |
|    | AEXIT=AAMB*AO                        | 096  |
|    | WRITE(6,253) AO                      | 097  |
|    | WRITE(6,251) EK                      | 098  |
|    | JO=1                                 | 099  |
| 0  | DO 3 J=1,JMAX                        | 100  |
|    | Q(1,J)=QOUT(J)                       | 101  |
|    | Q(2,J)=Q(1,J)                        | 1011 |
|    | A(2,J)=AEXIT                         | 1012 |
| 3  | A(1,J)=AEXIT                         | 102  |
|    | DO 91 I91=1,JMAX                     |      |
|    | CALL VEL(A(1,I91),AO,EK,THICK,F)     | 105  |
|    | B=(F*A(1,I91))**0.5                  | 106  |
|    | U1=Q(1,I91)/A(1,I91)                 | 107  |
|    | IF(U1.GT.B) GOTO 92                  | 108  |
|    | JTRANS(I91)=1                        | 109  |
|    | GOTO 91                              | 110  |
| 2  | JTRANS(I91)=1                        | 111  |

|  |      |
|--|------|
| CONTINUE   | 112  |
| X=0.0  | 113  |
| DO 30 J=1,IMAX   | 114  |
| X=X+DELX   | 115  |
| JO=JO+1  | 116  |
| JMO=JMAX=JO  | 117  |
| T=DELX*FLOAT(JO)   | 118  |
| CALL VEL(A(2,100),AO,EK,THICK,F1)                            | 1181 |
| VELM=(F1*A(2,100))*0.5                                       | 1182 |
| QCRIT=VELM*A(2,100)  | 1183 |
| RA=QCRIT/QDEF  | 1184 |
| SRA=RA*RA  | 1185 |
| REK1=1.5*EK/SRA  | 1186 |
| EXL=2.0  |      |
| EX=DELX*I  |      |
| CMAX=1.0=EXP(=EXL)   |      |
| CMOD=(1.0=EXP(=EXL*EX/EL))/CMAX                              |      |
| REK1=REK1/CMOD   |      |
| DELEK=REK1*EK  | 1187 |
| ISW=0  | 1188 |
| FMOD=(DELEK/DELX)*H(A(2,100),AO,THICK,ISW)                   | 1189 |
| EK=REK1  | 1190 |
| CALL VEL(A(2,100),AO,EK,THICK,F1)                            | 1191 |
| VELM=(F1*A(2,100))*0.5                                       | 1192 |
| QCRIT=VELM*A(2,100)  | 1193 |
| IF(QDEF,GE,QCRIT) STOP 56                                    | 1194 |
| DO 40 J=JO,JMO   | 119  |
| JT=J   | 120  |
| CALL DIFF(IFLAG,IALPHA,THICK)                                | 121  |
| CONTINUE   | 122  |
| WRITE(6,1)  I  | 123  |
| ISW=0  | 1231 |
| P=EK*H(A(2,100),AO,THICK,ISW)                                | 1232 |
| T=100.0*DELX   | 1233 |
| DELEN=P*0.5*(Q(2,100)/A(2,100))*2 = 0.5*(QOUT(100)/AEXIT)**2 | 1234 |
| WRITE(6,202) T,Q(2,100),A(2,100),P,DELEN,EK,QCRIT            | 1235 |
| DO 50 J=JO,JMO   | 124  |
| A(1,J)=A(2,J)  | 125  |
| Q(1,J)=Q(2,J)  | 126  |
| ISTEP=ISTEP+IMAX/11  | 127  |
| CONTINUE   | 128  |
| DO 203 K=JO,JMO,5  | 129  |
| ISW=0  |      |
| P=EK*H(A(1,K),AO,THICK,ISW)/981.0                            |      |
| ENIN=P*0.5*(Q(1,K)/A(1,K))*2/981.0                           | 131  |
| ENFI=0.5*(Q(1,K)/AEXIT)**2/981.0                             |      |
| ISW=0  |      |
| PEXIT=EK*H(AEXIT,AO,THICK,ISW)/981.0                         |      |
| PFRIC=ENIN=ENFI=PEXIT  |      |
| RES=PFRIC/(Q(1,K)**2)  | 134  |
| T=T+5.0*DELX   | 135  |
| WRITE(6,202)  T,Q(1,K),A(1,K),P,ENFI,PFRIC,RES      ,ENIN    |      |
| CONTINUE   | 137  |
| CONTINUE   | 138  |
| CONTINUE   | 139  |
| IF(IMAX=2000)600,600,603                                     | 140  |
| CONTINUE   | 141  |
| STOP   | 142  |
| WRITE(6,2002)  | 143  |

FORMATTED R. H. SECONDARY DATA RECEIVED  
STOP  
END

145  
146

OF SEGMENT, LENGTH 1008, NAME PF32

|    |   |     |
|----|---|-----|
|    | DIMENSION ARRAY(10,10),RHS(70),E(10),Q(2,300),A(2,300),         | 151 |
| 1  | QIN(300),V(2)   | 152 |
| 2  | JTRANS(300)   | 153 |
|    | COMMON JO,AO,JT,JMAX,JM,DELX,DELT,EK,THETA,QIN,A,Q,ARRAY,RHS    | 149 |
| 1  | JTRANS,MFOD   | 150 |
|    | INTEGER E   | 154 |
| 2  | FORMAT(1H,3(I4,3X),5(E10,3,3X))                                 | 155 |
|    | JTM=JT  | 156 |
|    | JT=JTM  | 157 |
|    | IFLAG=IFLAG+2   | 158 |
|    | IFLAG1=IFLAG+1  | 159 |
|    | V(1)=6  | 160 |
|    | IFLAG2=IFLAG+2  | 161 |
|    | CALL VEL(A(1,JT),AO,EK,THICK,F)                                 | 162 |
|    | B=F   | 163 |
|    | B=(B*A(1,JT))*0.5   | 164 |
|    | U=Q(1,JT)/A(1,JT)   | 165 |
|    | PSIPL=U*B   | 166 |
|    | PSIMI=U*B   | 167 |
|    | ARRAY(IFLAG,IFLAG)=1.0  | 168 |
|    | ARRAY(IFLAG1,IFLAG)=1.0   | 169 |
|    | ARRAY(IFLAG,IFLAG1)=PSIPL*2.0*U                                 | 170 |
|    | ARRAY(IFLAG1,IFLAG1)=PSIMI*2.0*U                                | 171 |
|    | IF(U,LT.0) GOTO 51  | 172 |
|    | WRITE(6,62) JT,JO,IFLAG,B,U,PSIPL,PSIMI,F                       | 173 |
| 51 | CONTINUE  | 174 |
| 50 | FORMAT(1H,6(E10,3,3X),4X,I4)                                    | 175 |
| 2  | IF(ABS(PSIPL)/DELT>THETA) GOTO 22                               | 176 |
| 3  | IALPHA=1  | 177 |
| 5  | CALL COEFF(1,1,JT,PSIPL,IFLAG,IFLAG)                            | 178 |
| 6  | CALL COEFF(2,1,JT,PSIPL,IFLAG,IFLAG)                            | 179 |
|    | RHS(IFLAG)=RHS(IFLAG)+A(1,JT)*(DELX/PSIPL)*G(Q(1,JT),A(1,JT))   | 180 |
| 7  | IFLAG1=IFLAG+1  | 181 |
| 8  | IF(ABS(PSIMI)/DELT>THETA) GOTO 14                               | 182 |
| 9  | IF(PSIMI/DELT>0.0) GOTO 116                                     | 183 |
| 11 | CALL COEFF(1,0,JT,PSIMI,IFLAG1,IFLAG)                           | 184 |
|    | CALL COEFF(2,0,JT,PSIMI,IFLAG1,IFLAG)                           | 185 |
|    | RHS(IFLAG1)=RHS(IFLAG1)+A(1,JT)*DELT*G(Q(1,JT),A(1,JT))         | 186 |
| 12 | IALPHA=2  | 187 |
|    | RETURN  | 188 |
| 14 | IF(IALPHA,GT.2) GOTO 20   | 189 |
| 15 | CALL COEFF(1,1,JT,PSIMI,IFLAG1,IFLAG)                           | 190 |
|    | CALL COEFF(2,1,JT,PSIMI,IFLAG1,IFLAG)                           | 191 |
|    | RHS(IFLAG1)=RHS(IFLAG1)+A(1,JT)*(DELX/PSIMI)*G(Q(1,JT),A(1,JT)) | 192 |
|    | IF(IFLAG,LT.2) GO TO 40   | 193 |
|    | DO 116 IARR=1,IFLAG1  | 194 |
| 16 | ARRAY(IARR,IFLAG2)=RHS(IARR)                                    | 195 |
| 16 | PAUSE 10  | 196 |
|    | IF(E(1).NE.IFLAG1) GOTO 100                                     | 197 |
|    | WRITE(6,110) JT,IFLAG1  | 198 |
| 10 | FORMAT(1H,4H JT=,I4,4X,8H IFLAG1=,I4)                           | 199 |
| 50 | JT1=JT+1  | 200 |
|    | INDEX=JT1   | 201 |
|    | DO 70 IJT=1,IFLAG1  | 202 |
|    | INDEX=INDEX+1   | 203 |
|    | Q(2,INDEX)=ARRAY(IJT,IFLAG2)                                    | 204 |
|    | IJT1=IJT+1  | 205 |
| 70 | A(2,INDEX)=ARRAY(IJT1,IFLAG2)                                   | 206 |

|    |   |     |
|----|---|-----|
| 40 | CALL SINEQ2(PSIPL,PSIMI,U,Q(2,JT),A(2,JT))                      | 208 |
| 17 | IFLAG=1   | 209 |
| 18 | IALPHA=1  | 210 |
|    | DO 31 IJ1=1,IFLAG1  | 211 |
|    | RHS(IJ1)=0.0  | 212 |
|    | DO 31 IJ2=1,IFLAG1  | 213 |
| 31 | ARRAY(IJ1,IJ2)=0.0  | 214 |
|    | RETURN  | 215 |
| 20 | CALL COEFF(1,1,JT,PSIMI,IFLAG1,IFLAG)                           | 216 |
|    | CALL COEFF(2,1,JT,PSIMI,IFLAG1,IFLAG)                           | 217 |
|    | RHS(IFLAG1)=RHS(IFLAG1)+A(1,JT)*(DELX/PSIMI)*G(Q(1,JT),A(1,JT)) | 218 |
|    | RETURN  | 219 |
| 14 | IF(IFLAG.GT.1) GOTO 11  | 220 |
|    | CALL COEFF(1,2,JT,PSIMI,IFLAG1,IFLAG)                           | 221 |
|    | CALL COEFF(2,2,JT,PSIMI,IFLAG1,IFLAG)                           | 222 |
|    | RHS(IFLAG1)=RHS(IFLAG1)+A(1,JT)*DELT*G(Q(1,JT),A(1,JT))         | 223 |
|    | GOTO 40   | 224 |
| 22 | CONTINUE  |     |
|    | IF((JT.EQ.J0).AND.(J0.EQ.2)) GOTO 60                            | 225 |
|    | IF(IALPHA.GT.1) GOTO 25   | 226 |
|    | PSIPL=THETA*ABS(PSIPL)/PSIPL                                    |     |
|    | U1=B*PSIPL  |     |
|    | Q(1,JT)=U1*A(1,JT)  |     |
|    | GOTO 3  |     |
| 23 | CALL COEFF(1,2,JT,PSIPL,IFLAG,IFLAG)                            | 227 |
|    | CALL COEFF(2,2,JT,PSIPL,IFLAG,IFLAG)                            | 228 |
|    | RHS(IFLAG)=RHS(IFLAG)+A(1,JT)*DELT*G(Q(1,JT),A(1,JT))           | 229 |
|    | GOTO 7  | 230 |
| 25 | CALL COEFF(1,0,JT,PSIPL,IFLAG,IFLAG)                            | 231 |
|    | CALL COEFF(2,0,JT,PSIPL,IFLAG,IFLAG)                            | 232 |
|    | RHS(IFLAG)=RHS(IFLAG)+A(1,JT)*DELT*G(Q(1,JT),A(1,JT))           | 233 |
| 26 | IALPHA=2  | 234 |
| 27 | GOTO 7  | 235 |
| 60 | WRITE(6,61)   | 236 |
|    | WRITE(6,62) JT,J0,IFLAG,B,U,PSIPL,PSIMI,F                       | 237 |
|    | STOP  | 238 |
| 90 | WRITE(6,91)   | 239 |
|    | STOP  | 240 |
| 00 | WRITE(6,101)  | 241 |
|    | STOP  | 242 |
| 61 | FORMAT(27H REQUIRE L.H. BOUNDARY DATA)                          | 243 |
| 91 | FORMAT(15H OVER/UNDERFLOW)                                      | 244 |
| 01 | FORMAT(19H MATRIX IS SINGULAR)                                  | 245 |
|    | END   | 246 |

OF SEGMENT, LENGTH 828, NAME DIFF

```

SUBROUTINE COEFF(IR1,K2,PSI,IR2,IR1,K2)
DIMENSION RHS(70),ARRAY(10,10),Q(2,300),A(2,300),QIN(300)
1,JTRANS(300)
COMMON JO,AO,JT,JHAX,JH,DELX,DELT,EK,THETA,QIN,A,Q,ARRAY,RHS
1,JTRANS,FMOD
U=Q(1,J)/A(1,J)
S=ABS(PSI)/THETA
IF(K2.NE.0) GOTO 3
GOTO (1,2),K1
1 L=2
IF(PSI.GT.0.0) GOTO 40
L=L
40 CONTINUE
IRL=IR2+L
ARRAY(IR1,IRL)=ARRAY(IR1,IRL)+(1.0=S)
RHS(IR1)=RHS(IR1)+S*Q(1,J)
RETURN
2 IF(PSI) 5,5,4
5 ARRAY(IR1,IR2+3)=ARRAY(IR1,IR2+3)+(1.0=S)*(PSI+2.0*U)
RHS(IR1)=RHS(IR1)+S*A(1,J)*(PSI+2.0*U)
RETURN
4 CONTINUE
ARRAY(IR1,IR2+1)=ARRAY(IR1,IR2+1)+(1.0=S)*(PSI+2.0*U)
RHS(IR1)=RHS(IR1)+S*A(1,J)*(PSI+2.0*U)
RETURN
3 GOTO (5,7),K1
6 GOTO(20,21),K2
20 CALL TINTER(PSI,J,X,1)
RHS(IR1)=RHS(IR1)+X
RETURN
21 CALL XINTER(PSI,J,X,1)
RHS(IR1)=RHS(IR1)+X
RETURN
7 GOTO(23,24),K2
23 CALL TINTER(PSI,J,X,2)
RHS(IR1)=RHS(IR1)+X*(PSI+2.0*U)
RETURN
24 CALL XINTER(PSI,J,X,2)
RHS(IR1)=RHS(IR1)+X*(PSI+2.0*U)
RETURN
30 WRITE(6,31)
31 FORMAT(27H REQUIRE L'H; BOUNDARY DATA)
STOP
END

```

251  
252  
249  
250  
253  
254  
255  
256  
257  
258  
259  
260  
261  
262  
263  
264  
265  
266  
267  
268  
269  
270  
271  
272  
273  
274  
275  
276  
277  
278  
279  
281  
282  
283  
284  
285  
286  
287  
288  
289  
290  
291

OF SEGMENT, LENGTH 354, NAME COEFF

```

SUBROUTINE (INICK,IPDA,JPDA,ISEL)
DIMENSION RHS(70),ARRAY(10,10),Q(2,300),A(2,300),QIN(300)
1,JTRANS(300)
COMMON JO,AO,JT,JMAX,IM,DELX,DELT,EK,THETA,QIN,A,Q,ARRAY,RHS
1,JTRANS,EMOD
K=1
IF(PHI,GT,0.0) GOTO 40
K=K
40 CONTINUE
JK=J+K
GOTO (1,2), ISEL
1 X=Q(1,J) * THETA*(Q(1,JK)-Q(1,J))/ABS(PHI)
RETURN
2 X=A(1,J) * THETA*(A(1,JK)-A(1,J))/ABS(PHI)
RETURN
END

```

```

293
294
295
296
297
298
299
300
301
302
303
304
305
306
307
308

```

```

) OF SEGMENT, LENGTH 91, NAME TINTER

```

|   |     |
|---|-----|
| DIMENSION RHS(70), ARRAY(10,10), Q(2,300), A(2,300), QIN(300)             | 313 |
| 1, JTRANS(300)  | 314 |
| COMMON JO, AO, JT, JHAX, JH, DELX, DELT, EK, THETA, QIN, A, Q, ARRAY, RHS | 311 |
| 1, JTRANS, FROD   | 312 |
| K=1   | 315 |
| IF(PHI.GT.0.0) GOTO 40  | 316 |
| K=K+1   | 317 |
| 40 CONTINUE   | 318 |
| J=J+K   | 319 |
| GOTO (1,2), ISEL  | 320 |
| 1 X=Q(2,J)-(ABS(PHI))*(Q(2,J)-Q(1,J))/THETA                               | 321 |
| RETURN  | 322 |
| 2 X=A(2,J)-(ABS(PHI))*(A(2,J)-A(1,J))/THETA                               | 323 |
| RETURN  | 324 |
| END   | 325 |

OF SEGMENT, LENGTH 92, NAME XINTER

```

SUBROUTINE P1NV(PBL0UT, Q00T, AIN)
DIMENSION PBL0UT(300), Q00T(300), AIN(300), QIN(300), ARRAY(10,10),
1RHS( 70), A(2,300), Q(2,300)
2, JTRANS(300)
COMMON JO, AO, JT, JMAX, JM, DELX, DELT, EK, THETA, QIN, A, Q, ARRAY, RHS
1, JTRANS, FNOP
IRET=0
6 FORMAT(4H EK=,E11.4,17H IS INCOMPATIBLE)
AO2=AO**2
S=EK
T=30.0*981.0
J=1
2 CONTINUE
IRET=IRET+1
IF(IRET.GT.100) GOTO 7
DO 1 J=1, JMAX
A2=((Q00T(J)**2)/(2.0)+EK*AO2)/(PBL0UT(J)+EK)
IF(A2.LT.AO2) GOTO 3
AIN(J)=A2**0.5
1 CONTINUE
RETURN
3 IF(EK.LT.T) GOTO 4
IF(J.GT.1) GOTO 4
WRITE(6,6) EK
EK=EK+EK/10.0
GOTO 2
4 WRITE(6,6) EK
J=2
S=S+S/10.0
EK=S
GOTO 2
7 WRITE(6,8)
8 FORMAT(24H EK,GT,100 MODIFICATIONS)
STOP
END

```

327  
328  
329  
330  
331  
332  
333  
334  
335  
336  
337  
338  
339  
340  
341  
342  
343  
344  
345  
346  
347  
348  
349  
350  
351  
352  
353  
354  
355  
356  
357  
358  
359  
360  
361

0 OF SEGMENT, LENGTH 157, NAME P1NV

|  |     |
|--|-----|
| FUNCTION G(Y,Z)  | 363 |
| DIMENSION Q(2,300),QIN(300),A(2,300),QOUT(300),AIN(300),     | 006 |
| 1YQ(300),YQ(300),IDENT(160),ARRAY(10,10),RHS(70),PBLOUT(300) | 007 |
| 2,JTPANS(300)  | 008 |
| COMMON JU,AO,JT,JMAX,JM,DELX,DELT,EK,THETA,QIN,A,Q,ARRAY,RHS | 004 |
| 1,JTRANS,FMOD  | 005 |
| R=ABS((100.0*Y*(4.0*Z/3.142)**0.5)/Z)                        | 364 |
| Y=ABS(Y)   | 365 |
| V=V/Z  | 366 |
| D=(4.0*Z/3.142)**0.5   | 367 |
| F=0.5*V**2*0.32/(D**0.25)                                    | 368 |
| G=F+FMOD   | 369 |
| RETURN   | 370 |
| END  | 371 |

OF SEGMENT, LENGTH 65, NAME G

|    |  |     |
|----|--|-----|
|    | DIMENSION RHS(70), QIN(300), ARRAY(10,10), A(2,300), Q(2,300)              | 374 |
| 1  | JTRANS(300)  | 375 |
|    | COMMON JU, AO, JT, JMAX, JMD, DELX, DELT, EK, THETA, QIN, A, Q, ARRAY, RHS | 376 |
| 1  | JTRANS, FMOO   | 377 |
| 2  | FORMAT(1H ,6(E11.4,3X),13,/,5(E11.4,3X))                                   |     |
|    | PATMOS=76.0*13.53  |     |
|    | THICK=0.3  | 379 |
|    | IF(PSIPL,LT.0.0) GOTO 21   |     |
|    | IS=1   |     |
|    | GOTO 22  |     |
| 21 | IS=-1  |     |
| 22 | CONTINUE   |     |
|    | GOTO 31  |     |
| 25 | CONTINUE   |     |
|    | A2=(RHS(1)-RHS(2))/(PSIPL*PSIMT)   | 384 |
|    | Q2=RHS(1)-(PSIPL*2.0*U)*A2   | 385 |
|    | IF(A2,LT.AO) GOTO 111  |     |
|    | Q2=-Q2   | 386 |
|    | RETURN   | 388 |
| 11 | CONTINUE   |     |
|    | WRITE(6,112) A2,AO   |     |
| 12 | FORMAT(1H ,2(E11.4,4X))  |     |
|    | CALL VEL(A1,AO,EK,THICK,F)   |     |
|    | B1=(A1*F)**0.5   |     |
|    | CALL VEL(A2,AO,EK,THICK,F)   |     |
|    | B2=(A2*F)**0.5   |     |
|    | WRITE(6,112) B1,B2,A(1,JT)   |     |
|    | RETURN   |     |
| 13 | CONTINUE   | 389 |
|    | JTRANS(JT)=IS  |     |
| 3  | FORMAT(8H LABEL81)   |     |
| 1  | W1=A2  | 390 |
| 4  | FORMAT(7H LABEL1)  |     |
|    | W2=Q2  | 391 |
|    | Q1=Q(1,JT)   | 392 |
|    | A1=A(1,JT)   | 393 |
|    | U1=Q1/A1   | 394 |
|    | ISW=0  |     |
|    | P1=EK*H(A1,AO,THICK,ISW) + PATMOS  |     |
|    | ENKIN=0.5*(U1**2)  | 396 |
|    | RATIO=ENKIN/P1   | 397 |
|    | IF(RATIO,GT.1.0) GOTO 91   | 398 |
|    | R=0.5*RATIO  | 399 |
|    | S1=1.0   | 400 |
|    | GOTO 92  | 401 |
| 91 | B=2.0*RATIO  | 402 |
|    | S1=1.0   | 403 |
| 92 | CONTINUE   | 404 |
|    | B=0  |     |
|    | IF(B,LT.0.0) B=1.0   |     |
| 17 | FORMAT(3H B=,E11.3,4X,14)  | 416 |
| 29 | ERR=0.01   |     |
| 11 | CONTINUE   |     |
|    | IR=0   |     |
| 12 | A2=A1/B  | 405 |
|    | IF((B,LT.0.0).AND.(IR,GT.0)) GOTO 25                                       |     |
|    | ISK=-1   |     |
|    | P2=EK*H(A2,AO,THICK,ISW) + PATMOS  |     |

```

CALL VEL(A2,A0,EK,THICK,F)
X2=U1**2
IR=IR+1
FN1=P1+p2=X2
FN2=X2-2,0*P2
FX=B*FN1**2=(B+1,0)*FN2*X2
DP2=F*A1/(B**2)
DFX=FN1**2+2,0*B*FN1*DP2=FN2*X2+2,0*X2*(B+1,0)*DP2
DELR=FX/DFX
R=B+DELB
ARG=DELB/R
PER=100,0*ABS(ARG)
IF(ABS(ARG).LT.ERR) GOTO 6
IF(IR.GT.1000) GOTO 27
GOTO 12
7 WRITE(6,10)
10 FORMAT(17H ZERO CONVERGENCE)
24 FORMAT(20H NO SOLN, OBTAINABLE)
STOP
8 WRITE(6,9)
9 FORMAT(16H NUMERICAL ERROR)
STOP
6 CONTINUE
IF(H.LT.0,0) GOTO 25
A2=A1/B
CALL VEL(A2,A0,EK,THICK,F)
VE=(A2*F)**0.5
ARG1=2,0*THETA+ERR*U2
ARG2=2,0*THETA-ERR*U2
ARG=U2-VE
AARG=ABS(ARG)
IF(AARG.GT.ARG1) GOTO 25
AARG2=ABS(ARG2)
IF(AARG.LT.AARG2) GOTO 14
ERR=ERR/2,0
GOTO 11
14 CONTINUE
IF(AARG.GT.THETA) GOTO 15
U2=VE+THETA*AARG/ARG
15 CONTINUE
Q2=U2*A2
W1=A(1,JT)
W2=Q(1,JT)
W3=W2/W1
CALL VEL(W1,A0,EK,THICK,F)
W4=(W1*F)**0.5
W5=VE+W4
W6=W4*W3
W7=VE-Q2/A2
WRITE(6,17) B,K
WRITE(6,2) W1,W2,W3,W4,W5,W6,JT,A2,Q2,U2,VE,W7
RETURN
26 IF(IR.NE.0) GOTO 25
IF(IB.GT.100) GOTO 26
IB=IB+1
B=B/2,0
GOTO 29
27 CONTINUE

```

420  
421  
422  
423  
424  
425  
426  
427  
428  
434  
415  
433

STOP 1  
END

OF SEGMENT, LENGTH 563, NAME STMEQ2

REBABS(100.0\*Y\*(4.0\*Z/3.142)\*\*0.5)/Z  
RETURN  
END

437  
438  
439

OF SEGMENT, LENGTH 33, NAME RE

|   |     |
|---|-----|
| B=(X/3.142)**0.5 *T                       | 442 |
| B2=B**2                                   | 443 |
| B3=B*B2                                   | 444 |
| C2=(X*Y)/3.142                            | 445 |
| PA=3.142*X                                | 446 |
| PA2=PA**0.5                               | 447 |
| G=T/(PA2*(B2=C2))+1.0/X=1.0/(PA2*B)       | 448 |
| F=B+Y/(X**2)+C2/(PA2*B3) = 1.0/(3.142*B2) | 449 |
| F=0.5*Z*F                                 | 450 |
| RETURN                                    | 451 |
| END                                       | 452 |

OF SEGMENT, LENGTH 85, NAME VEL

|  |     |
|--|-----|
| A2=X/3,142                             | 455 |
| C2=(X+Y)/3,142                         | 456 |
| B=A2**0.5+Z                            | 457 |
| B2=B**2                                | 458 |
| ARG=(1.0-C2/B2)/(1.0-C2/A2)            |     |
| IF((ARG.LT.0.9).AND.(ISW.EQ.1)) GOTO 1 |     |
| F=ALOG(ARG)                            |     |
| H=0.5*(F+C2/A2-C2/B2)                  | 460 |
| RETURN                                 | 461 |
| 1 ISW=1                                |     |
| B=0.0                                  |     |
| RETURN                                 |     |
| END                                    | 462 |

OF SEGMENT, LENGTH 79, NAME H

|    |  |     |
|----|--|-----|
|    | DIMENSION QB(300),BO(300),QINT(300),QIN(300)                 | 465 |
| 1  | JTRANS(300)  | 466 |
|    | COMMON JO,AO,JT,JMAX,JH,DELX,DELT,EK,THETA,QIN,A,Q,ARRAY,RHS | 467 |
| 1  | JTRANS,FNOB  | 468 |
|    | JM2=JM#2   | 469 |
|    | FJM1=FLOAT(JM#1)   | 470 |
|    | FJM=FLOAT(JM)  | 471 |
|    | FJMAX=FLOAT(JMAX)  | 472 |
|    | FJMAX1=FJMAX-1.0   | 473 |
|    | JM1=FJM1   | 474 |
|    | DO 101 KO#1, JM  | 475 |
|    | FKO1=FLOAT(KO#1)   | 476 |
| 01 | QB(KO)=QIN(KO)-QIN(1)+(QIN(JM)-QIN(1))*FKO1/FJM1             | 477 |
|    | DO 102 JO#2, JM1   | 478 |
|    | FJO1=FLOAT(JO#1)   | 479 |
|    | B=0.0  | 480 |
|    | DO 103 JOO#2, JH1  | 481 |
|    | FJOO1=FLOAT(JOO#1)   | 482 |
| 03 | B=B+QB(JOO)*SIN(FJO1*FJOO1*3.142/FJM1)                       | 483 |
| 02 | BO(JO)=2.0*B/FJM1  | 484 |
|    | DO 104 JOO#1, JHAX   | 485 |
|    | FJOO1=FLOAT(JOO#1)   | 486 |
|    | C=0.0  | 487 |
|    | DO 105 KOO#2, JH1  | 488 |
|    | FKOO1=FLOAT(KOO#1)   | 489 |
| 05 | C=C+BO(KOO)*SIN(FJOO1*FKOO1*3.142/FJMAX1)                    | 490 |
| 04 | QINT(JOO)=C+QIN(1)+(QIN(JM)-QIN(1))*FJOO1/FJMAX1             | 491 |
|    | RETURN   | 492 |
|    | END  | 493 |

OF SEGMENT, LENGTH 250, NAME PA

STOP 10  
END

OF SEGMENT, LENGTH 15, NAME GJR

NAME #PF32, CORE 14653, LOWER AREA 1181, PROGRAM 6806

COMPILATION \* NO ERRORS